

ผลของการเสื่อมของพอลิเอธิลีนไกลคอล 600 ต่อการจางของสีและการเชื่อมโยงข้าม  
ในเปลือกแคปซูลเจลาตินนึ่ม



นางวิณา นิตยสุทธิ

จุฬาลงกรณ์มหาวิทยาลัย

บทคัดย่อและแฟ้มข้อมูลฉบับเต็มของวิทยานิพนธ์ตั้งแต่ปีการศึกษา 2554 ที่ให้บริการในคลังปัญญาจุฬาฯ (CUIR)  
เป็นแฟ้มข้อมูลของนิสิตเจ้าของวิทยานิพนธ์ ที่ส่งผ่านทางบัณฑิตวิทยาลัย

The abstract and full text of theses from the academic year 2011 in Chulalongkorn University Intellectual Repository (CUIR)  
are the thesis authors' files submitted through the University Graduate School.

วิทยานิพนธ์นี้เป็นส่วนหนึ่งของการศึกษาตามหลักสูตรปริญญาเภสัชศาสตรมหาบัณฑิต

สาขาวิชาเภสัชอุตสาหกรรม ภาควิชาวิทยาการเภสัชกรรมและเภสัชอุตสาหกรรม

คณะเภสัชศาสตร์ จุฬาลงกรณ์มหาวิทยาลัย

ปีการศึกษา 2560

ลิขสิทธิ์ของจุฬาลงกรณ์มหาวิทยาลัย

EFFECT OF DEGRADATION OF PEG 600 ON COLOR FADING AND CROSSLINKING  
IN SOFT GELATIN CAPSULE SHELL



A Thesis Submitted in Partial Fulfillment of the Requirements  
for the Degree of Master of Science in Pharmacy Program in Industrial Pharmacy  
Department of Pharmaceutics and Industrial Pharmacy  
Faculty of Pharmaceutical Sciences  
Chulalongkorn University  
Academic Year 2017  
Copyright of Chulalongkorn University



วิธินา นิตยสุทธิ : ผลของการเสื่อมของพอลิเอธิลีนไกลคอล 600 ต่อการจางของสีและการเชื่อมโยงข้ามในเปลือกแคปซูลเจลละตินนิ่ม (EFFECT OF DEGRADATION OF PEG 600 ON COLOR FADING AND CROSSLINKING IN SOFT GELATIN CAPSULE SHELL) อ.ที่ปรึกษาวิทยานิพนธ์หลัก: ผศ. ญ. ดร.จิตติมา ชัชวาลย์สายสินธ์, 131 หน้า.

การเกิดออกซิเดชันของพอลิเอธิลีนไกลคอล 600 ซึ่งเป็นของเหลวที่ชอบน้ำและมักใช้บรรจุในแคปซูลนิ่มทำให้เกิดพอร์มาลดีไฮด์ซึ่งเป็นตัวออกซิไดซ์ วัตถุประสงค์ของการศึกษานี้เพื่อศึกษาผลของพอร์มาลดีไฮด์ต่อการจางของสีบิลเลเยนท์บลูและการเชื่อมโยงข้ามของเจลละตินในเปลือกแคปซูลนิ่ม และเพื่อหาความเป็นไปได้ในการยับยั้งการเกิดออกซิเดชันของพอลิเอธิลีนไกลคอล 600 ด้วยสารต้านออกซิเดชัน สูตรตำรับที่นำมาบรรจุแคปซูลมีจำนวน 9 สูตรตามการออกแบบทดลองแบบแฟคทอเรียล ซึ่งประกอบด้วย พอลิเอธิลีนไกลคอล 600 โดยมีน้ำ (ร้อยละ 0, 5, 10 โดยน้ำหนัก) และดี-แอลฟา-โทโคฟีรอล (ร้อยละ 0, 0.001, 0.05 โดยน้ำหนัก) ในปริมาณแตกต่างกันอย่างละ 3 ระดับ สูตรตำรับดังกล่าวบรรจุในแคปซูลซึ่งไม่แต่งสีและแต่งสีเปลือกด้วยบิลเลเยนท์บลู เก็บแคปซูลที่เตรียมได้ในขวดแก้วสีชาภายใต้สภาวะที่ควบคุมอุณหภูมิ 30 องศาเซลเซียสและความชื้นสัมพัทธ์ร้อยละ 75 เป็นเวลา 90 วัน และศึกษาคุณสมบัติทางเคมีกายภาพของแคปซูล ผลการศึกษาพบว่าพอลิเอธิลีนไกลคอล 600 เกิดออกซิเดชัน และปริมาณน้ำที่เติมในสูตรตำรับเป็นปัจจัยที่มีผลต่อการก่อพอร์มาลดีไฮด์ซึ่งวิเคราะห์ที่ 14 วัน อย่างมีนัยสำคัญ (ค่า  $p = 0.001$ ) ปริมาณสูงสุดของดี-แอลฟา-โทโคฟีรอลในการศึกษานี้ไม่สามารถยับยั้งการเกิดออกซิเดชันของพอลิเอธิลีนไกลคอล 600 ได้ การจางของสีแคปซูลไม่สามารถสังเกตเห็นได้ด้วยตาเปล่า อย่างไรก็ตามค่าบ่งชี้ความแตกต่างของสีซึ่งวัดที่ 90 วัน เพิ่มขึ้นจากวันแรกและปริมาณของสีลดลงในบางสูตรตำรับ รวมทั้งเกิดการเคลื่อนของบิลเลเยนท์บลูในเปลือกแคปซูลเข้าในของเหลวที่บรรจุ นอกจากนี้พบการเชื่อมโยงข้ามในเปลือกแคปซูลเจลละตินด้วยเทคนิคฟูเรียร์ทรานสฟอร์มอินฟราเรด ซึ่งสอดคล้องกับผลการศึกษาการละลายของแคปซูล จากผลการทดลองสรุปได้ว่าออกซิเดชันของพอลิเอธิลีนไกลคอล 600 ทำให้เกิดพอร์มาลดีไฮด์ซึ่งทำให้เกิดปัญหาการเชื่อมโยงข้ามของเจลละตินมากกว่าการจางของสีบิลเลเยนท์บลูในเปลือกแคปซูล

ภาควิชา วิทยาการเภสัชกรรมและเภสัช  
อุตสาหกรรม

ลายมือชื่อนิสิต .....  
ลายมือชื่อ อ.ที่ปรึกษาหลัก .....

สาขาวิชา เภสัชอุตสาหกรรม

ปีการศึกษา 2560



## ACKNOWLEDGEMENTS

Foremost, I would like to express my sincere gratitude to my thesis advisor, Assistant Professor Jittima Chatchawalsaisin, Ph.D., for her patience, motivation, and support throughout my study.

I am immensely grateful to Sumaporn Kasemsumran, Ph.D, at Kasetsart Agricultural and Agro-Industrial Product Improvement Institute for her suggestion and comments on NIR part in this thesis. Without her suggestion, this part of thesis could not have been possible.

I would like to thank Graduate School Thesis Grant, Graduate School, Chulalongkorn University for financial support. A very special gratitude goes to Chulalongkorn University Drug and Health Products Innovation Promotion Center, Faculty of Pharmaceutical Sciences, for providing research facilities. Moreover, I am also grateful to scientists, staff, and classmates in the Department of Pharmaceutics and Industrial Pharmacy, Faculty of Pharmaceutical Sciences, Chulalongkorn University, for their kind support throughout my study.

## CONTENTS

	Page
THAI ABSTRACT .....	iv
ENGLISH ABSTRACT .....	v
ACKNOWLEDGEMENTS .....	vi
CONTENTS .....	vii
LIST OF TABLES .....	x
LIST OF FIGURES .....	xi
LIST OF ABBREVIATIONS .....	xx
CHAPTER I INTRODUCTION.....	1
CHAPTER II LITERATURE REVIEW .....	3
1. Soft gelatin capsules.....	3
2. Fill compositions.....	3
3. Shell compositions.....	6
4. Color stability.....	7
5. Crosslinking in gelatin capsule shell.....	14
6. Near-infrared (NIR) spectroscopy .....	17
6.1 Source and type of absorption band in NIR.....	17
6.2 Quantitative analysis by NIR .....	18
6.3 Determination of water in NIR.....	21
7. Model drug.....	22
CHAPTER III MATERIALS AND METHOD .....	24
1. Preparation of soft gelatin capsule .....	25
2. Characterization of soft gelatin capsules.....	28

	Page
2.1 Appearance .....	28
2.2 Thickness .....	28
2.3 Hardness .....	28
2.4 Moisture content .....	28
2.5 Determination of formaldehyde content and water in liquid fill.....	29
2.6 Color Determination.....	33
2.7 <i>In vitro</i> dissolution test.....	33
2.8 Investigation of molecular interaction in gelatin shell by Fourier transform infrared spectroscopy (FT-IR).....	34
CHAPTER IV RESULTS AND DISCUSSION .....	35
1. Characterization of soft gelatin capsule .....	35
1.1 Appearance.....	35
1.2 Thickness.....	35
1.3 Hardness.....	36
1.4 Moisture content in capsule shell.....	39
1.5 Water content in liquid fill .....	42
1.6 Determination of formaldehyde content.....	47
1.7 Color determination.....	57
1.8 Investigation of molecular interaction in gelatin shell by Fourier transform infrared spectroscopy (FT-IR).....	65
1.9 <i>In vitro</i> dissolution test .....	68
CHAPTER V CONCLUSIONS.....	73
REFERENCES .....	74
Appendix I: Physicochemical properties of soft gelatin capsules .....	85



	Page
Appendix II: Statistical analysis .....	87
Appendix III: Pretreatment of NIR spectra, and calibration and validation of PLS models for prediction of water in liquid fill.....	90
Appendix IV: Pretreatment of NIR spectra and calibration and validation of the PLS models for prediction of formaldehyde in liquid fill .....	100
Appendix V: IR spectra of gelatin capsule shell.....	115
Appendix VI Dissolution profile of ibuprofen soft gelatin capsules .....	127
VITA.....	131



## LIST OF TABLES

Table 2- 1 Stability properties of some coloring agents (Modified from Handbook of pharmaceutical excipient (36)).....	8
Table 3- 1 Compositions of fill formulations in soft gelatin capsules.....	26
Table 3- 2 Ingredient of capsule shell .....	27
Table 4- 1 Pretreatment of NIR spectra in the region of 5,000-5,400 and 5,900-7,700 $\text{cm}^{-1}$ , RMSEC and $r^2$ of calibration, also RMSEP and $r^2$ of internal validation ....	43
Table 4- 2 Pretreatment of NIR spectra in the region of 4,000-10,000 $\text{cm}^{-1}$ , RMSEC and $r^2$ of calibration, also RMSEP and $r^2$ of internal validation.....	53
Table 4- 3 Pretreatment of NIR spectra in the region of 4,000-10,000 $\text{cm}^{-1}$ , RMSEC and $r^2$ of calibration, also RMSEP and $r^2$ of internal validation.....	54
Table I- 1 Average thickness (mm, n = 3) of non colored gelatin capsule shells.....	85
Table I- 2 Average thickness (mm, n = 3) of colored gelatin capsule shells.....	85
Table I- 3 Formaldehyde content (n=2, ppm) in the liquid fill of colored capsules determined by GC-MS and model M36-2 of NIR technique.....	86
Table II- 1 ANOVA results for capsule hardness at 90 days .....	87
Table II- 2 ANOVA results for % moisture content in capsule shells at 90 days.....	87
Table II- 3 ANOVA results for formaldehyde content in liquid fill at 14 days .....	88
Table II- 4 ANOVA results for % increase of formaldehyde at 14 days .....	88
Table II- 5 ANOVA results for delta E at 90 days.....	89
Table II- 6 Two-sample independent t-test between total color contents in the capsules at 1 and 90 days.....	89

## LIST OF FIGURES

Figure 2- 1 Brilliant blue FCF structure (51) .....	10
Figure 2- 2 Structure of intermediate I (a) and II (b) occurring during degradation of brilliant blue FCF due to oxidation by potassium persulfate (51) .....	11
Figure 2- 3 Structure of oxidation products of brilliant blue-R : .....	11
Figure 2- 4 Diagram representing the CIELAB color space .....	14
Figure 2- 5 Structure of the main methylols and crosslinks formed in the hardening reaction of gelatin and formaldehyde(70). .....	16
Figure 2- 6 Structure of ibuprofen.....	22
Figure 3 - 1 A set of die plate used for soft gelatin capsule preparation .....	27
Figure 4- 1 Soft gelatin capsules: non colored capsules after storage for 1 day (a) and 90 days (b); colored capsules after storage for 1 day (c) and 90 days (d),.....	35
Figure 4- 2 Hardness (n=3) of gelatin capsule shells for non colored formulation 1, 2, 3 (a); non colored formulation 1, 4, 5 (b); colored formulation 1, 2, 3 (c); colored formulation 1, 4, 5 (d) .....	36
Figure 4- 3 Hardness (n=3) of gelatin capsule shells for non colored formulation 2, 6, 7 (a); non colored formulation 3, 8, 9 (b); colored formulation 2, 6, 7 (c); colored formulation 3,8,9 (d).....	37
Figure 4- 4 %Moisture content (n=3) of gelatin capsule shells for non colored formulation 1, 2, 3 (a); non colored formulation 1, 4, 5 (b); colored formulation 1, 2, 3 (c); colored formulation 1, 4, 5 (d) .....	39
Figure 4- 5 %Moisture content (n=3) of gelatin capsule shells for non colored formulation 2, 6, 7 (a); non colored formulation 3, 8, 9 (b); colored formulation 2, 6, 7 (c); colored formulation 3,8,9 (d).....	40




Figure 4- 6 Scatter plot between hardness and moisture content of non colored capsules.....	41
Figure 4- 7 Scatter plot between hardness and moisture content of colored capsules.....	41
Figure 4- 8 External validation of W1 model showing predicted water content in liquid fill, with deviation. ....	44
Figure 4- 9 Water content in liquid fill (n=3) for non colored formulation 1, 2, 3 (a); non colored formulation 1, 4, 5 (b); colored formulation 1, 2, 3 (c); colored formulation 1, 4, 5 (d).....	45
Figure 4- 10 Water content in liquid fill (n=3) for non colored formulation 2, 6, 7 (a); non colored formulation 3, 8, 9 (b); colored formulation 2, 6, 7 (c); colored formulation 3,8,9 (d) .....	46
Figure 4- 11 % Formaldehyde increase in the liquid fill of colored capsule formulation 1, 2, 3 (a); colored capsule formulation 2, 6, 7 (b); colored capsule formulation 1, 4, 5 (c); colored capsule formulation 3, 8, 9 (d) .....	49
Figure 4- 12 Main effect plot for formaldehyde content at 14 days: Effect of initial water content.....	50
Figure 4- 13 Main effect plot for % increase of formaldehyde at 14 days: Effect of initial water content.....	50
Figure 4- 14 NIR spectrum in the range 4,000-10,000 $\text{cm}^{-1}$ of neat PEG 600 .....	51
Figure 4- 15 External validation of M35 model showing predicted formaldehyde content in liquid fill, with deviation .....	55
Figure 4- 16 External validation of M36-2 model showing predicted formaldehyde content in liquid fill, with deviation .....	55
Figure 4- 17 Spectra of PEG 600  , PEG 600 with 10% w/w water  , liquid fill of sample  .....	56

Figure 4- 18 Delta E (n=3) of gelatin capsule shells for non colored formulation 1, 2, 3 (a); non colored formulation 1, 4, 5 (b); colored formulation 1, 2, 3 (c); colored formulation 1, 4, 5 (d) .....	58
Figure 4- 19 Delta E (n=3) of gelatin capsule shells for non colored formulation 2, 6, 7 (a); non colored formulation 3, 8, 9 (b); colored formulation 2, 6, 7 (c); colored formulation 3, 8, 9 (d) .....	59
Figure 4- 20 Scatter plot between delta E and maximum remaining formaldehyde during storage of colored capsules.....	60
Figure 4- 21 Total color content of each formulation capsules at 1 and 90 days .....	62
Figure 4- 22 Scatter plot between brilliant blue content in capsule shell and delta E at 90 days of colored capsules .....	62
Figure 4- 23 Scatter plot between brilliant blue content in capsule shell at 90 days and maximum remaining formaldehyde in liquid fill during storage of colored capsules .....	63
Figure 4- 24 Scatter plot between brilliant blue content in liquid fill and maximum remaining formaldehyde during storage of colored capsules .....	63
Figure 4- 25 Scatter plot between brilliant blue contents in the liquid fill and shell during storage of colored capsules .....	64
Figure 4- 26 Scatter plot between water contents and brilliant blue contents in liquid fill of colored capsules at 90 days .....	64
Figure 4- 27 FTIR spectrum of freshly prepared soft gelatin capsule shell.....	65
Figure 4- 28 FT-IR spectra of of gelatin capsule shell of non colored formulation 2 containing no ibuprofen at different time points .....	66
Figure 4- 29 FT-IR spectra of gelatin capsule shell of colored formulation 2 containing no ibuprofen at different time points .....	66

Figure 4- 30 Scatter plot between maximum remaining formaldehyde content during storage and beginning time of crosslinking .....	67
Figure 4- 31 Scatter plot between maximum moisture content in the shell during storage and beginning time of crosslinking .....	68
Figure 4- 32 Example of dissolution of cross-linked ibuprofen soft gelatin capsules for colored formulation (CSG-2) at 1 (1D), 30 (30D) and 90 (90D) days .....	69
Figure 4- 33 Example of dissolution of cross-linked ibuprofen soft gelatin capsules for colored formulation CSG-9 at 1 (1D), 30 (30D) and 90 (90D) days .....	70
Figure 4- 34 FT-IR spectra of gelatin capsule shell of colored formulation CSG-2 containing ibuprofen at different time points .....	70
Figure 4- 35 FT-IR spectra of gelatin capsule shell of colored formulation CSG-9 containing ibuprofen at different time points .....	71
Figure 4- 36 Example of pellicle formed during dissolution test of colored ibuprofen soft gelatin capsule (CSG-2) at 90 days, after 30 min (a) and 60 min (b) ....	71
Figure 4- 37 Relative beginning time of gelatin crosslinking for studied formulations.....	72
Figure III- 1 Pretreatment of NIR spectra for PLS model W1: No pretreatment .....	90
Figure III- 2 Pretreatment of NIR spectra for PLS model W2: MSC.....	90
Figure III- 3 Pretreatment of NIR spectra for PLS model W3: SNV.....	91
Figure III- 4 Pretreatment of NIR spectra for PLS model W4: MSC 1 <sup>st</sup> derivative with Norris-Williams.....	91
Figure III- 5 Pretreatment of NIR spectra for PLS model W5: MSC 1 <sup>st</sup> derivative with Savitzky-Golay .....	92
Figure III- 6 Pretreatment of NIR spectra for PLS model W6: MSC 2 <sup>nd</sup> derivative with Norris-Williams.....	92

Figure III- 7 Pretreatment of NIR spectra for PLS model W7: MSC 2 <sup>nd</sup> derivative with Savitzky-Golay .....	93
Figure III- 8 Pretreatment of NIR spectra for PLS model W8: SNV 1 <sup>st</sup> derivative with Norris-Williams.....	93
Figure III- 9 Pretreatment of NIR spectra for PLS model W9: SNV 1 <sup>st</sup> derivative with Savitzky-Golay .....	94
Figure III- 10 Pretreatment of NIR spectra for PLS model W10: SNV 2 <sup>nd</sup> derivative with Norris-Williams.....	94
Figure III- 11 Pretreatment of NIR spectra for PLS model W11: SNV 2 <sup>nd</sup> derivative with Savitzky-Golay .....	95
Figure III- 12 Calibration and validation of PLS model W1 .....	96
Figure III- 13 Calibration and validation of PLS model W2.....	96
Figure III- 14 Calibration and validation of PLS model W3 .....	96
Figure III- 15 Calibration and validation of PLS model W4 .....	97
Figure III- 16 Calibration and validation of PLS model W5 .....	97
Figure III- 17 Calibration and validation of PLS model W6.....	97
Figure III- 18 Calibration and validation of PLS model W7.....	98
Figure III- 19 Calibration and validation of PLS model W8.....	98
Figure III- 20 Calibration and validation of PLS model W9 .....	98
Figure III- 21 Calibration and validation of PLS model W10.....	99
Figure III- 22 Calibration and validation of PLS model W11 .....	99
Figure IV- 1 Pretreatment of NIR spectra for PLS model M34: No pretreatment ...100	
Figure IV- 2 Pretreatment of NIR spectra for PLS model M35: MSC.....	100
Figure IV- 3 Pretreatment of NIR spectra for PLS model M36: SNV .....	101

Figure IV- 4 Pretreatment of NIR spectra for PLS model M37: MSC 1 <sup>st</sup> derivative with Norris-Williams.....	101
Figure IV- 5 Pretreatment of NIR spectra for PLS model M38: MSC 1 <sup>st</sup> derivative with Savitzky-Golay .....	102
Figure IV- 6 Pretreatment of NIR spectra for PLS model M39: MSC 2 <sup>nd</sup> derivative with Norris-Williams.....	102
Figure IV- 7 Pretreatment of NIR spectra for PLS model M40: MSC 2 <sup>nd</sup> derivative with Savitzky-Golay .....	103
Figure IV- 8 Pretreatment of NIR spectra for PLS model M41: SNV 1 <sup>st</sup> derivative with Norris-Williams.....	103
Figure IV- 9 Pretreatment of NIR spectra for PLS model M42: SNV 1 <sup>st</sup> derivative with Savitzky-Golay .....	104
Figure IV- 10 Pretreatment of NIR spectra for PLS model M43: SNV 2 <sup>nd</sup> derivative with Norris-Williams.....	104
Figure IV- 11 Pretreatment of NIR spectra for PLS model M44: SNV 2 <sup>nd</sup> derivative with Savitzky-Golay .....	105
Figure IV- 12 Pretreatment of NIR spectra for PLS model M34-2: OSC.....	105
Figure IV- 13 Pretreatment of NIR spectra for PLS model M35-2: MSC-OSC.....	106
Figure IV- 14 Pretreatment of NIR spectra for PLS model M36-2: SNV-OSC .....	106
Figure IV- 15 Pretreatment of NIR spectra for PLS model M37-2: OSC-1 <sup>st</sup> derivative with Norris-Williams.....	107
Figure IV- 16 Pretreatment of NIR spectra for PLS model M38-2: OSC 1 <sup>st</sup> derivative with Savitzky-Golay .....	107
Figure IV- 17 Pretreatment of NIR spectra for PLS model M39-2: OSC 2 <sup>nd</sup> derivative with Norris-Williams.....	108



Figure IV- 18 Pretreatment of NIR spectra for PLS model M40-2: OSC 2 <sup>nd</sup> derivative with Savitzky-Golay .....	108
Figure IV- 19 Calibration and validation of PLS model M34.....	109
Figure IV- 20 Calibration and validation of PLS model M35.....	109
Figure IV- 21 Calibration and validation of PLS model M36.....	109
Figure IV- 22 Calibration and validation of PLS model M37.....	110
Figure IV- 23 Calibration and validation of PLS model M38.....	110
Figure IV- 24 Calibration and validation of PLS model M39.....	110
Figure IV- 25 Calibration and validation of PLS model M40.....	111
Figure IV- 26 Calibration and validation of PLS model M41.....	111
Figure IV- 27 Calibration and validation of PLS model M42.....	111
Figure IV- 28 Calibration and validation of PLS model M43.....	112
Figure IV- 29 Calibration and validation of PLS model M44.....	112
Figure IV- 30 Calibration and validation of PLS model M34-2 .....	112
Figure IV- 31 Calibration and validation of PLS model M35-2 .....	113
Figure IV- 32 Calibration and validation of PLS model M36-2 .....	113
Figure IV- 33 Calibration and validation of PLS model M37-2 .....	113
Figure IV- 34 Calibration and validation of PLS model M38-2 .....	114
Figure IV- 35 Calibration and validation of PLS model M39-2 .....	114
Figure IV- 36 Calibration and validation of PLS model M40-2 .....	114
Figure V- 1 FT-IR spectra of of gelatin capsule shell formulation 1; non colored (a) and colored (b) containing no ibuprofen at different time points .....	115
Figure V- 2 FT-IR spectra of of gelatin capsule shell formulation 3; non colored (a) and colored (b) containing no ibuprofen at different time points.....	116

Figure V- 3 FT-IR spectra of of gelatin capsule shell formulation 4; non colored (a) and colored (b) containing no ibuprofen at different time points.....	117
Figure V- 4 FT-IR spectra of of gelatin capsule shell formulation 5; non colored (a) and colored (b) containing no ibuprofen at different time points.....	118
Figure V- 5 FT-IR spectra of of gelatin capsule shell formulation 6; non colored (a) and colored (b) containing no ibuprofen at different time points.....	119
Figure V- 6 FT-IR spectra of of gelatin capsule shell formulation 7; non colored (a) and colored (b) containing no ibuprofen at different time points.....	120
Figure V- 7 FT-IR spectra of of gelatin capsule shell formulation 8; non colored (a) and colored (b) containing no ibuprofen at different time points.....	121
Figure V- 8 FT-IR spectra of of gelatin capsule shell formulation 9; non colored (a) and colored (b) containing no ibuprofen at different time points.....	122
Figure V- 9 FT-IR spectra of gelatin capsule shell of colored formulation 1 (a) and colored formulation 3 (b) containing ibuprofen at different time points.....	123
Figure V- 10 FT-IR spectra of gelatin capsule shell of colored formulation 4 (a) and colored formulation 5 (b) containing ibuprofen at different time points.....	124
Figure V- 11 FT-IR spectra of gelatin capsule shell of colored formulation 6 (a) and colored formulation 7 (b) containing ibuprofen at different time points.....	125
Figure V- 12 FT-IR spectra of gelatin capsule shell of colored formulation 8 (a) and colored formulation 9 (b) containing ibuprofen at different time points.....	126
Figure VI- 1 Dissolution profiles of ibuprofen soft gelatin capsules for colored formulation 1 (a) and formulation 3 (b) at 1 (1D), 30 (30D) and 90 (90D) days	127
Figure VI- 2 Dissolution profiles of ibuprofen soft gelatin capsules for colored formulation 4 (a) and formulation 5 (b) at 1 (1D), 30 (30D) and 90 (90D) days.....	128
Figure VI- 3 Dissolution profiles of ibuprofen soft gelatin capsules for colored formulation 6 (a) and formulation 7 (b) at 1 (1D), 30 (30D) and 90 (90D) days .....	129

Figure VI- 4 Dissolution profiles of ibuprofen soft gelatin capsules for colored formulation 8 (a) and formulation 9 (b) at 1 (1D), 30 (30D) and 90 (90D) days ..... 130



## LIST OF ABBREVIATIONS

BHA	Butylated hydroxyanisole
BHT	Butylated hydroxytoluene
CSG	Colored soft gelatin capsule
FT-IR	Fourier transform infrared
GC-MS	Gas chromatography – mass spectrometry
h	hour
min	Minute
MSC	Multiplicative scatter correction
NIR	Near infrared
OSC	Orthogonal signal correction
PEG	Polyethylene glycol
PLS	Partial least square
PRESS	Prediction residual error sum of squares
RH	Relative humidity
RMSEC	Root mean square error of calibration
RMSEP	Root mean square error of prediction
SG	Non colored soft gelatin capsule
SNV	Standard normal variate
T <sub>g</sub>	Glass transition temperature
Vitamin E TPGS	D- $\alpha$ -Tocopheryl polyethylene glycol 1000 succinate
°C	Degree celsius

## CHAPTER I

### INTRODUCTION

Soft gelatin capsules have several advantages in pharmaceutical products such as protecting the encapsulated drugs from external environment, improving patients compliance, improving oral bioavailability of the low aqueous solubility compounds (1).

The soft gelatin capsule is composed of shell and fill materials. Commonly, gelatin is a main ingredient in the shell. Other ingredients in the shell are water and plasticizer, also may include color that needs for aesthetic and identification purposes. The fill material may be in a form of solution, suspension or emulsion with lipophilic or hydrophilic based vehicles. An appropriate fill formulation will allow an active ingredient to be absorbed better (2).

Physical and chemical quality attributes of soft gelatin capsules are usually of concern to formulation scientists. Major challenges are interactions between the fill and the shell material, as well as dynamic migration of chemicals including moisture between fill material, capsule shell, and the external atmosphere.

Generally, vehicle used in soft gelatin capsules may be classified into 2 types. The lipophilic vehicles such as soybean oil, corn oil are often used for dissolving oil soluble active ingredient. The hydrophilic vehicles such as PEGs, propylene glycol are used as solvent or co-solvent in the fill formulations of more polar active ingredients. In this case, PEGs of molecular weight not less than 400 are more desirable because relatively low molecular weights of PEGs are likely to diffuse into gelatin shell and act as plasticizer (3).

PEG of pharmaceutical grade may contain formaldehyde which is limited at a maximum of 30 ppm in European Pharmacopoeia 8.0. In addition, formaldehyde can be further formed by PEG autoxidation under stress condition or aging (4-6). Formaldehyde is an oxidizing agent which can affect the properties of the drug

products. It was proved to worsen stability of some drugs (7, 8) and induce crosslinking in gelatin capsules (9-11). It may also be involved in color fading of indigo carmine in coated tablets (12).

As for other solid dosage forms, color of soft gelatin capsules should be maintained during shelf life indicating acceptable quality. However, color fading of soft gelatin capsule can occur through migration of water soluble dye from the shell into hydrophilic vehicles. For the capsule containing PEGs as vehicle, it is also possible that during storage, aging of PEGs or autoxidation would produce formaldehyde resulting in color degradation by oxidation reaction.

Consequently, in the present study, the effects of formaldehyde occurred in PEG 600 on color fading and crosslinking of soft gelatin capsule shells were investigated. Moreover, possibility of inhibition of PEG 600 oxidation by a selected antioxidant was also studied.

#### **Objective of the study**

1. To investigate the effect of degradation product of PEG 600 on color fading and crosslinking in soft gelatin capsule shells.
2. To determine the amount of antioxidant that can inhibit oxidation of polyethylene glycol 600 in fill formulations of soft gelatin capsules.

## CHAPTER II

### LITERATURE REVIEW

#### 1. Soft gelatin capsules

Soft gelatin capsules are a single-unit solid dosage form that widely used in pharmaceutical industry because several advantages such as masking unpleasant odour and taste of drug substance, protecting the encapsulated drugs from light and external environment, improving patients compliance and providing high content uniformity of low-dose drugs. Moreover, fill materials can be developed as liquid and semi-solid formulations which can improve bioavailability and decrease variability of drug concentration in plasma through improved solubility and absorption. Soft gelatin capsules have two parts that must be considered in research and development, so called fill and shell.

#### 2. Fill compositions

Fill materials of soft gelatin capsules can be formulated as liquid or semi-solid, suspensions, solutions or emulsions. It should be compatible with capsule shells to accomplish physically stable capsule product. The fill materials have broadly categorized into two groups:

##### 1. Hydrophobic materials

This group of materials include free fatty acids (e.g., oleic acid), mineral oil, soybean oil and vegetable oil. The formulation may be classified as lipid based fill formulations.

##### 2. Hydrophilic materials

This group of materials include polyethylene glycols (PEGs), propylene glycol, polysorbate 80, poloxamers, glycerin, ethyl alcohol and water. PEGs have been widely used as fill materials in soft gelatin capsules. They can improve solubility of poorly soluble drugs and well miscible with water that sometimes required in formulation. Appropriate molecular weights of PEGs in fill formulation are 400 to 600.

Earlier studies showed that PEGs with difference molecular weight had plasticizing effect on gelatin film. Low molecular weight liquid PEGs such as 300 and PEG 400 could interact with gelatin more than higher molecular weight PEG such as 600 because of more polar groups (-OH) than can develop hydrogen bonds with gelatin (3). The lower molecular weight PEGs also showed more affinity to water and hygroscopicity (13). One of major problems of PEGs is that autoxidative reaction with air can produce degradation products which may deteriorate product quality (7, 14-16).

### **Autoxidation of polyethylene glycol**

Autoxidation is an oxidation reaction of substrate by molecular oxygen, or also called air-oxidation (17). Heat and light can expedite peroxides to become peroxy radicals that induce chain propagation (18). During manufacturing process of PEGs, hydrogen peroxide is often added as an initiator in polymerization and it cannot be removed absolutely during purification (19). The peroxide impurities can be further formed by autoxidative degradation of PEG, depending on aging and storage conditions (20).

Autoxidation in PEG occurs by reaction of  $O_2$  with PEG and then followed by three chain processes - initiation, propagation and termination. The initiation process is derived from cleavage of weak bond in PEG by electron transfer process producing free radical. Then the propagation process is started when the free radical reacts with molecular oxygen providing peroxy radical. In the final process, termination occurs through radical combination reaction which leads to producing aldehyde products (21).

Johnson and Taylor reported that peroxides as intermediate impurities in autoxidation of PEG 400 solution could occur only when PEG was exposed to air. When the storage condition was  $80^\circ\text{C}$  in nitrogen atmosphere autoxidation did not occur (8). Another study was performed with PEG 6000 at  $80^\circ\text{C}$  in the air and vacuum atmosphere. The results showed that no degradation of PEG 6000 in vacuum atmosphere while in the air PEG degradation occurred and formic esters were formed



(22). This therefore indicated that oxygen in the air was needed in autoxidation of PEG.

It was also possible that during manufacturing process of some dosage forms such as, factors i.e. high temperature and agitation could increase the rate of peroxide formation (23).

Formaldehyde has been reported as a major degradation product of PEG oxidation (5-7). This substance can provide an undesirable effect in the product formulated with PEG. For example, formaldehyde in soft gelatin capsule induced gelatin crosslinking that led to a decrease in dissolution of the drug products (24).

Hom et al. studied about oxygen permeability into the fill material of soft gelatin capsule. They found that oxygen permeability was increased with increasing relative humidity of storage conditions. Moreover, when the plasticizer such as glycerin in the capsule shell was increased oxygen permeability into the film was increased (25).

The effect of stress conditions applied to PEG was studied by Li et al. PEG 400 and PEG 600 was filled into headspace vials which were then kept in a 40°C and 75%RH chamber for one night. The formaldehyde amounts determined by GC-MS were 102.5 and 65.2 ppm in PEG 400 and PEG 600, respectively (26).

Hemenway et al. have studied about impurities formation in pure PEG 400 and 50% PEG 400 solution in water, stored in glass vials, at 40°C and 50°C. Aldehyde and organic acid impurities in the samples were determined by high performance liquid chromatography. The result showed that aqueous PEG 400 contained more amounts of formaldehyde and formic acid than pure PEG 400 (6).

Frontini and Mielck investigated decomposition of PEG 6000 by oxidative reaction and found that water was needed for formation of ethylene glycol which was further oxidized to be formaldehyde (5). However, McGinity and Hill reported that 5-10% of water in formulation could prevent further peroxide production (27) and hence formaldehyde formation in PEG, but could not reduce initially existed peroxides.

Another study showed that formaldehyde initially presented in 40% PEG 400 solution containing O<sup>6</sup>-benzylguanine in sealed glass ampules mainly caused degradation of the drug (7).

Hemenway et al. studied about effects of adding some antioxidants into 50% PEG 400 solution in water placed in sealed headspace glass vials stored at 40°C for 90 days. The result showed that 0.02% butylated hydroxyanisole (BHA), 0.02% butylated hydroxytoluene (BHT), 0.5% ascorbic acid and 10% Vitamin E TPGS could inhibit formation of formaldehyde in PEG 400 (6).

Puz et al. compared antioxidant activity of BHT, ferrous sulfate, and ethylene diamine tetra acetic acid (EDTA) in coated controlled release tablet having PEG 3350 in the coating material. The result showed that BHT, a free radical scavenger antioxidant was the most effective to inhibit sulfoxide formation through PEG autoxidation (28).

Byun et al. investigated an antioxidant activity of  $\alpha$ -tocopherol and BHT in polylactic acid (PLA) films with or without PEG 400. The result showed that pure PLA film, PLA film with BHT and PEG 400, and PLA film with BHT, PEG 400 and  $\alpha$ -tocopherol had 2,2-diphenyl-1-picrylhydrazyl (DPPH) radical scavenging activity of 0, 14 and 90% respectively. This meant  $\alpha$ -tocopherol might have high activity in radical scavenger activity (29).

Stein and Bindra studied effect of adding water into PEG based fill formulation with and without BHA as antioxidant in hard gelatin capsules. The formulation with water 5%w/w and BHA exhibited the best dissolution and no pellicle formation was observed (30).

### 3. Shell compositions

Generally, shell formulation of soft gelatin capsule consists of film-forming agent, such as gelatin, water and plasticizer. The formulation may have other additives such as colors, flavors, opacifiers and preservatives. The type and amount of additives, including plasticizers, can affect on shell properties. For example, the

plasticizer helps to improve flexibility of gelatin film. The common plasticizers used are such as glycerol, sorbitol and propylene glycol. Water remained in the shell after drying stage can also act as plasticizer because it can reduce glass transition temperature ( $T_g$ ) of anhydrous gelatin (31). However, upon storage water may further evaporate resulting in brittleness of gelatin shell. Low-volatile substances such as glycerol are more effective plasticizers. Plasticizing effectiveness of glycerol results from its greater hygroscopicity than other polyols (32). Furthermore, glycerol has lower  $T_g$  ( $-93^\circ\text{C}$ ) when compared with sorbitol ( $-3^\circ\text{C}$ ) (32). When glycerol was used as plasticizer in soft gelatin capsule, oxygen permeability was increased under high humidity (25).

Properties of gelatin shells contributes to the quality of product. High temperature and humidity can cause physicochemical properties of soft gelatin capsule shell changed. One of critical problems of soft gelatin capsule is gelatin crosslinking due to inappropriate storage conditions and chemicals (9, 10, 33). Hakata et al. reported disintegration time of soft gelatin capsule was remarkably delayed when stored at  $40^\circ\text{C}$  or higher (34).

Furthermore, color fading of soft gelatin shell is also a quality problem under concern as it can indicate product quality and stability. As with other dosage forms, coloring agents are mainly used in soft gelatin capsules for attractive appearance and identification. Color fading may be caused by color migration from the shell into the fill materials which contain favorable vehicle, and/or due to color instability.

#### **4. Color stability**

In pharmaceutical products, dye and lake that can be used must be certified as FD&C and D&C grades. The chemical structure of dye molecule consists of two parts including (1) chromophore which is the main skeleton indicating the light stability of a dye and (2) auxochromes which are substituent groups (35). Each coloring agent has different stability when exposed to chemicals and environment as shown in Table 2-1.

Table 2- 1 Stability properties of some coloring agents (Modified from Handbook of pharmaceutical excipient (36))

Color	FD&C grade	Oxidizing agents	Reducing agents	Heat	Light	Acid	Base
Brilliant blue FCF	FD&C Blue no.1	Moderate	Poor	Good	Moderate	Very good	Moderate
Indigo carmine	FD&C Blue no.2	Poor	Good	Good	Very poor	Moderate	Poor
Fast green FCF	FD&C Green no.3	Poor	Very poor	Good	Fair	Good	Poor
Erythrosine	FD&C Red no.3	Fair	Very poor	Good	Poor	Insoluble	Good
Allura red AC	FD&C Red no.40	Fair	Fair	Good	Moderate	Good	Moderate
Tartrazine	FD&C Yellow no.5	Fair	Fair	Good	Good	Good	Moderate
Sunset yellow	FD&C Yellow no.6	Fair	Fair	Good	Moderate	Good	Moderate

There were many published articles that reported about stability of certain dyes.

Nalliah studied about food dyes, i.e. FD&C blue no.1, FD&C red no.40 and FD&C yellow no.5 oxidized by oxidizing oxone, using iron (II) sulfate as a catalyst. Highly oxidative radicals,  $SO_4^{\cdot-}$  could decolorize these dyes (37).

Garrett and Carper could predict thermal stability of coloring agents such as FD&C yellow no. 6 and D&C red no. 33 in a liquid preparation of sulfa drugs at various temperatures. The colors were mixed in liquid multisulfa preparation. The results showed that high temperature could increase a decrease rate of color absorbance (38).

Photosensitivity of certified dyes in tablet was studied under normal and exaggerated light, with or without light protector (39-46). The results indicated that high intensity of light increased color fading rate and amber glass bottle could

prevent color fading better than other colored glasses (georgia green, emerald green, champagne green). Moreover, ultraviolet absorber (2,4-dihydroxybenzophenone) could prevent FD&C blue no.1 or brilliant blue from fading.

The effects of pH and temperature on some dyes, including FD&C red no. 4, blue no. 1, and yellow no. 5 were also studied. The color of the tablet surface and total dye contents were measured at different temperatures and pH. FD&C red no.4 was the most stable dye under all studied conditions. FD&C yellow no.5 showed poor stability in pH 5 and 7 buffered tablets at high temperatures of 60 °C and 80 °C; while FD&C blue no.1 was more stable. However, at 25 °C, all dyes were stable under the studied pH levels (47).

Brownley and Lachman studied the stability of FD&C red no. 4, FD&C yellow no. 5, FD&C green no. 3, and FD&C blue no. 1 and FD&C blue no. 2 with lactose in pH 6.6 to 6.8 buffered solution. Only FD&C blue no. 2 (or indigo carmine) was unstable under light. The degradation mechanism of FD&C blue no. 2 was explained by reduction to a semiquinone which was followed by oxidation (48). Some materials used as pharmaceutical excipients such as dextrose, lactose and sucrose in solutions also increased fading rate of FD&C blue no. 2, while mannitol and sorbitol did not (49).

Color instability has also been reported in several films with PEG. Teckoe et al. investigated color stability of coated tablets with and without PEG in formulation and concluded that formaldehyde appearing in PEG may lead to color fading in coated tablets (12). This result was confirmed by Brown et al. who suggested that fading of indigo carmine in film coated tablets was increased when PEG was used as plasticizer in coating formulation (50).

Brilliant blue FCF, categorized in triarylmethane dyes is one of widely used synthetic dyes in pharmaceutical industry. The structure shown in Figure 2-1 is based on a central triphenylmethane structure which is substituted with amine derivatives, with or without sulfonic acid groups. It is anionic with the disodium salt of sulfonic acid. From Table 2-1, it is moderately stable when there is an oxidizing agent,

suggesting that when it interacts with an oxidizing agent, oxidation occurs and hence the color is faded.

Gosetti et al. had investigated degradation pathway of brilliant blue FCF which was oxidized by potassium persulfate, under sunlight irradiation. LC-MS was used to determine intermediates obtained from degradation of brilliant blue dye. There were two intermediates, I or II, occurring during degradation depending on molar dye/persulfate ratio. At the 1/1 and 1/10 molar ratios of dye/persulfate, the intermediate I (Figure 2-2(a)) could give change to solution color, observed by eyes, from brilliant blue to dark blue color. This was because of hydroxylation of the dye molecule, electrophilic addition reaction of hydroxyl group on aromatic rings. Five aromatic rings, or the chromophore, of the blue color were still present. At 1/100 molar dye/persulfate ratios, intermediate II (Figure 2-2(b)) was formed by loss of a methyl group of two  $-\text{SO}_2$  groups and of a fragment of molecule bound to the aminic group together with addition of  $-\text{OH}$  group to the central carbon atom. This resulted in loss of one aromatic ring and the color was faded (51).

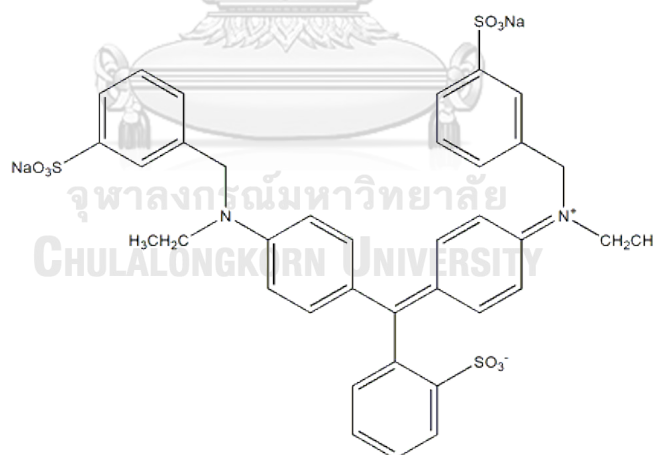


Figure 2- 1 Brilliant blue FCF structure (51)

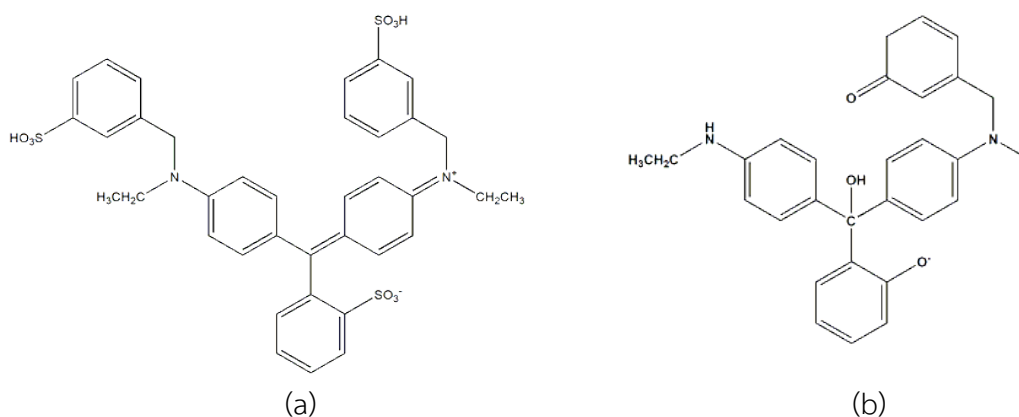


Figure 2- 2 Structure of intermediate I (a) and II (b) occurring during degradation of brilliant blue FCF due to oxidation by potassium persulfate (51)

Nadupalli et al. used spectrophotometer to investigate oxidation mechanism of the reaction between brilliant blue-R and hypochlorite. The experiment was carried out at 25 °C. After oxidation reaction occurred, three separated products as shown in Figure 2-3 (a,b,c) were identified by <sup>1</sup>H- and <sup>13</sup>C-NMR (52).

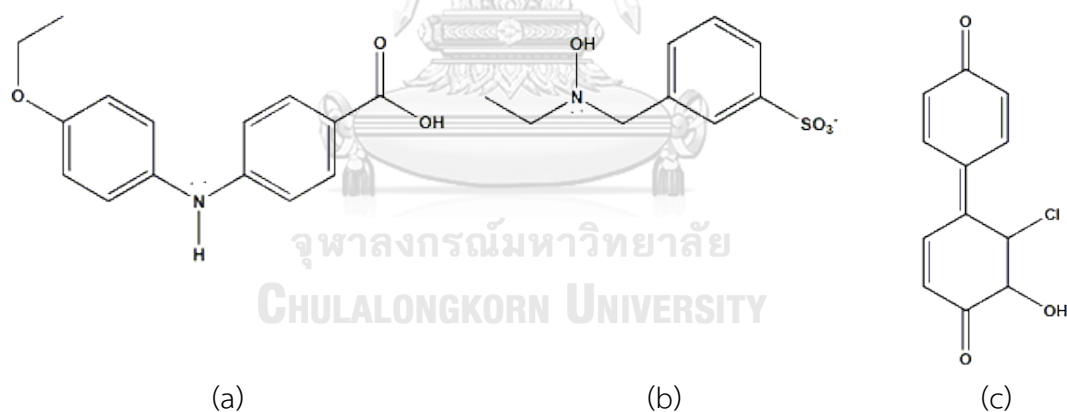


Figure 2- 3 Structure of oxidation products of brilliant blue-R : 4-(4-ethoxyphenylamino)benzoic acid (a), 3-[(ethyl-hydroxyamino)methyl]benzene sulfonic acid (b) and 6'-chloro-5'-hydroxybicyclohexylidene-2,5,2'-triene-4,4'-dione (c), (52)

PEGs have been widely used as vehicle in fill formulation of soft gelatin capsules. The reactive impurities and degradation product of PEG i.e. formic acid and

formaldehyde may cause oxidative degradation of color such as brilliant blue in the capsule shell.

However, as PEG is a hydrophilic vehicle which is miscible with water soluble dye, it may be also possible that color fading results from dye migration from the capsule shell in to the fill containing PEG. There has been reported that water soluble dyes such as FD&C red no. 3, FD&C blue no.1, FD&C violet no.1, could form hydrogen bonding with type A and B gelatin in solid solution at 1:10 to 1:5 dye gelatin ratios, resulting in a slow release of dye in distilled water at 27°C (53).

#### **Determination of color stability and color fading**

The stability of coloring agents is one of quality control in soft gelatin capsule formulation because of their sensitivity to environment and chemicals. As mentioned above, color degradation could lead to color fading (51, 52, 54). The change in color can be measured by several techniques.

Color measurement by spectrophotometry technique is based on full spectrum color measurement and producing precise data from spectral analysis of samples' reflectance, absorbance and transmittance.

Yasri et al. used UV-vis spectrophotometer to measure absorbance of violet colored product developed by telomerization of formaldehyde and tryptamine at a maximum wavelength of 558 nm (55).

Liang et al. also applied UV-vis spectrophotometer to analyze absorption spectra of yellow colored solution obtained from reaction between persulfate and iodide and the absorbance of color was determined at 352 nm (56).

Turi et al. used fadeometer equipped with spectrophotometer to determine fading and predict stability of lake colors, including aluminum lakes of FD&C yellow no.5, FD&C blue no.1, FD&C red no.2, FD&C red no.3, FD&C red no.5 and FD&C yellow no.6, in compressed and sugar-coat tablets that exposed to light (57), and to predict light stability of dye colors, including FD&C blue no. 2, FD&C yellow no. 5, and FD&C yellow no. 6, in solutions with and without excipient such as lactose, sucrose, PEG 6000 (58).



Urbanyi et al. used reflectance attached Beckman DU spectrophotometer to observe stability of colors, including FD&C violet no.1, FD&C blue no.1, FD&C red no.1, FD&C green no.3, D&C yellow no.10, in tablets. The method could measure the reflected light from upper or lower surface of the tablet (59).

However, due to full spectrum measurement, the measured data from spectrophotometry technique is beyond the data that can be observed by human eyes.

Alternatively, colorimetry which is a similar technique to spectrophotometry, but with reducing color data that correlate to human color perception, is more suitable for determination of color difference and hence it can be used for routine color quality control of final product and during manufacturing process.

Basically, in colorimetry technique, color may be represented in three characteristics of light: hue, saturation, and brightness. Commission de International de l'Eclairage (CIE) has defined the system of color measurement on three main stimuli: red (700 nm), green (546.1 nm), and blue (435.8 nm). Human eyes can see all colors in combination of these stimuli, called tristimulus values, X, Y, Z respectively.

However, tristimulus system is not simply understood in term of object's color. The theory of opponent color, so called 3-dimensional rectangular L, a, b color space (CIELAB) were developed (60). As shown in Figure 2-4 which is L, a, b rectangular color space, "lightness" is indicated by L-axis where the value of 0 signifies black and the value of 100 is white. The colors of "red and green" are indicated by a-axis where the positive values are red and the negative values are green. The colors of "yellow and blue" are indicated by b-axis where the positive values are yellow and the negative values are blue (60).

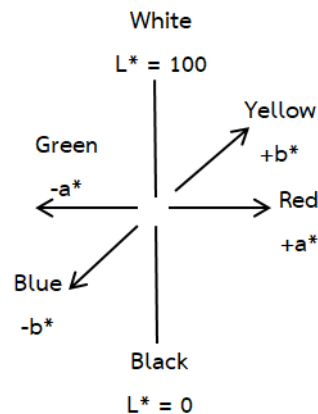


Figure 2- 4 Diagram representing the CIELAB color space

The delta values in this color scale, i.e. delta L\*, delta a\* and delta b\*, specify difference between standard and sample in L\*, a\* and b\*. The total color difference, delta E\* can be calculated by following formula.

$$\Delta E^* = [(\Delta L^*)^2 + (\Delta a^*)^2 + (\Delta b^*)^2]^{1/2}$$

$$\Delta L^* = L^* \text{ sample} - L^* \text{ standard}$$

$$\Delta a^* = a^* \text{ sample} - a^* \text{ standard}$$

$$\Delta b^* = b^* \text{ sample} - b^* \text{ standard}$$

Tolerances may be set for each delta value to indicate whether difference between the standard and samples is too much, resulting in delta values are out of tolerances.  $\Delta E^*$  is a single value, so it does not indicate which values are out of tolerances.

จุฬาลงกรณ์มหาวิทยาลัย  
CHULALONGKORN UNIVERSITY

## 5. Crosslinking in gelatin capsule shell

There are many factors such as external environment, humidity, temperature or chemicals such as aldehydes that can cause gelatin crosslinking, so control of these factors during manufacturing process and storage of gelatin capsule shell is needed.

Hakata et al. studied the effect of storage temperature, i.e. 25 °C, 40 °C and 60 °C on physicochemical properties of soft gelatin capsule shell. Fifty capsules were stored in an amber glass bottle with stopper. It was found that when the

capsules were stored at 40°C for six months, disintegration time of capsules were prolonged similar to that of capsule which was treated with 1% formaldehyde at 20°C (34).

Dey et al. investigated effect of accelerated storage conditions, 40°C and 75%RH, of hard gelatin capsule, a decrease of etodolac dissolution was observed after 20 weeks, while this was not observed when the capsules were stored at 25°C (61).

Regarding to chemicals, formaldehyde is the most frequently reported chemical component that has been involved with gelatin crosslinking. Formaldehyde can be found as an impurity or degradation product in many pharmaceutical excipients such as polysorbate 80 (62, 63), polyethylene glycol (22, 64, 65) which may be used in formulation in gelatin capsules. It was reported as volatile agent found in soft gelatin capsules (66).

Dissolution problem of capsules due to formaldehyde induced gelatin crosslinking was investigated by many researchers (10, 24, 63, 67). Ofner et al. determined the amounts of formaldehyde that could result in crosslinking of hard gelatin capsule. It was found that hard gelatin capsules with 120 ppm of formaldehyde mixed with lactose showed slower dissolution, while hard gelatin capsule with 20 ppm of formaldehyde had the same gelatin dissolution profile compared with that of the control capsules (68).

Albert et al. also used  $^{13}\text{C}$  NMR spectroscopy to investigate crosslinking reaction of gelatin with formaldehyde solution. The result confirmed that the reaction was initiated by formation of lysine-methylol (lysine- $\text{CH}_2\text{OH}$ ) which was followed by arginine-methylol (arginine- $\text{CH}_2\text{OH}$ ) formation and subsequently led to arginine-lysine crosslinking (69) and arginine-arginine crosslinking (70).

Gelatin cross-linked by formaldehyde could also be investigated by Fourier transform infrared (FTIR) spectroscopy. The principle component regression (PCR) was able to discriminate the spectra of crosslinked gelatin as a function of time. The first three PCs, lysine-methylol as PC#3 (7%), followed by arginine-methylol as PC#2

(14%) and by the arginine-lysine as PC#1 (68%) (71) agreed with the result from  $^{13}\text{C}$  NMR (69).

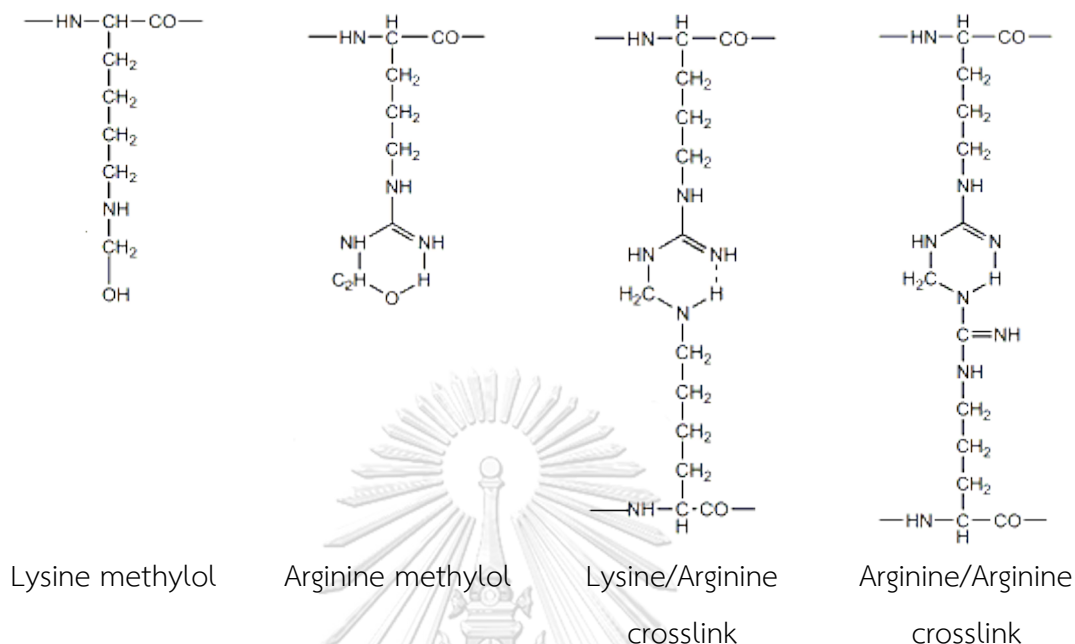


Figure 2- 5 Structure of the main methylols and crosslinks formed in the hardening reaction of gelatin and formaldehyde(70).

Bottom et al. investigated the effect of formaldehyde levels in soft gelatin capsule shell. It was shown that 80 ppm of formaldehyde in soft gelatin capsules led to a reduction of dissolution compared with the capsules having 20 ppm formaldehyde (24).

Hakata et al. spiked 0-3% formaldehyde into soft gelatin capsules to induce different degrees of crosslinking. Disintegration time was significantly increased when the capsules were stored at 40°C. Swelling was decreased, while gel strength of capsule shell was increased when formaldehyde content was increased (72).

Tengroth et al. studied crosslinking in soft gelatin capsule by placing the capsules in formaldehyde atmosphere for 6 h. Methylol peak was detected by FTIR spectroscopy at 1030 and 1080  $\text{cm}^{-1}$  due to addition of formaldehyde to the primary amines of lysine and arginine which led to crosslinking of gelatin (73). These results were confirmed by Salsa et al, who used FT-IR spectroscopy to study crosslinking of gelatin dispersed in a potassium bromide pellet on which formaldehyde was

sprayed. High intensity of  $1039\text{ cm}^{-1}$  peak, identified as C-O stretching, appeared at time 0 min. However, after 10 min, the intensity of this peak was decreased, while the intensity of peak at  $1,080\text{ cm}^{-1}$  was increased (71). Tengroth et al. also observed that little downward shifted (about  $2.5\text{ cm}^{-1}$ ) of amide II peak that consisted of C-N stretching and N-H bending was shown for cross-linked capsule, compared with untreated capsules. However, this downward shift may independent on aldehyde used but it could be attributed to H-bond breaking due to loss of water observed in hardened capsules (73).

Gold et al investigated crosslinking in soft gelatin capsules using near-infrared spectroscopy. Different levels of formaldehyde were added into PEG 400 filled in the soft gelatin capsules. The results showed that saturated crosslinking of soft gelatin shell was found with 185 ppm of formaldehyde (74).

Gelatin crosslinking usually provides retardation of *in vitro* dissolution because of formation of pellicle which is poorly soluble in medium used in *in vitro* testing. However, this problem does not affect the bioavailability of drug because enzyme can break down insoluble pellicle (61, 75).

## 6. Near-infrared (NIR) spectroscopy

Nowadays, NIR spectroscopy is one of process analytical technology that has been used in both qualitative and quantitative analysis in pharmaceutical industry for raw material control, product quality control, and process monitoring. It has many advantages. For examples, it is a nondestructive technique and does not need to prepare sample before analysis; it can be used in real time analysis. Thus, time taken for quality control is reduced and use of organic solvent can be avoided. However, it still has limited use because disadvantages such as strong absorbance of water can interfere other compounds.

### 6.1 Source and type of absorption band in NIR

NIR region is in wavenumber of 780-2526 nm or wavelength  $12820\text{-}3959\text{ cm}^{-1}$ . Absorption band in NIR region caused by fundamental vibration of functional group –

CH, -NH, -OH, -SH that are related to overtones and combinations. Overtone region, in the wavenumber 780-2000 nm, is attributed to asymmetry in multilevel energy transitions in molecule occurring at multiples of fundamental vibrational frequency, called anharmonic oscillator. Combination vibration, in wavenumber 1900-2500 nm, is caused by vibrational interactions in polyatomic molecules. The frequencies of this vibration are the sum of the interacting frequencies. The characteristics of NIR absorption band are broad, overlap and weak intensity when compared with mid-infrared (76).

Sample characteristics need to be considered when choosing the optimal measurement mode of NIR. For example, transmittance mode is usually used for transparent samples, while modes of diffuse transmittance or diffuse reflectance which relies on individual scattering and absorption is used for unclear liquid, semi-solid and solid samples. Sample preparation is a very important step, especially for solid sample that have large variation due to scattering effect caused by variation in packing density of powder and/or particle size. While, for liquid sample, the scattering effect was hardly observed (77). In addition, moisture in solid samples should be removed and temperature of liquid samples should be controlled before NIR measurement.

## 6.2 Quantitative analysis by NIR

NIR spectra are broad and overlapped. For quantitative analysis of material, NIR has to be calibrated with a reference method.

Many physical and chemical characters of compounds can cause the deviation from the linear relationship between NIR spectra and concentrations of interested compound. Pretreatment of NIR raw spectra may be a necessary step to reduce systematic variation of the spectra by diminishing or standardizing impact of interfering parameters, such as noise, light scattering from physical variation in samples, path length variations, in order to generate linear correlation between light

absorption and concentration of interested compound that complies to Beer's law (77).

Two common techniques used in spectra pretreatment are (1) scatter correction method including multiplicative scatter correction (MSC) and standard normal variate (SNV)] and (2) spectral derivative including Norris-Williams derivation and Savitzky-Golay derivation Both derivation techniques require smoothing the NIR spectra before calculating the derivative values.

(1) Multiplicative scatter correction (MSC) and standard normal variate (SNV)

The principle of these methods is removing non-linearity in the spectra caused by scattering effect of particles found in the samples. The calculation is based on the MSC and SNV equations:

$$\text{MSC equation} \quad z_i = (x_i - a)/b$$

While,  $x_i$  = raw NIR spectra

$z_i$  = NIR spectra after pretreatment

$a$  = intercept

$b$  = slope of least square regression of value  $x_1, x_2, \dots, x_p$  with reference spectra  $r_1, r_2, \dots, r_p$

$$\text{SNV equation} \quad z_i = (x_i - m)/s$$

While  $x_i$  = raw NIR spectra

$z_i$  = NIR spectra after pretreatment

$m$  = mean

$s$  = standard deviation of the value  $x_i$

The main challenge of MSC is to determine suitable reference spectrum. Generally, the reference spectrum is average of spectra in calibration set (78).

SNV is different from MSC in that the reference spectrum is not necessary. Each spectrum is processed on its own. Consequently, SNV does not consist of a

least square fitting in their factor assessment. However, the results from SNV and MSC are the same in many applications.

## (2) Spectral derivative

This technique can be used to remove the scattering effect produced by diffuse reflectance and to decrease baseline shift, overlapping peaks and other negative effects on the signal to noise ratio (79). This technique is worthy and most frequently used in pretreatment. It can enhance resolution of NIR spectra when increasing derivative order, but reduce the strength of spectra and signal to noise ratio. Consequently, optimal derivative order is important in this technique. Commonly used methods are such as Savitzky-Golay derivation and Norris-Williams derivation (or gap derivation). Derivation can be done as first, second or higher derivative order. Mostly, first and second derivative orders are applied.

First-order derivative is the rate of change of absorption spectrum regarding wavelength. First-order derivative spectral passes zero at the same wavelength as maximum absorbance ( $\lambda_{\max}$ ) of the absorption spectrum. It starts and finishes at zero. Second-order derivative band, the lowest point is the same wavelength as a zero order band's maximum. When higher orders of derivatives are used, the signal-to-noise ratio decreases. In addition, smoothing may be used to improve the signal-to-noise ratio of spectrum (80).

Principal component regression (PCR) and partial least-squares (PLS) regression are widely used in multivariate regression methods in quantitative NIR analysis. Limitation of PCR is that calculation process uses only effect of variation of independent variables, while PLS regression combines effect of dependent and independent variables to generate calibration model.

The number of samples should be adequate to provide spectra for generating a calibration model with acceptable performance in prediction. Two sets of samples, i.e. calibration set and test set (or internal validation set), are required to generate and verify the calibration model, respectively. Root mean square error of calibration (RMSEC), root mean square error of prediction (RMSEP), and the regression



coefficient ( $R^2$ ) are calculated and used for choosing of a suitable calibration model (81). RMSEC and RMSEP indicate the performance of NIR model. Generally, the closer values of RMSEC and RMSEP to zero, the better model. Prediction residual error sum of squares (PRESS) and root mean square error of cross validation (RMSECV) are used to determine the optimum number of factors. Usually, PRESS is plotted as a function of the number of PLS factors. When the PRESS value reaches minimum, its corresponding PLS factors is selected as the optimum one for a PLS quantitative model (82).

When the model is chosen, accuracy and precision of NIR model should be compared with the reference method. This can be done by using the external validation set. This sample set has to be prepared and the concentration of analyte is determined by both NIR and the reference method. The deviation of the predicted results from the results of reference method is then calculated.

The calibration model can be constructed with full range of spectra. However, due to broaden and overlapped spectra of NIR, specific wavelength or wavenumber ranges may be chosen to generate the appropriate calibration model rather than full range.

### 6.3 Determination of water in NIR

NIR is a common method used for determination of water in various samples because of the strength and unique combination band of water at 1940 nm (83).

Cho et al. used NIR spectroscopy to determine water content in ethanol. The calibration set were prepared by varying water concentrations from 1-19% in the total sample number of fifteen. For validation set, the samples were prepared with water concentration at 3%, 5% and 7%. All spectra were collected at room temperature. Water band at 1450 nm was noticeably observed with increasing water concentrations. The 1120-1730 nm range was therefore used for construction of calibration model. Partial Least Squares (PLS) technique was chosen to construct the

calibration model with second derivative spectra. The predicted value agreed with the result from the reference method with standard deviation of 0.15-0.19% (84).

Zhou et al. used NIR spectroscopy to determine moisture in a drug substance, using Karl Fischer titration as reference method. The hygroscopic drug substance consisted of 0.5-11.4 %w/w water content. A spectral range of 1350-1500 nm and 1850-1936 nm were chosen to build the calibration model. Total spectra of 129 resulted from 43 samples were pretreated and divided into a calibration set of 90 spectra and a test set of 39 spectra. The result showed that first derivative of spectra in the region of 1850-1936 nm offered the best calibration model with standard errors of prediction (SEP) 0.11 %w/w (85).

Mantanus et al. used NIR spectroscopy to determine 1-8% moisture content in pellets using thermogravimetric balance as reference method. A region in wavelength of 6102-4247  $\text{cm}^{-1}$  was chosen to build the calibration model. Pre-treatment of raw spectra by multiplicative scatter correction (MSC) was the most suitable. RMSEC and RMSEP was reported as 0.163% and 0.167% respectively (86).

## 7. Model drug

One advantage of soft gelatin capsules is improving solubility of poorly soluble drugs through formulating in liquid form. Many of the Biopharmaceutics Classification System (BCS) class II drugs that have low solubility and high permeability have been formulated in this dosage form. Ibuprofen classified as BCS class II drug was chosen as model drug in this study. The structure of this drug is shown in Figure 2-6. It has a carboxylic group in molecule and pKa is 4.5-4.6 (87).

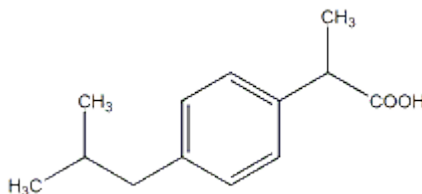


Figure 2- 6 Structure of ibuprofen

Patel et al. investigated soft gelatin capsules of carboxylic drugs which had PEG 400 and PEG 600 as vehicles. The results showed that factors affecting decomposition of the drugs included hydroxyl group content of the vehicles, water content, alkali level and drug concentrations in the formulations. It was postulated that drug stability in the formulations could be improved by using ionized form of the drug, decreasing hydroxyl group content of vehicle and increasing water in the formulations (88).



### CHAPTER III

## MATERIALS AND METHOD

#### Materials

Absolute ethanol (American Chemical Society grade, Merck KGaA., Darmstadt, Germany)

Brilliant blue FCF dye or FD&C blue no.1 (Sensient Technologies (Thailand) Co., Ltd., Bangkok, Thailand)

D- $\alpha$ -tocopherol polyethylene glycol 1000 succinate (Sigma-Aldrich., Saint Louis, USA)  
Deionized water

Formaldehyde 37% solution (Ajax Finechem Pty., Ltd., Scoresby, Australia)

Glycerine USP (99.5%, S. Tong Chemicals Co., Ltd., Nonthaburi, Thailand)

Ibuprofen (Albemarle Corporation, South Carolina, U.S.A.)

Magnesium chloride ( $MgCl_2$ , Analytical reagent, Ajax Finechem Pty. Ltd., New South Wales, Australia)

Pharmaceutical gelatin type A, bloom strength 180 (Cartino gelatin Co., Ltd., Samutprakarn, Thailand)

Polyethylene glycol 600 (Merck KGaA., Darmstadt, Germany)

Potassium dihydrogen orthophosphate ( $KH_2PO_4$ , Analytical reagent, Ajax Finechem Pty. Ltd., New South Wales, Australia)

P-toluenesulfonic acid (Carlo Erba Reagents SAS., Val de Reuil, France)

Sodium chloride ( $NaCl$ , Analytical reagent, Ajax Finechem Pty. Ltd., New South Wales, Australia)

Sodium hydroxide pellets (American Chemical Society grade, Carlo Erba Reagent SpA, Rodano, Milan, Italy)

## Equipment

Analytical balance (A200S, Sartorius, Goettingen, Germany)

Amber glass bottle 100 ml (Tan Soon Huat product Co., Ltd., Bangkok, Thailand)

Clear glass vials 20 ml with PTFE/white silicone septa (Ligand Scientific Co., Ltd., Nonthaburi, Thailand)

Desiccator

Digital caliper (150 mm/0.01 mm, China)

Dissolution apparatus II (VK7000, VanKel, New York City, USA)

Fourier transform infrared spectrometer (Nicolet iS10, Thermo Scientific, Wisconsin, USA)

Hot plate (EGO, Oberderdingen, Germany)

Moisture analyzer (HR83 Halogen Moisture Analyzer, Mettler Toledo, Columbus, USA)

Near infrared spectrometer (Antaris II, Thermo Scientific, Wisconsin, USA) and Antaris II analyzer series S (Thermo Fisher Scientific Inc., USA)

Texture analyzer (TA.XT plus, Stable Micro Systems, Ltd., Surrey, England)

UV spectrophotometer (UV-1800, Shimadzu, Tokyo, Japan)

Sonicator (S70H, Elmasonic, Frankfurt, Germany)

## Method

### 1. Preparation of soft gelatin capsule

#### 1.1 Fill formulation

The formulations were composed of polyethylene glycol (PEG) 600 and contained varied amounts of water and/or D- $\alpha$ -tocopherol. PEG 600 was chosen as a hydrophilic vehicle in this study because it shows lower hygroscopicity and hence reduced water migration (1), also it has less plasticizing effect for gelatin film, comparing with other liquid PEG such as PEG 400 (3).

Vitamin E TPGS as H-atom donor or free radical scavenger was chosen for antioxidant activity to inhibit oxidation of PEG 600 and amounts of free  $\alpha$ -tocopherol were 0.001 and 0.05% based on recommended range in Handbook of

Pharmaceutical Excipients (89). Furthermore, a certain amounts of water, i.e. 5% and 10% were added in PEG 600 because there was an evidence that 5%w/w of water could inhibit formaldehyde formation by prevent peroxide formation (27).

Total of nine liquid-filled formulations were designed, as tabulated in Table 3-1.

Table 3- 1 Compositions of fill formulations in soft gelatin capsules

Formulation	PEG 600	Water	D- $\alpha$ -tocopherol
1	100	-	-
2	90	10	-
3	95	5	-
4	100	-	0.001*
5	100	-	0.05*
6	90	10	0.001*
7	90	10	0.05*
8	95	5	0.001*
9	95	5	0.05*

\*Percentage based on the amount of PEG 600

Effects of water and d-alpha-tocopherol levels were evaluated through formulation 1, 2, 3, and formulation 1, 4 and 5, respectively. Combined effects of d-alpha-tocopherol at high and low water levels were investigated through formulation 2, 6, 7 and 3, 8, 9, respectively. Statistical analysis, if any, was carried out by Minitab 17.

Only for in vitro dissolution test, 150 mg ibuprofen was added and dissolved into the fill formulation.

## 1.2 Shell formulation

Gelatin shell was composed of gelatin, glycerin, brilliant blue and water. Brilliant blue was chosen as a model color in this study because it is more stable under light comparing with indigo carmine. Thus, the effect of light on color stability during storage was reduced. The shell formulation is shown in Table 3-2.

The gelatin shell was prepared by dispersing granular gelatin in the solution of glycerin and brilliant blue and left for 20 min before heating the mixture in a water bath at 60°C for 45 minutes. Subsequently, gelatin mass was sonicated for 2 hours to eliminate bubbles. The warm gelatin mass was then spread on 20 cm x 29 cm cooled glass plates to form two gelatin sheets. After that one gelatin sheet was laid on an in-house die plate as shown in Figure 3-1. Pouches on the gelatin sheet were formed with an aid of 2 bar compressed air. The pouches were sealed with another gelatin sheet to form empty capsules.

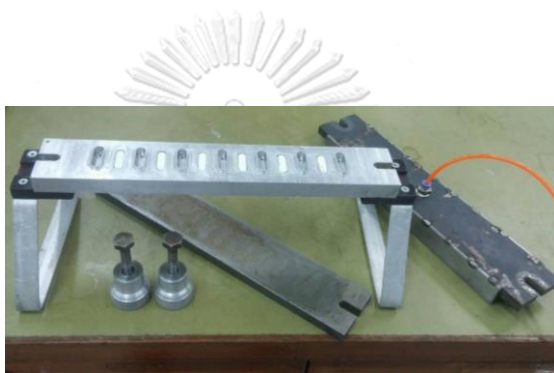


Figure 3 - 1 A set of die plate used for soft gelatin capsule preparation

Table 3- 2 Ingredient of capsule shell

Ingredient	Amount (g)
Gelatin	43
Deionized water	38
Glycerol	19
Brilliant blue	0.01
Total	100

The empty capsule was injected with the fill through the needle no.18. Each capsule contained 600 mg of fill material.

The filled capsules were dried in a glass desiccator containing saturated magnesium chloride solution to produce approximately 32% RH at an ambient

temperature for 12 h. Then, 20 capsules of each formulation were kept in 100 ml amber glass bottles and stored at 30°C and 75% relative humidity (RH). After storage time of 1, 7, 14, 30, 60 and 90 days, unless otherwise stated, the capsules were taken and characterized. The non-color capsules also prepared and tested for control.

In this study, the whole colored and non colored capsules which contained fill formulation numbers 1 to 9, were coded as CSG-1 to CSG-9, and SG-1 to SG-9, respectively.

## **2. Characterization of soft gelatin capsules**

### **2.1 Appearance**

The color fading of soft gelatin capsules were visually inspected under white background. Capsule swelling and leakage was observed.

### **2.2 Thickness**

Thickness of capsule shell was determined by digital vernier caliper. At each time point, three capsules of each formulation were cut and their shell thickness were measured on 4 positions. The average value was reported.

### **2.3 Hardness**

The hardness of soft gelatin capsules was measured by Texture Analyser TA.XT plus (Stable Micro Systems, Ltd., Surrey, England). The test was carried out using compression mode at 50% strain. The speed of probe was 0.5 mm/s. Three capsules were tested and average value was reported.

### **2.4 Moisture content**

The moisture content of soft gelatin capsules shells was gravimetrically determined at 105°C using moisture analyzer (HR83 Halogen Moisture Analyzer, Mettler Toledo, Columbus, USA). The soft capsule shell was cut and the liquid on the shell surface was removed using lint free wiper. Three capsule shells were analyzed and the average value was reported.



## 2.5 Determination of formaldehyde content and water in liquid fill

### 2.5.1 Gas chromatography/mass spectrometry (GC/MS)

Formaldehyde content in the fill formulations after storage time of 1, 14, 30 and 90 days was determined by GC/MS using Agilent model 7890B headspace autosampling unit. The method was modified from the previous work (90). Briefly, HP-INNOWAX, with 30 m length, 0.25 mm i.d. and 0.25  $\mu\text{m}$  film thickness was used as chromatography column. Helium was used as the carrier gas and flow rate was set constantly at 1.5 mL/min with an initial loop fill pressure of 15 psi and final loop fill pressure of 10 psi. Inlet temperature was 170 $^{\circ}\text{C}$  and a ratio of gas flow through the column and split line, i.e. split ratio, was 300:1. The standard solutions and samples were equilibrated in headspace at 60 $^{\circ}\text{C}$  for 15 min. The temperature of loop and transfer line was set at 120 $^{\circ}\text{C}$ . Mass selective detector performed at 20-150 amu was used for identification and selected ion monitoring (SIM) mode was used for quantitative analysis. The m/z values selected in SIM mode for diethoxymethane which is derivatized compound of formaldehyde were 31, 59, 103.

### Standard preparation

As formaldehyde content was determined through measuring diethoxymethane which is its derivitized compound. Acidified ethanol was prepared by 1% w/v of p-toluenesulfonic acid in ethanol ACS grade and used to derivitize formaldehyde to obtain diethoxymethane. Standard solutions of formaldehyde were prepared by diluting a 50  $\mu\text{g}/\text{ml}$  formaldehyde stock solution in acidified ethanol to 0.5, 1, 2, 5, 10, 20 and 25  $\mu\text{g}/\text{ml}$ . Five ml of the standard solution was filled into 20 ml vials and seal immediately with septum and paraffin film before use.

### Sample preparation

Fill material in the soft gelatin capsules were accurately weighed 500 mg into 20 ml clear glass vials. Five ml of acidified ethanol was added and the vial was sealed immediately with septum and paraffin film. After that, the solutions was sonicated for 1 min to completely dissolved the mixture.

#### 2.5.2 Near infrared spectroscopy (NIR)

NIR was used to determine formaldehyde and water contents in the fill. The results were analysed by Unscrambler X 10.4. The reference values were weights of formaldehyde and water. Calibration models were established as the following:

Standard solutions of 10-200 ppm formaldehyde in PEG 600 which contained a range of 10-200 mcg formaldehyde per gram of solution were diluted from a 1000 mcg/g formaldehyde stock solution.

Standard solutions of formaldehyde in PEG 600 with 5%w/w and 10%w/w water were prepared in the same way as the standard solutions with no added water.

Consequently, the total standard solutions of 767 were prepared and examined by NIR in transmittance mode in a range of 4000-10000  $\text{cm}^{-1}$  with a setting of 16 scans and 8  $\text{cm}^{-1}$  resolution via Thermo RESULT Integration program by Antaris II analyzer series S, Thermo Fisher Scientific Inc., USA.

The standard spectra were randomly divided by the software into 690 spectra and 77 spectra for calibration set and test set, respectively, and used for construction of calibration model.

However, prior to constructing the model, the NIR spectra of full region (4000-10000  $\text{cm}^{-1}$ ) were pretreated with different methods as follows:

	First step	Second step
1	No pretreatment	-
2	Multiplicative Scatter Correction, MSC	-
3	Standard Normal Variate, SNV	-
4	Multiplicative Scatter Correction, MSC	1 <sup>st</sup> derivative and Norris-Williams derivation
5		1 <sup>st</sup> derivative and Savitzky-Golay derivation
6		2 <sup>nd</sup> derivative and Norris-Williams derivation
7		2 <sup>nd</sup> derivative and Savitzky-Golay derivation
8	Standard Normal Variate, SNV	1 <sup>st</sup> derivative and Norris-Williams derivation
9		1 <sup>st</sup> derivative and Savitzky-Golay derivation
10		2 <sup>nd</sup> derivative and Norris-Williams derivation
11		2 <sup>nd</sup> derivative and Savitzky-Golay derivation

After pretreatment, PLS regression was used to generate the calibration model. The values of root mean square error of calibration (RMSEC) and root mean square error of prediction (RMSEP) were used for suggestion a predictive model. Normally, the small values of RMSEC and RMSEP suggest better model.

The calibration model was then validated by using external validation set of spectra which were obtained from the same concentrations of formaldehyde

solution in PEG 600 (10-200 mcg/g) with no water or with 5%w/w and 10%w/w of water. Each matrix contains 20 validation samples, so the total validation samples of 60 were prepared.

Aldehydes have carbonyl group in which C=O stretching shows strong absorption in the mid-infrared but relatively weak absorption in near-infrared. The possibility of analyzing formaldehyde in PEG 600, therefore, was very poor, especially when water which has strong absorption was present in the sample. In this case, the technique of orthogonal signal correction (OSC) was also applied to eliminate variation due to interfering strong absorbance data of water (OSC components) from spectra that is not related to interested absorbance of formaldehyde.

In addition, for more information, standard solutions of 0-50 %w/w water in PEG 600 were prepared. They were examined by NIR with the same setting and resulting spectra were used to generate calibration model for prediction of water content. The total standards spectra of 31 were randomly divided by the software into 25 spectra and 6 spectra for calibration set and test set, respectively. These spectra used for construction of calibration model. External validation set of 0-50%w/w water content were also prepared to validate the model.

Water region in NIR spectra was strongly observed at  $5000-5400\text{ cm}^{-1}$  and  $5900-7700\text{ cm}^{-1}$ . This region was chosen to generate water calibration model through partial least square regression. The same pretreatment techniques as above calibration model were tried to transform NIR spectra before generate the calibration model.

### **Sample preparation**

Three capsules of each formulation were cut and the fills were removed and placed in clear glass vials. The vial was immediately closed with plastic cap before examination by NIR.

## 2.6 Color Determination

### 2.6.1 Colorimeter

The soft capsule was cut and the liquid on the shell surface was removed using lint free wiper. The color of three capsule shells was measured with spectrophotometer (Ultrascan XE, Hunterlab, Virginia, USA). Average delta L, delta a, delta B and delta E values of shell color were compared with that of freshly prepared (within 1 day) shell which was used as reference.

### 2.6.2 UV-Visible spectrophotometer

Brilliant blue dye standard solutions in water of 0.5, 1, 2, 3 and 4 µg/ml were prepared and analysed at the maximum wavelength of 629 nm using UV-visible spectrophotometer.

To measure the color of both shell and liquid fill, each soft gelatin capsule was cut and the shell and liquid fill were weighed accurately. The shell was then dissolved in deionized water under sonication for 15 min and made to the volume of 25 ml. The liquid fill was dissolved in deionized water and then adjusted to the volume of 5 ml. The concentration of brilliant blue in the shell and the liquid fill were analyzed using UV-Visible spectrophotometer (UV-1800, Shimadzu, Tokyo, Japan) at the maximum wavelength of 629 nm. Three capsules were tested and average values of color content were reported.

## 2.7 *In vitro* dissolution test

Soft gelatin capsules containing 150 mg ibuprofen in different fill formulations were prepared and stored as previously described in section 1.1. After storage time of 1, 30 and 90 days, dissolution of three colored capsules in each formulation was studied using USP dissolution apparatus II, at a paddle speed of 50 rpm (VK7000, Vankel, New York City, USA). A dissolution medium was 900 ml of pH 7.2 phosphate buffer solution kept at 37°C. Ten mL of samples were taken at 10, 20, 30, 45 and 60 min from dissolution vessels and analyzed using UV

spectrophotometry at detection wavelength of 264 nm. The medium was replaced with ten mL fresh medium after each sampling.

### **2.8 Investigation of molecular interaction in gelatin shell by Fourier transform infrared spectroscopy (FT-IR)**

The soft gelatin capsule with and without ibuprofen was cut and the liquid on the shell surface was removed using lint free wiper. The gelatin capsule shell were examined by FT-IR Nicolet iS10 (Thermo Scientific, Wisconsin, USA) in the region of  $600\text{-}4000\text{ cm}^{-1}$  with 32 scans and  $4\text{ cm}^{-1}$  resolution.



## CHAPTER IV

### RESULTS AND DISCUSSION

#### 1. Characterization of soft gelatin capsule

##### 1.1 Appearance

After preparation, soft gelatin capsules were in yellowish and transparent blue colors for non colored and colored gelatin capsule shells, respectively (Figure 4-1(a), 1(c)). The capsules slightly leaked along the seal. This could be a result of insufficient force applied during capsules preparation. Leakage could cause some capsules stucked together. Color fading was not visually observed after storage for 90 days, as shown in Figure 4-1(b), 1(d).



Figure 4- 1 Soft gelatin capsules: non colored capsules after storage for 1 day (a) and 90 days (b); colored capsules after storage for 1 day (c) and 90 days (d),

##### 1.2 Thickness

The thickness of capsule shell was varied in the range of 0.53 - 0.98 mm and 0.37 - 0.92 mm for non colored and colored capsules, respectively. Average values were reported in the Table I-1 and Table I-2 (Appendix I). No swelling of capsule was visually observed. However, inconsistently increased or decreased capsule thickness may be caused by water loss due to evaporation and water absorption into the shell (91).

### 1.3 Hardness

Hardness of capsules were measured at each time point and the results are shown in Figure 4-2 and Figure 4-3.

In general, hardness of capsules was also changed inconsistently during storage. High hardness values resulted from hardening capsules and above approximately 3000 g capsules were broken during the test. Relatively low hardness values mostly observed at 90 days were caused by softening and sticky capsules such as the values measured for formulations 2, 6 and 7 which contained high level of added water (10%). Therefore, this behavior may be due to the water contents in these capsules. It was also possible that gelatin shell absorbed more moisture from atmosphere during storage. The water molecules can act as plasticizer in gelatin film. Excess water molecule in gelatin film would provide softening gelatin shell.

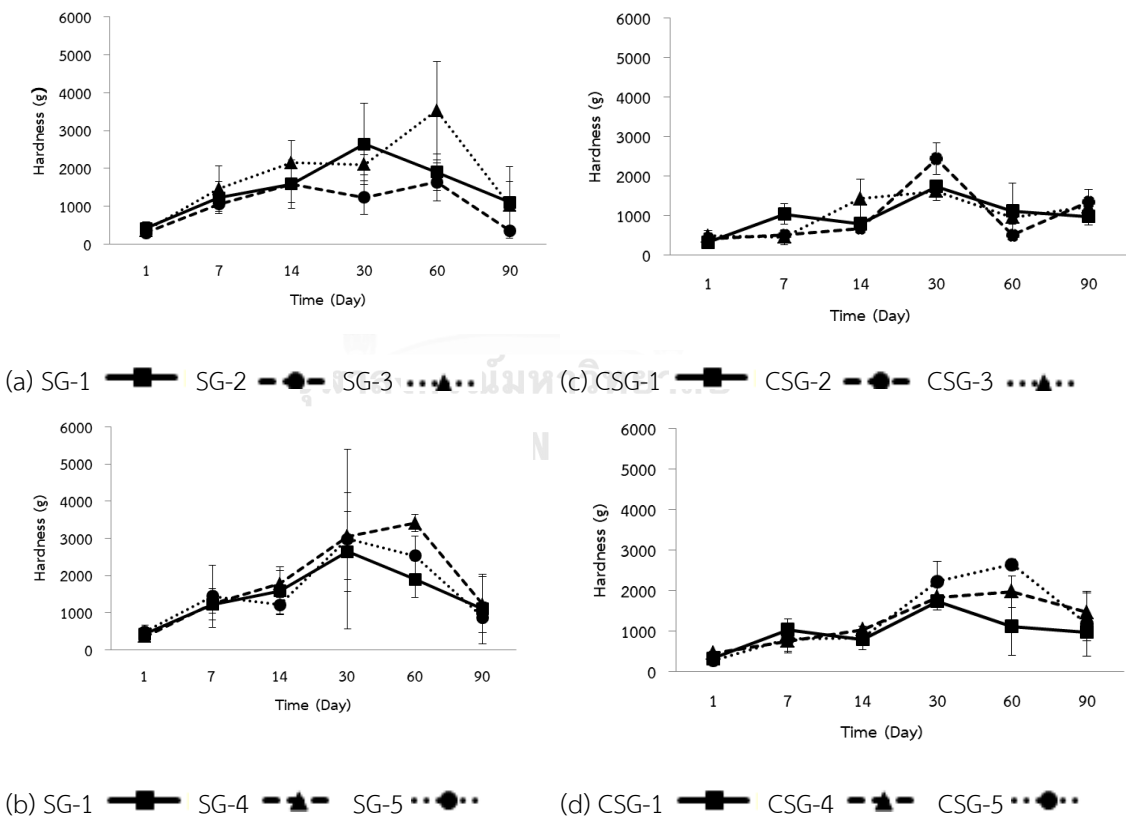


Figure 4- 2 Hardness (n=3) of gelatin capsule shells for non colored formulation 1, 2, 3 (a); non colored formulation 1, 4, 5 (b); colored formulation 1, 2, 3 (c); colored formulation 1, 4, 5 (d)



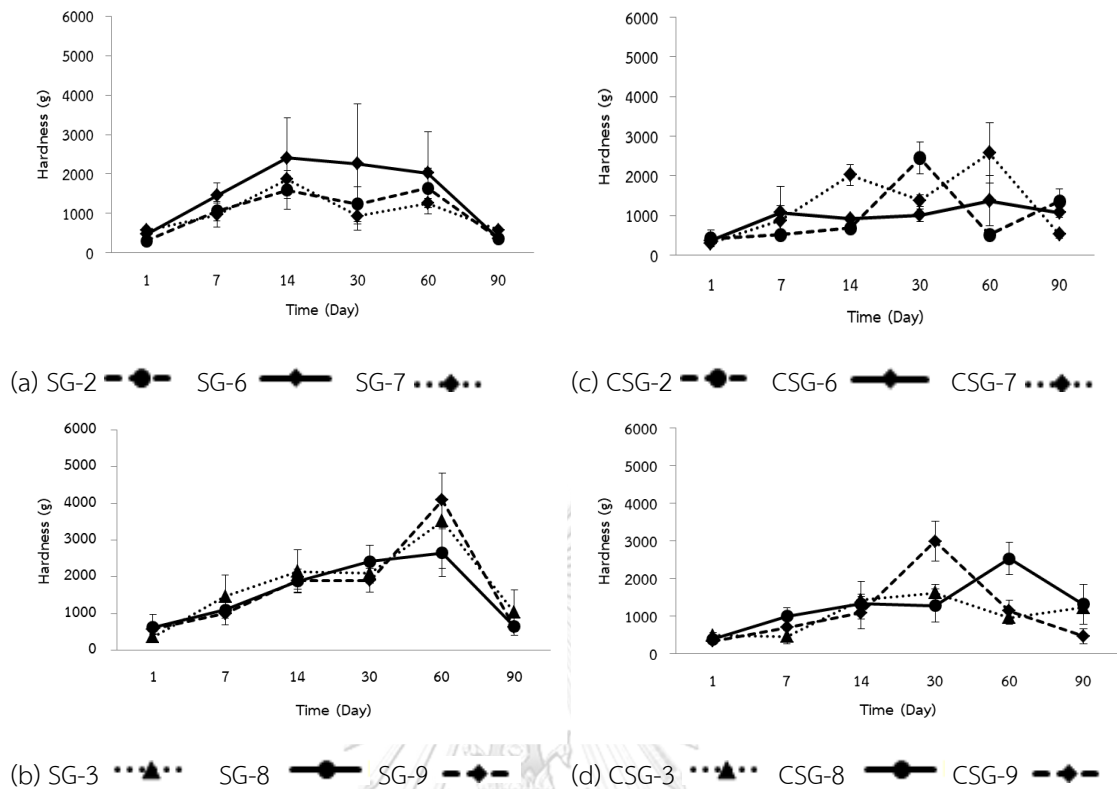


Figure 4- 3 Hardness (n=3) of gelatin capsule shells for non colored formulation 2, 6, 7 (a); non colored formulation 3, 8, 9 (b); colored formulation 2, 6, 7 (c); colored formulation 3,8,9 (d)

In addition, the moisture content in the capsule shell could escape to the atmosphere as well as into the liquid fill containing PEG 600 which is hygroscopic and having high affinity to water. Loss of moisture in the shell may result in hardening capsules, such as non colored capsule of formulation 4 at 30 and 60 days.

Serajuddin et al. investigated on water migration from soft capsule shell into the liquid fills which have varied affinity to water. They found that the amount of water migrating from the capsule shell into PEG 400 which is more affinity to water was higher (6.3%) than Gelucire 44/14:PEG 400 (1.1%) (92). Upon water migration, water soluble substances such as water soluble dye or drug could migrate together with water (93).

Plasticizing effect may also result from intimate contact of PEG 600 with gelatin shell during storage. PEG 600 could partition in glycerol plasticized gelatin

shell and modify mechanical properties of the capsules. PEGs can also act as plasticizer; and lower molecular weight PEGs have higher plasticizing effect for gelatin films (3). Armstrong et al. reported a high water soluble substance, i.e. 4-hydroxybenzoic acid could migrate into the shell of soft gelatin capsule higher than low water soluble substance, i.e. acetaminophen (3).

In this study, hardness of capsules could not be always systematically related to the fill formulations. Statistical analysis of hardness at 90 days showed that there is no significant factor affecting on hardness of capsules as shown in Table II-1 (Appendix II) although there might be an effect of color on hardness (p-value of block = 0.052).

Causes of change in capsule hardness due to chemical migration from or into the shell maybe affected by many factors such as temperature, contact time and nature of chemicals which may not be taken into account. It was also possible that chemical migration could occur dynamically providing fluctuation of hardness value during storage (94). In this study, the temperature was controlled in stability chamber; therefore the hardness behavior could be caused by combining effect of PEG contact time and dynamic water migration.

### 1.4 Moisture content in capsule shell

In the shell formula of soft gelatin capsules studied, the water content was 38%; and normally final moisture content after tumbling and tray dryer in manufacturing industry is 4-10% (95). Consequently, the water content which should be added into the fill material and not deteriorate the gelatin shell has been recommended at a maximum of 10% (96).

In the present study, after 12 h in 32%RH desiccator or 1 day in graphs, the moisture content of the capsule shells were varied in the range of 2.32-4.77% and 1.73-2.56% for non colored and colored capsules, respectively. During storage, the moisture contents of gelatin shell were varied slightly with a limit of 1.36-4.84% and 1.58-4.26% for non colored and colored capsules, respectively (Figure 4-4 and Figure 4-5).

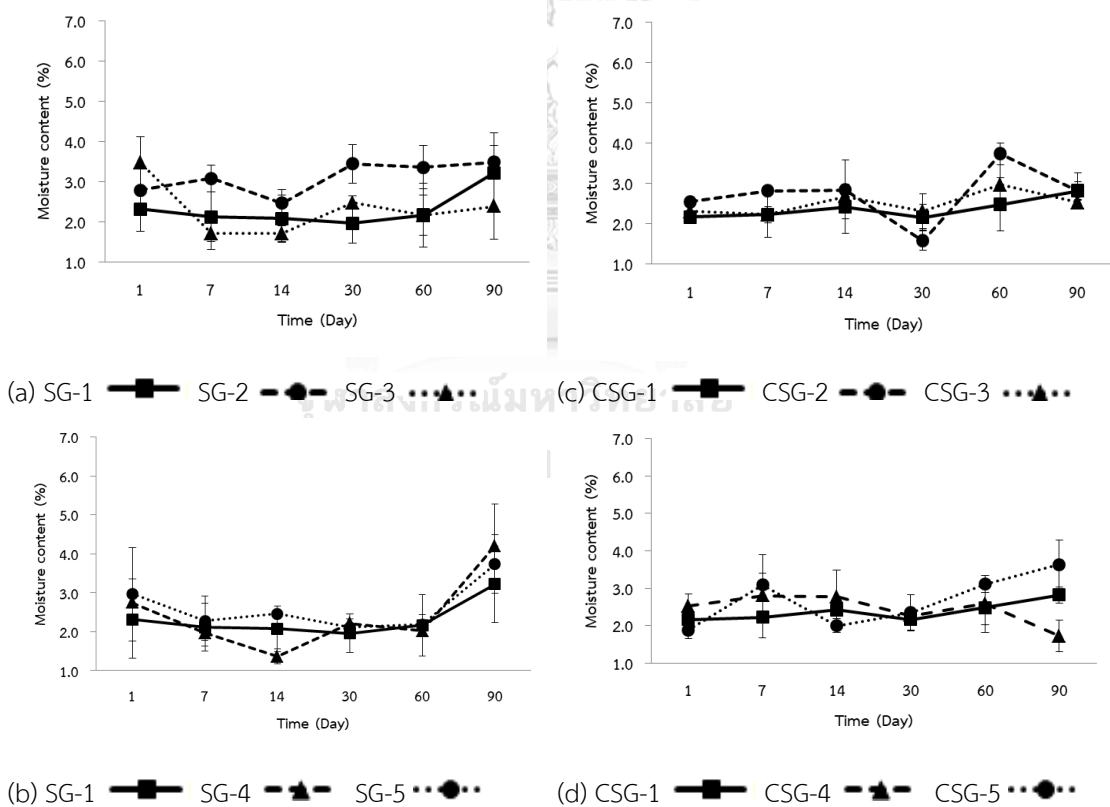


Figure 4- 4 %Moisture content (n=3) of gelatin capsule shells for non colored formulation 1, 2, 3 (a); non colored formulation 1, 4, 5 (b); colored formulation 1, 2, 3 (c); colored formulation 1, 4, 5 (d)

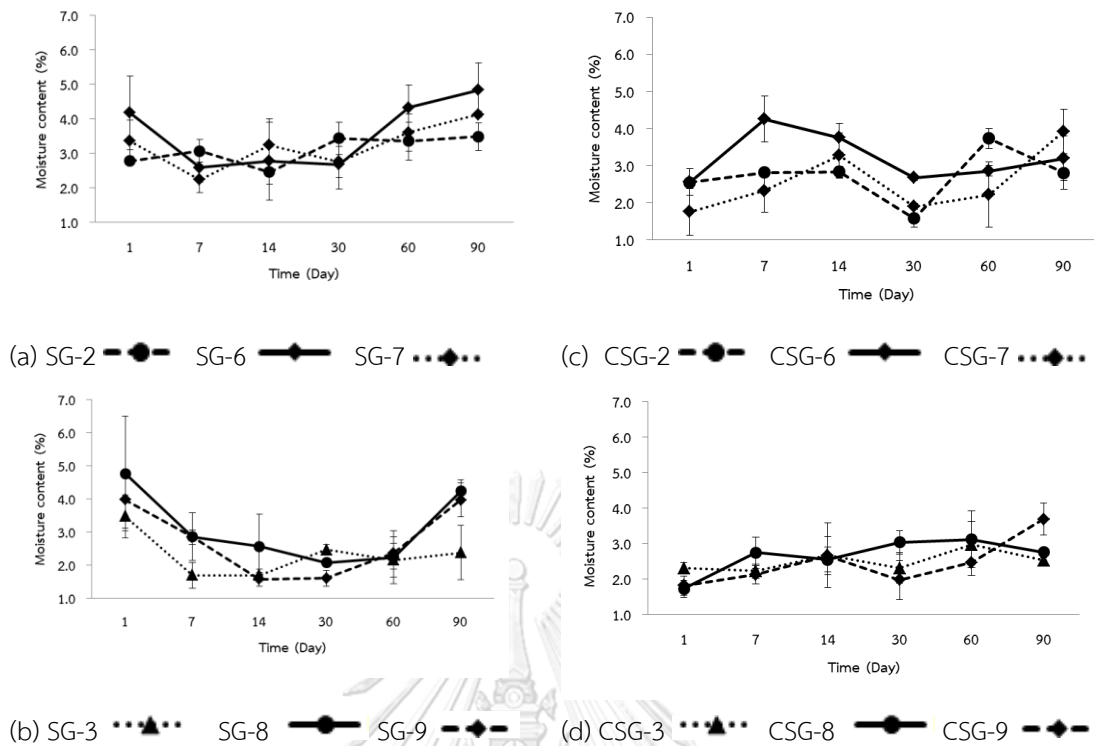


Figure 4- 5 %Moisture content (n=3) of gelatin capsule shells for non colored formulation 2, 6, 7 (a); non colored formulation 3, 8, 9 (b); colored formulation 2, 6, 7 (c); colored formulation 3,8,9 (d)

Statistical analysis of moisture content in capsule shell at 90 days showed that block or color addition affected moisture content (p-value = 0.027). Moreover, alpha-tocopherol in the fill material was likely to be an important factor affecting %moisture content in the capsule shells (p-value = 0.069). The results are shown in Table II-2 (Appendix II).

As discussed earlier, moisture contents in the gelatin shell could be a factor affecting capsule hardness. Scatter plots between hardness and % moisture content of non-colored and colored capsules show that hardness of non colored capsules were more related to the moisture content as  $R^2$  value, 0.2966 (p=0.000) was higher, comparing with that of colored capsules which contained water soluble brilliant blue and hence a more complex system (Figure 4-6 and Figure 4-7).

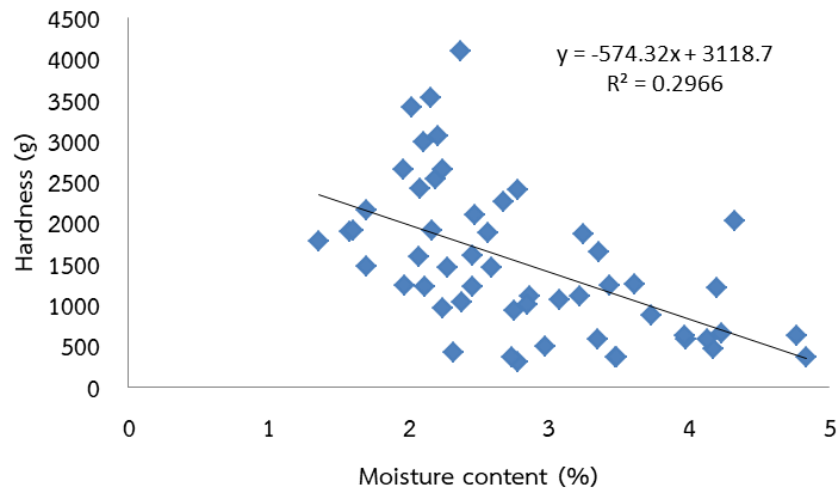


Figure 4- 6 Scatter plot between hardness and moisture content of non colored capsules

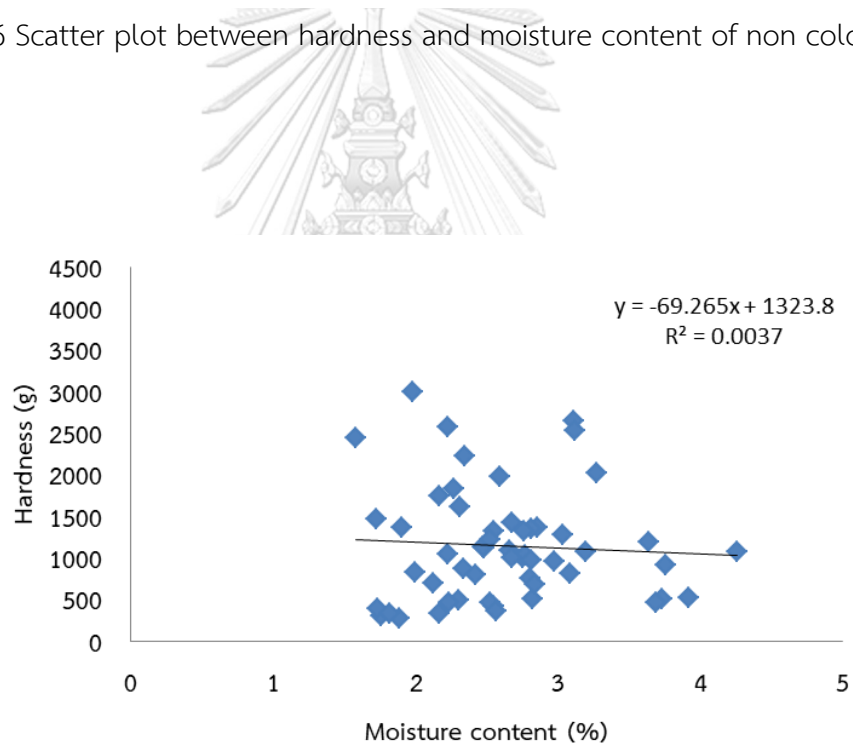


Figure 4- 7 Scatter plot between hardness and moisture content of colored capsules

### 1.5 Water content in liquid fill

Moisture content in the capsule shells can migrate into the liquid fill as discussed earlier (92). This moisture content could be residual moisture after drying, also atmospheric moisture that was absorbed and permeate through the shell into PEG 600 which is hydrophilic material in the liquid fill. Any water soluble component such as water soluble dye in the shell could migrate together with water (97).

In this study, water content in the liquid fill was determined by NIR. NIR spectra are classified to three regions: (1) the high wavelength region between 6500 to 9000  $\text{cm}^{-1}$  ascribed to first overtone of O-H stretching and second overtone of C-H stretching; (2) the wavelength between 5350 to 5900  $\text{cm}^{-1}$  ascribed to first overtone of C-H stretching and (3) the wavelength between 4800 to 5300  $\text{cm}^{-1}$  ascribed to combination of O-H stretching and second overtone of C=O carbonyl group stretching of aldehyde (98).

For water determination, the spectrum in the range of 5,000-5,400 and 5,900-7,700  $\text{cm}^{-1}$  was pretreated by different methods prior to constructing a calibration model (Figure III-1 – Figure III-11, Appendix III) and the results are shown as shown in Table 4-1 and Figure III-12 – Figure III-22 (Appendix III). The selected model for calibration was W1 with RMSEP of 2.4270 and  $R^2$  of 0.9778 using three factors. The results were validated with external validation set of samples as shown in Figure 4-8 from which water content could be predicted in a range of 0-50%w/w with deviation 1.07-3.47.

Table 4- 1 Pretreatment of NIR spectra in the region of 5,000-5,400 and 5,900-7,700  $\text{cm}^{-1}$ , RMSEC and  $r^2$  of calibration, also RMSEP and  $r^2$  of internal validation

Code	Pretreatment of spectra			RMSEC	$r^2$	RMSEP	$r^2$	Factor
	Scatter correction	Derivative	Smoothing					
W1	-	-	-	3.9628	0.9251	2.4270	0.9778	3*
W2	MSC	-	-	3.6708	0.9357	3.4398	0.9555	3
W3	SNV	-	-	4.097	0.9281	2.6014	0.9737	3
W4	MSC	1 <sup>st</sup> derivative	Norris-Williams derivation	3.919	0.9302	3.3784	0.9559	3
W5	MSC	1 <sup>st</sup> derivative	Savitzky-Golay derivation	2.8268	0.9619	5.8131	0.8729	3
W6	MSC	2 <sup>nd</sup> derivative	Norris-Williams derivation	3.9494	0.9256	5.3499	0.8923	3
W7	MSC	2 <sup>nd</sup> derivative	Savitzky-Golay derivation	5.0022	0.8806	7.0778	0.8115	3
W8	SNV	1 <sup>st</sup> derivative	Norris-Williams derivation	4.151	0.9262	3.7076	0.9465	3
W9	SNV	1 <sup>st</sup> derivative	Savitzky-Golay derivation	4.3122	0.9203	3.0164	0.9646	3
W10	SNV	2 <sup>nd</sup> derivative	Norris-Williams derivation	4.8434	0.8995	3.0162	0.9646	3
W11	SNV	2 <sup>nd</sup> derivative	Savitzky-Golay derivation	4.1459	0.9264	2.6144	0.9734	3

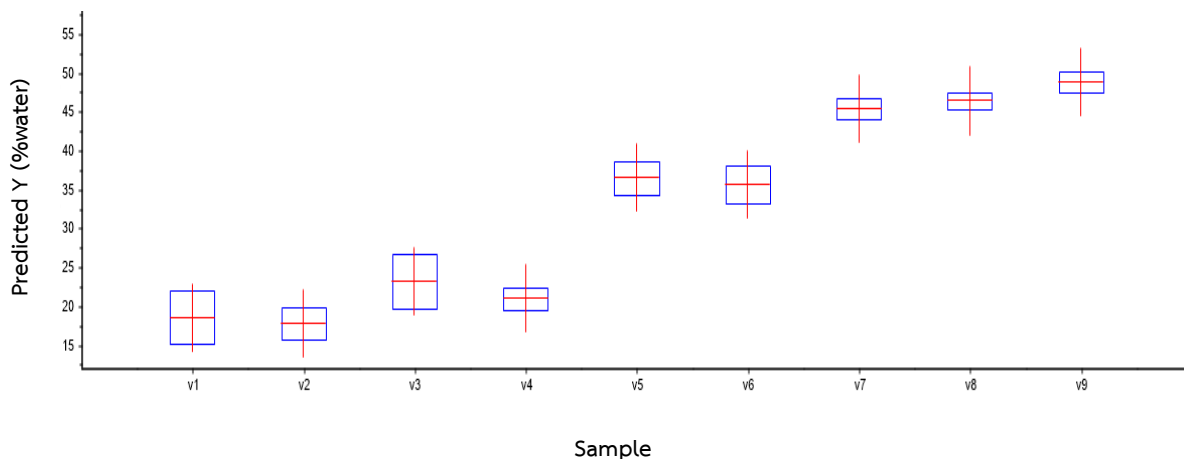
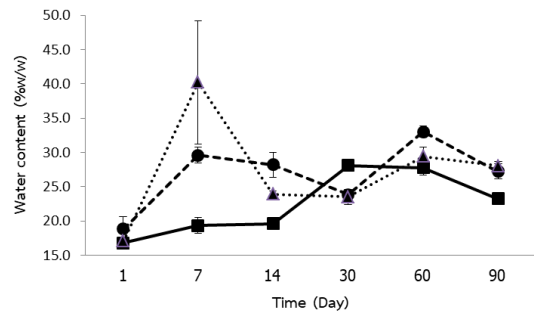
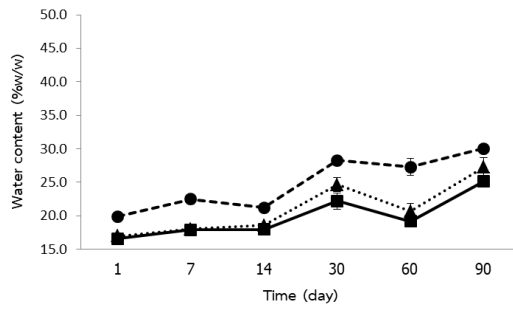


Figure 4- 8 External validation of W1 model showing predicted water content in liquid fill, with deviation.

When the calibration model was applied to predict water content in the liquid fill during storage, the predicted water contents ranged in 16.29-30.67%w/w and 16.07-40.22%w/w for non colored and colored capsules, respectively. Water content in liquid fill that was predicted by model W1 and plotted in Figure 4- 9 and Figure 4- 10.

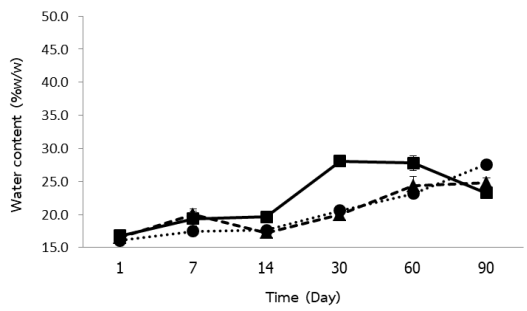
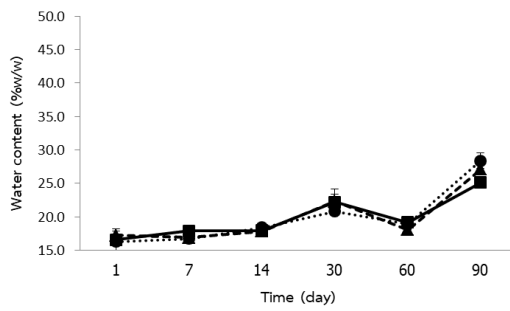
These predicted values of water contents may be higher than the actual amount that should be in the liquid fill for soft capsules. It was possibly due to that weighing which was the reference method was not a method of choice to determine water content. In addition, external validation was carried out on the same day as calibration set so temperature variation was not taken into the model. Consequently, the results were used for investigating only trend of water content from which the water content was found to increase during storage. This corresponded to high affinity of PEG 600 to water (13).





(a) SG-1 —■— SG-2 -●- SG-3 ...▲...

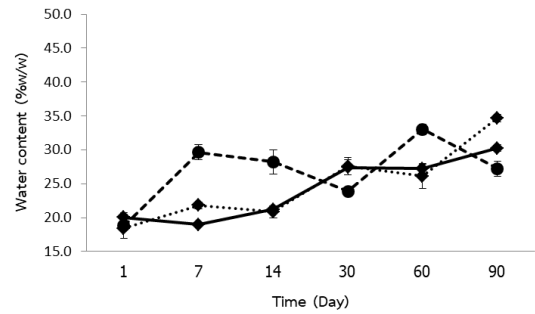
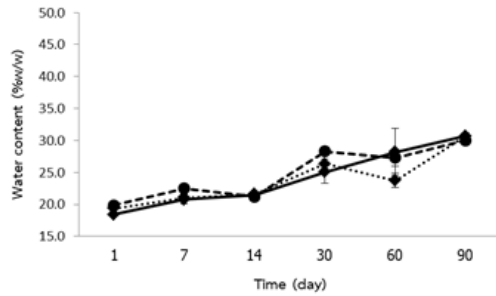
(c) CSG-1 —■— CSG-2 -●- CSG-3 ...▲...



(b) SG-1 —■— SG-4 -▲- SG-5 ...●...

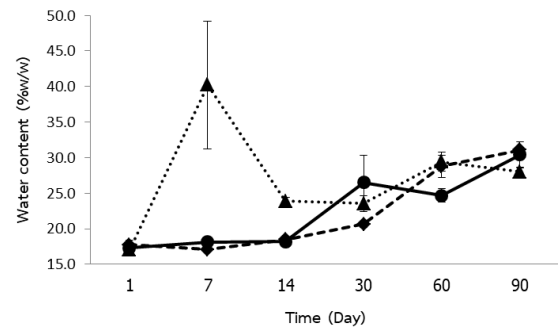
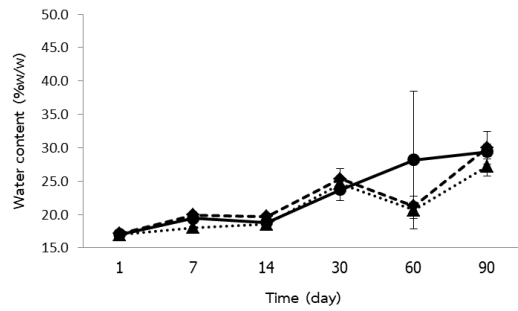
(d) CSG-1 —■— CSG-4 -▲- CSG-5 ...●...

Figure 4- 9 Water content in liquid fill (n=3) for non colored formulation 1, 2, 3 (a); non colored formulation 1, 4, 5 (b); colored formulation 1, 2, 3 (c); colored formulation 1, 4, 5 (d)



(a) SG-2 ● SG-6 ◆ SG-7 ▲

(c) CSG-2 ● CSG-6 ◆ CSG-7 ▲



(b) SG-3 ▲ SG-8 ● SG-9 ◆

(d) CSG-3 ▲ CSG-8 ● CSG-9 ◆

Figure 4- 10 Water content in liquid fill (n=3) for non colored formulation 2, 6, 7 (a); non colored formulation 3, 8, 9 (b); colored formulation 2, 6, 7 (c); colored formulation 3,8,9 (d)

## 1.6 Determination of formaldehyde content

### 1.6.1 Gas chromatography/mass spectrometry (GC/MS)

Formaldehyde has been reported as impurities with a limit of 30 ppm (99) and degradation product of PEG (4).

Formaldehyde contents in the liquid fill of each formulation were analyzed by GC-MS at 1, 14, 30 and 90 days. The results of formaldehyde content and % formaldehyde increase are tabulated in Table I-3 in Appendix I and plotted in Figure 4-11.

Overall results suggested that formaldehyde contents in the liquid fill were increased up to 14 days of storage and then it was decreased continuously. The maximum formaldehyde content was 61.9 ppm found at 14 days for formulation 1 containing neat PEG 600 in the liquid fill. The significant factor that affected both formaldehyde contents and % formaldehyde increase at 14 days (Table II-3 and Table II-4, Appendix II) was the initial water content in the liquid fill ( $p$ -value = 0.001). More initial water contents resulted in less formaldehyde at 14 days (Figure 4-12). The % formaldehyde increase was minimized when the initial moisture content was 5% as observed for formulation 3 and 9 (Figure 4-11(d)) and main effect plot shown in Figure 4-13. This was because the formaldehyde content of these formulation were greatest at 1 day after preparation.

The increase of formaldehyde content was reaction product of PEG autoxidation. However, the results did not agree with that reported by Hemenway et al. who indicated that the presence of water in 50% PEG 400 solution resulted in more formaldehyde determined at 14 days being 99 and 73 ppm, respectively (6). However, McGinity and Hill suggested that 5-10% water could decrease peroxide intermediate that forms formaldehyde in autoxidation of PEG (27).

Hemenway et al. also reported that 10% vitamin E TPGS, which is H-atom donor antioxidant, in 50% PEG 400 solution could inhibit formation of formaldehyde.

In the present study, the maximum alpha-tocopherol of 0.05% which is equivalent to vitamin E TPGS 0.153 % was too little to inhibit PEG autoxidation.

Formaldehyde is a volatile substance. It can diffuse into the gelatin shell, also may be able to diffuse out from the shell into the atmosphere. The measured formaldehyde was the remaining content in the liquid fill after it diffused and reacted with any chemicals in the gelatin shells during storage time. Therefore, the more formaldehyde diffused into the gelatin shell, the less remaining formaldehyde content that was measured in the liquid fill. However, measurement of formaldehyde content in the liquid fill only could be misleading result because formaldehyde formed in liquid fill could be consumed to the shell and loss during storage (100).

The formaldehyde which diffused into the gelatin shell could be consumed by gelatin cross-linking reaction and oxidation reaction in the shell. Shelley et al. reported that aldehyde content greater than 100 ppm could cause gelatin crosslinking in the soft gelatin capsules shell (100). Another evidence showing that formaldehyde can migrate from liquid fill into the shell and adding formaldehyde at least 185 ppm induced crosslinking was carried out by Gold et al. (74). While, Teckoe et al. have found that color fading in film coated tablets was caused by formaldehyde content 7-10 ppm measured after 6 months (12). In addition, reduction of formaldehyde may be attributed to conversion to formic acid in PEG solution (6).

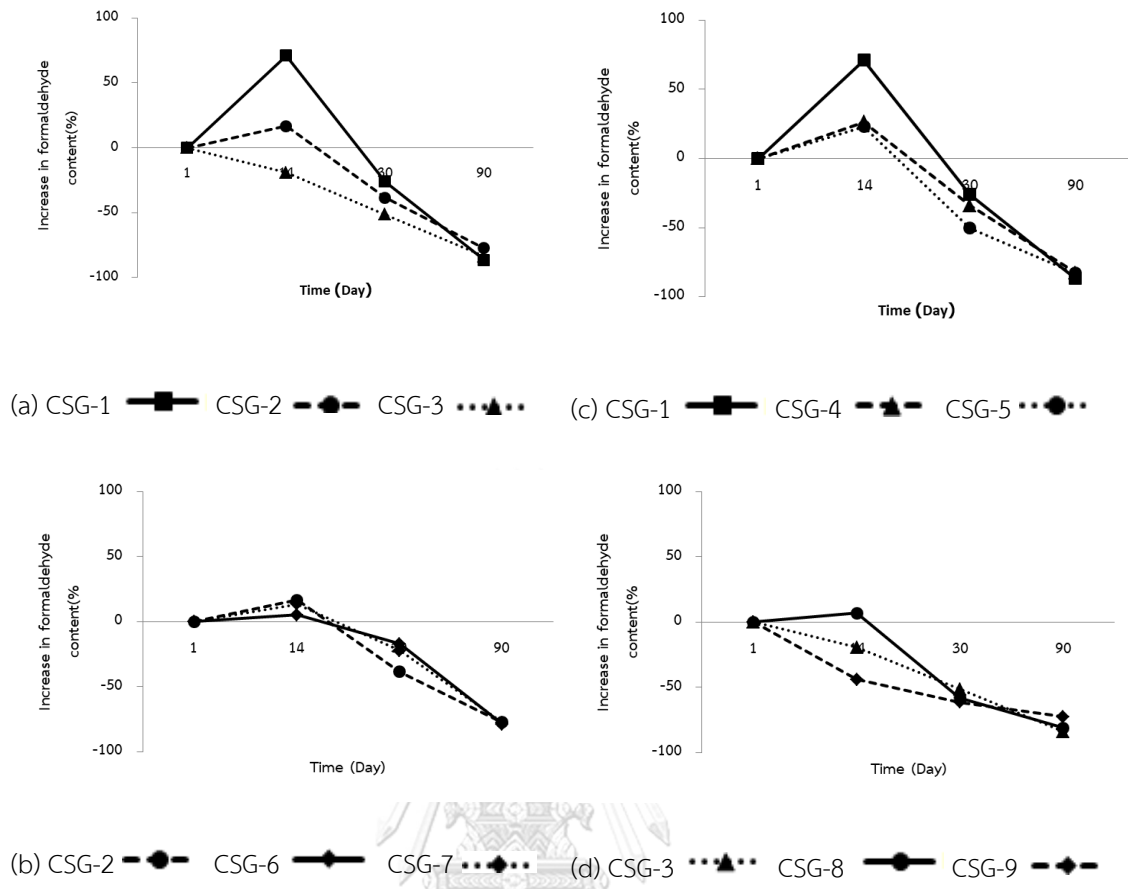


Figure 4- 11 % Formaldehyde increase in the liquid fill of colored capsule formulation 1, 2, 3 (a); colored capsule formulation 2, 6, 7 (b); colored capsule formulation 1, 4, 5 (c); colored capsule formulation 3, 8, 9 (d)

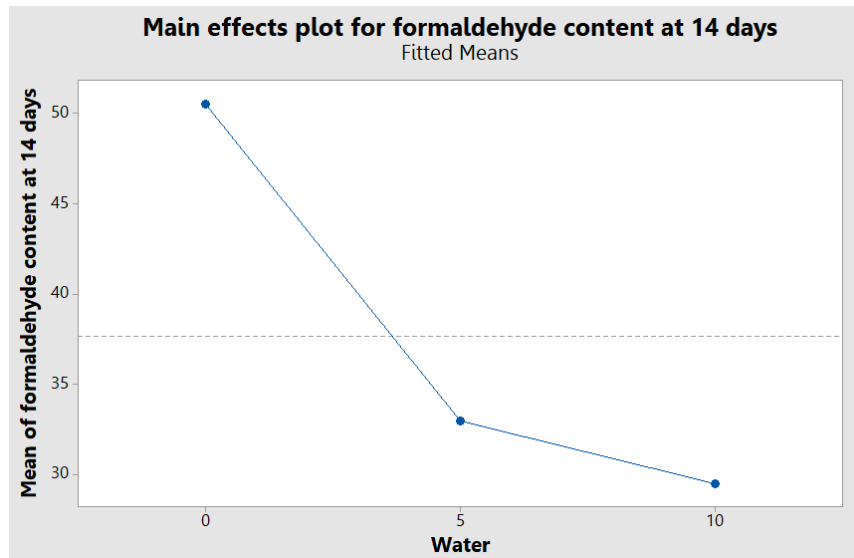


Figure 4- 12 Main effect plot for formaldehyde content at 14 days: Effect of initial water content

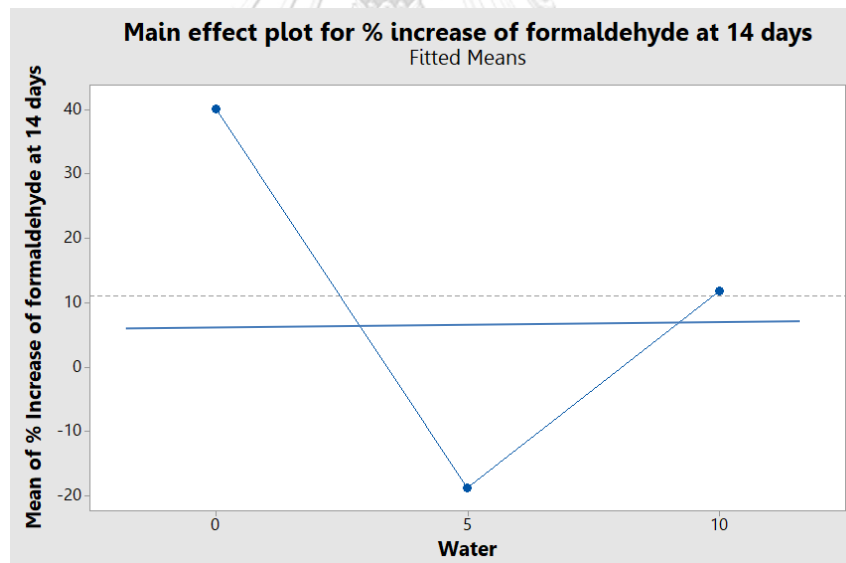


Figure 4- 13 Main effect plot for % increase of formaldehyde at 14 days: Effect of initial water content

### 1.6.2 Near-infrared spectroscopy (NIR)

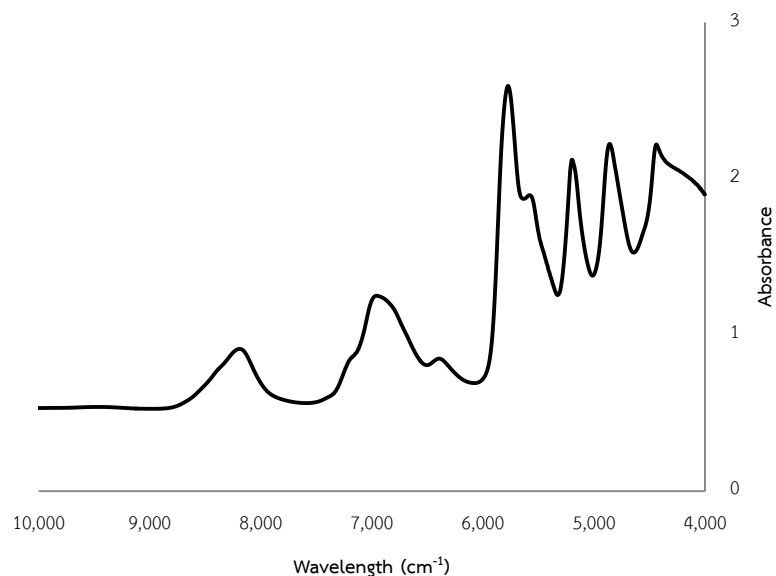


Figure 4- 14 NIR spectrum in the range 4,000-10,000 cm<sup>-1</sup> of neat PEG 600

When PEG 600 was examined with NIR, the spectrum of PEG 600 showed main peaks centered around 8187.36, 6920.7, 5770.28, 5197.47, 4858.96 and 4434.07 cm<sup>-1</sup> (Figure 4-14). Hydroxyl groups of PEG 600 showed strong O-H stretching vibration band at centered around 7030 cm<sup>-1</sup> while O-H bending showed absorption centered around 4331, 4872 and 5173 cm<sup>-1</sup> (101).

Formaldehyde has carbonyl group having C=O stretching in the second overtone of simple noncyclic aliphatic compounds. An example for second overtone of aliphatic aldehyde, such as propionaldehyde, is at 5100 cm<sup>-1</sup> (102).

Calibration model were generated with whole NIR spectra, 4,000-10,000 cm<sup>-1</sup>, and the weighed amounts of formaldehyde filled in neat PEG 600 and PEG 600 with 5% and 10% water. The NIR spectra were pretreated with different method, the results shown in Figure IV-1 - Figure IV-18 (Appendix IV) and capability of the model was suggested by the value of RMSEC, RMSEP, r<sup>2</sup> and number of factors applied (Table 4-2 and Figure IV-19 - Figure IV-29, Appendix IV). Accordingly, model M35 with RMSEP of 35.592 and R<sup>2</sup> of 0.638 using five factors was selected. The model

was validated with external validation set of samples from which formaldehyde content ranging from -109.78 – 156.27 could be predicted with deviation 38.64-139.21 (Figure 4-15). The great values of deviation signified that the selected model was not appropriate for prediction of formaldehyde content in PEG 600 with and without water.

The invalid model resulted from systematic variation in the NIR spectra that was not related to interested response (formaldehyde concentration). This could be explained that formaldehyde absorbed only in small NIR region (1890-1900 nm). Therefore, variation in raw spectra which was not related to the response contributed to inaccurate multivariate model. To eliminate unwanted systematic variation in the spectra, it could be done by removing the spectral region which is unrelated to the response by mathematically orthogonal converting to the response. In this study, the absorbance of water in the standard solutions interfered the spectral region of formaldehyde, so the OSC method was used to remove the effect of water in the standard set before pretreatment using common methods.

The results are shown as Model M34-2 – M40-2 in Table 4-3 and Figure IV-30 - Figure IV-36 (Appendix IV). The values of RMSEP and  $R^2$  were improved. The best model to predict formaldehyde in PEG 600 with water was M36-2, having RMSEP and  $R^2$  of 24.208 and 0.832, respectively, using one factor. The results were validated with external validation set of samples as shown in Figure 4-16 from which formaldehyde content could be predicted ranging from 29.53 - 221.09 with deviation of 34.87 – 105.5.



Table 4- 2 Pretreatment of NIR spectra in the region of 4,000-10,000  $\text{cm}^{-1}$ , RMSEC and  $r^2$  of calibration, also RMSEP and  $r^2$  of internal validation

Code	Pretreatment of spectra			RMSEC	$r^2$	RMSEP	$r^2$	Factor
	Scatter correction	Derivative	Smoothing					
M34	-	-	-	42.064	0.494	38.698	0.571	4
M35	MSC	-	-	41.453	0.508	35.592	0.638	5
M36	SNV	-	-	41.456	0.508	35.658	0.636	5
M37	MSC	1 <sup>st</sup> derivative	Norris-Williams derivation	43.998	0.446	37.288	0.602	5
M38	MSC	1 <sup>st</sup> derivative	Savitzky-Golay derivation	44.382	0.437	37.576	0.596	5
M39	MSC	2 <sup>nd</sup> derivative	Norris-Williams derivation	50.112	0.282	48.645	0.323	4
M40	MSC	2 <sup>nd</sup> derivative	Savitzky-Golay derivation	49.58	0.297	47.357	0.358	4
M41	SNV	1 <sup>st</sup> derivative	Norris-Williams derivation	51.128	0.252	50.64	0.266	4
M42	SNV	1 <sup>st</sup> derivative	Savitzky-Golay derivation	50.661	0.266	49.961	0.286	4
M43	SNV	2 <sup>nd</sup> derivative	Norris-Williams derivation	50.069	0.283	48.692	0.322	4
M44	SNV	2 <sup>nd</sup> derivative	Savitzky-Golay derivation	49.444	0.300	47.257	0.361	4

Table 4- 3 Pretreatment of NIR spectra in the region of 4,000-10,000  $\text{cm}^{-1}$ , RMSEC and  $r^2$  of calibration, also RMSEP and  $r^2$  of internal validation

Code	Pretreatment of spectra				RMSEC	$r^2$	RMSEP	$r^2$	Factor
	OSC	Scatter correction	Derivative	Smoothing					
M34-2	✓	-	-	-	32.302	0.702	29.943	0.743	1
M35-2	✓	MSC	-	-	27.952	0.776	26.774	0.795	1
M36-2	✓	SNV	-	-	26.518	0.799	24.208	0.832	1
M37-2	✓	-	1 <sup>st</sup> derivative	Norris-Williams derivation	32.439	0.699	30.061	0.741	1
M38-2	✓	-	1 <sup>st</sup> derivative	Savitzky-Golay derivation	32.336	0.701	30.083	0.741	1
M39-2	✓	-	2 <sup>nd</sup> derivative	Norris-Williams derivation	32.446	0.699	30.091	0.741	1
M40-2	✓	-	2 <sup>nd</sup> derivative	Savitzky-Golay derivation	32.115	0.705	30.127	0.740	1

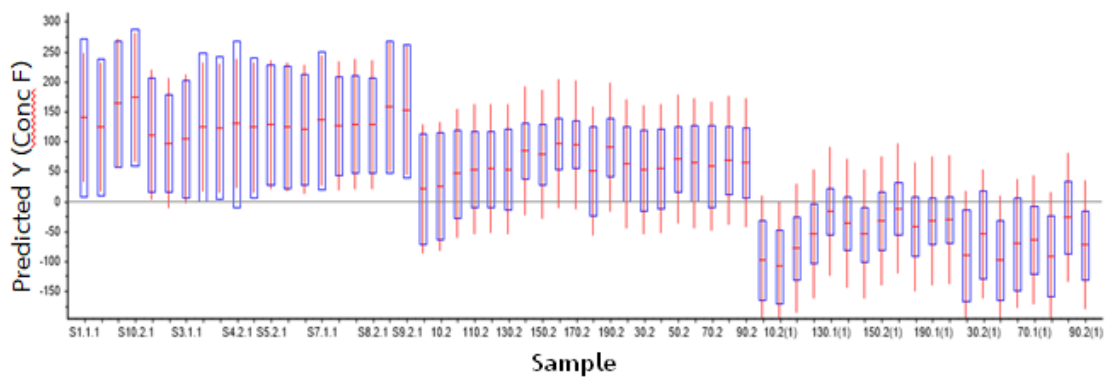


Figure 4- 15 External validation of M35 model showing predicted formaldehyde content in liquid fill, with deviation

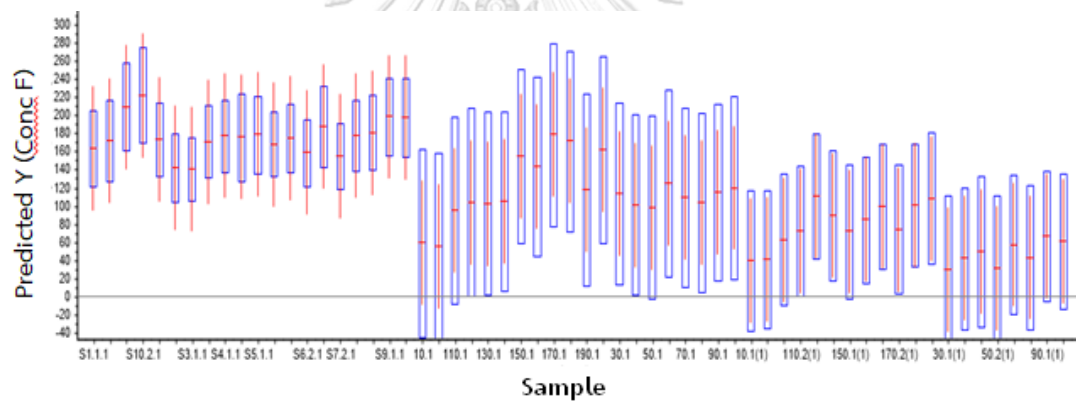


Figure 4- 16 External validation of M36-2 model showing predicted formaldehyde content in liquid fill, with deviation

However, when the model M36-2 was used to predict formaldehyde content in liquid fill of the stored capsules, the predicted values and deviation were considerably high and far beyond the values obtained from GC-MS method at the same time points (Table I-3, Appendix I) This can be explained by inaccurate reference method used as discussed earlier. Also the water content that was taken in the calibration model did not represent actual water contents in the samples during storage. Therefore, forms of the sample spectra and the spectra used in constructing the model were rather different (Figure 4-17).

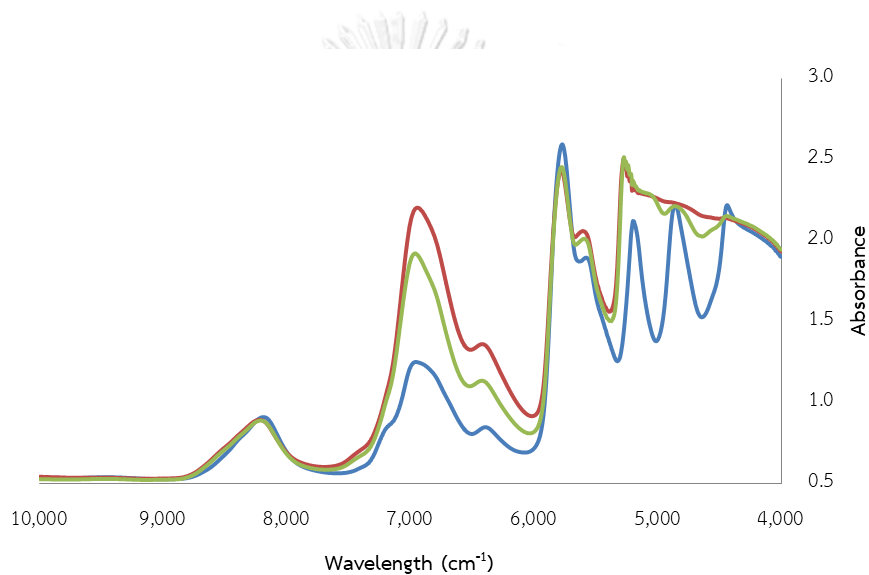


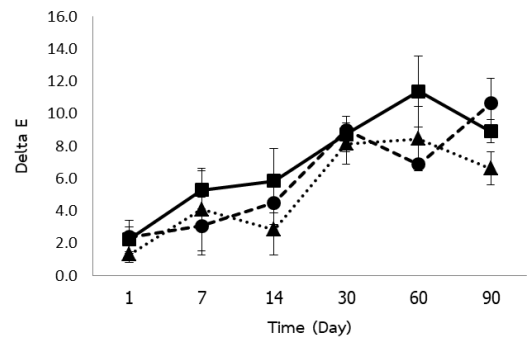
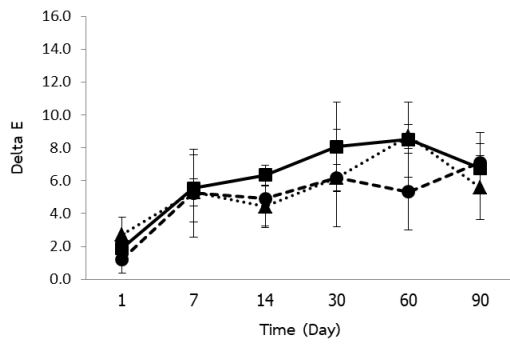
Figure 4- 17 Spectra of PEG 600 —, PEG 600 with 10% w/w water —, liquid fill of sample —

## 1.7 Color determination

### 1.7.1 Colorimeter

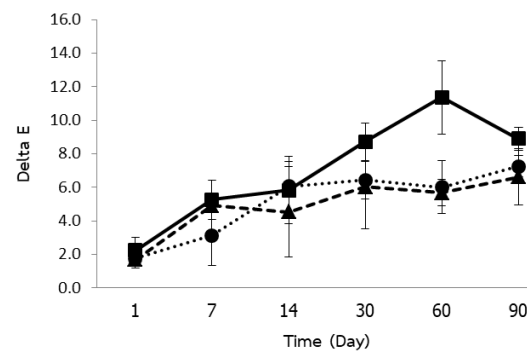
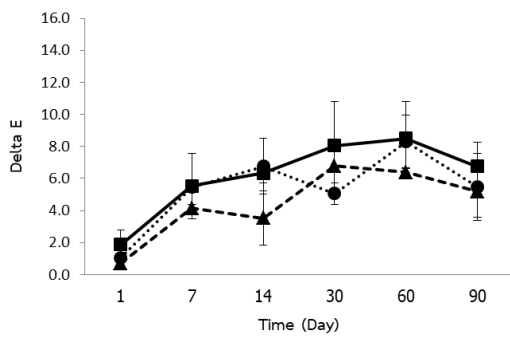
Color of soft gelatin capsule shell was measured by CIELAB color scale. The values are shown in three axes, L\* axis which runs from top to bottom showing brightness of color or called black and white. While the positive of a\* axis is red and negative of a\* axis is green. The positive b\* axis is yellow and negative b\* axis is blue. Delta E value is total color difference that can be calculated from three axes values. The detail of the technique is described in Chapter 2

The color of capsule shells after 1 day of preparation was measured as reference for each formulation. The delta E values of stored capsule shells are plotted and shown in Figure 4-18 and Figure 4-19. The delta E value were up to 11.81 and 12.12 for non colored formulation 9 and colored formulation 7 containing high level of d-alpha-tocopherol with 5% and 10% initial water content, respectively. Although, color fading could not be visually observed, the delta E values of non colored and colored capsules were likely to increase, indicating color change in both non colored and colored capsules. The increased delta E value of non colored shell was attributed to a more positive value, indicating yellow color, of b-axis. However, variation of color change was relatively high for both non colored and colored capsule shell.



(a) SG-1 —■— SG-2 - -●- SG-3 ...▲...

(c) CSG-1 —■— CSG-2 - -●- CSG-3 ...▲...



(b) SG-1 —■— SG-4 - -▲- SG-5 ...●...

(d) CSG-1 —■— CSG-4 - -▲- CSG-5 ...●...

Figure 4- 18 Delta E (n=3) of gelatin capsule shells for non colored formulation 1, 2, 3 (a); non colored formulation 1, 4, 5 (b); colored formulation 1, 2, 3 (c); colored formulation 1, 4, 5 (d)

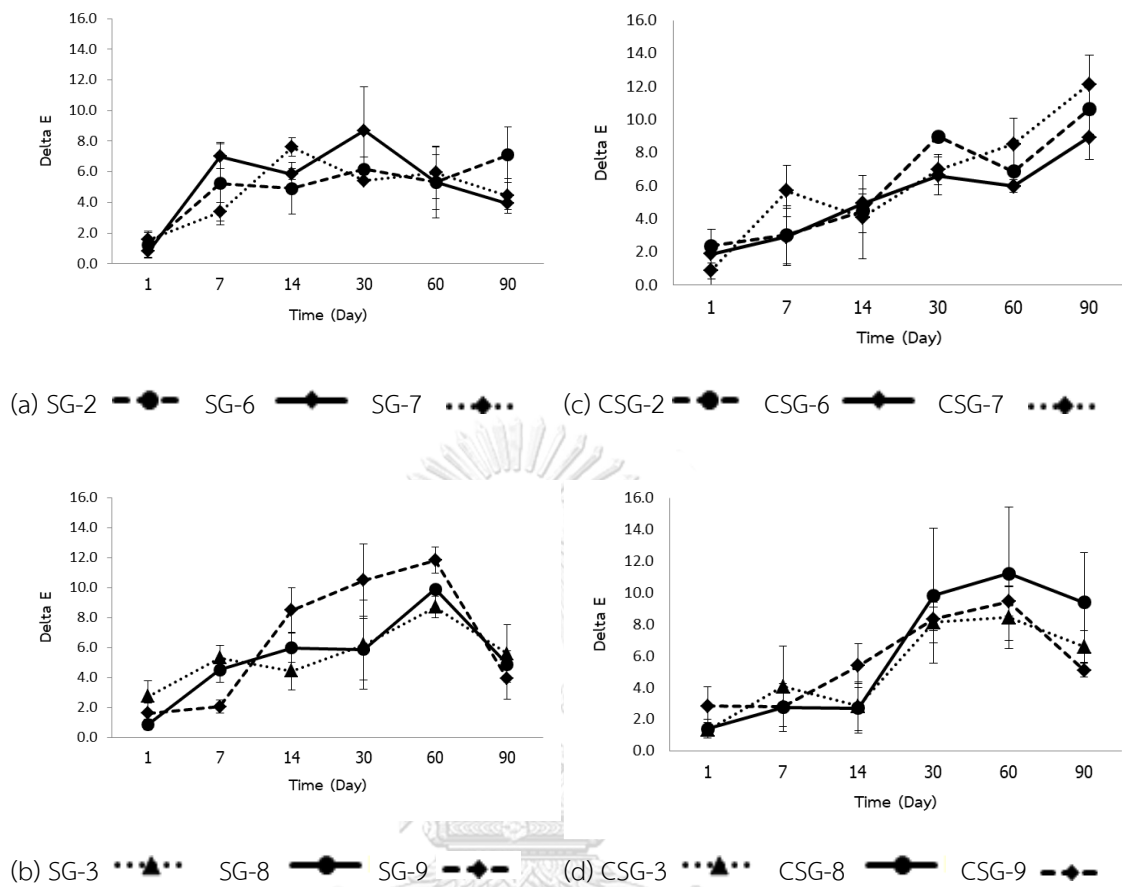


Figure 4- 19 Delta E (n=3) of gelatin capsule shells for non colored formulation 2, 6, 7 (a); non colored formulation 3, 8, 9 (b); colored formulation 2, 6, 7 (c); colored formulation 3, 8, 9 (d)

จุฬาลงกรณ์มหาวิทยาลัย  
CHULALONGKORN UNIVERSITY

Teckoe et al. found that fading of indigo carmine lake occurred in film coated tablets in which PEG was use as detackifier after 6 months of storage. The delta E of these tablets was more than 7 and the measured formaldehyde was 7-10 ppm. Color fading was not visually observed for PEG-free coated tablet where the delta E was 2.5. (12).

The delta E value can also differentiate haziness of film. Byun et al. reported that polylactic acid (PLA) film with PEG 400, BHT and  $\alpha$ -tocopherol gave a more hazy film having delta E value about 0.08, while the pure PLA film had delta E value of 0 (29).

Brilliant blue could be degraded by potassium persulfate as oxidizing agent (51). There were two intermediates which were intermediate I which could be visually observed in dark blue color, obtained when the molar dye/persulfate ratios were 1/1 and 1/10. This was because the chromophore of brilliant blue color was still present. Another intermediate II was non-color when the molar dye/persulfate ratio was increased to 1/100.

It was proposed that once the capsule shell was exposed to formaldehyde which is an oxidizing agent, color oxidation could occur. Therefore, the delta E values at 90 days were plotted against the maximum remaining formaldehyde that present the formulation during storage. It is shown that the greater delta E values or more color change were found at lower remaining formaldehyde (Figure 4-20). The correlation between delta E at 90 days and maximum remaining formaldehyde in liquid fill was not significant (p-value = 0.066)

Therefore, it was possible that formaldehyde was consumed in color oxidation, resulting in color change. However, the delta E value cannot specify shade of color change whether it was lighter or darker.

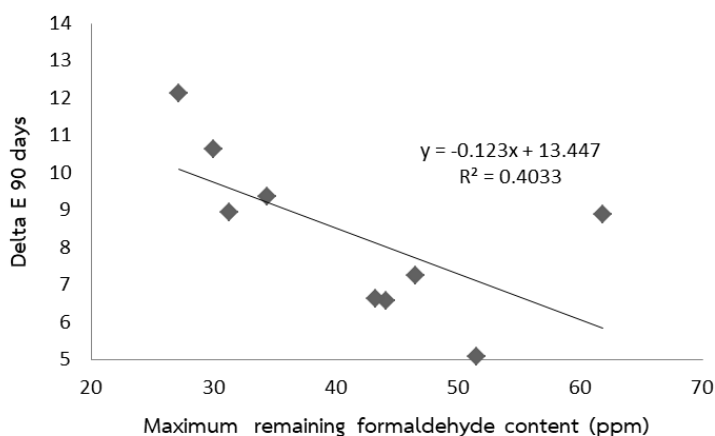


Figure 4- 20 Scatter plot between delta E and maximum remaining formaldehyde during storage of colored capsules

Statistical analysis (Table II-5, Appendix II) showed that addition of water and/or d-alpha-tocopherol did not significantly affect color change or delta E value



at 90 days. However, the results were significant difference between non colored and colored capsules ( $p = 0.003$ ).

### 1.7.2 UV-Visible spectrometer

UV visible spectroscopy was used for determine brilliant blue contents in both shell and in liquid fill. Total color content in fill and shell at 1 and 90 days was shown in Figure 4-21.

Statistical analysis using sample independent t-test comparing between the total brilliant blue contents both in the shell and liquid fill at 1 day and 90 days indicated significant color degradation only for formulation CSG-3 ( $p$ -value = 0.022), CSG-5 ( $p$ -value = 0.021), CSG-6 ( $p$ -value = 0.006), and CSG-8 ( $p$ -value = 0.027) (Table II-6, Appendix II). The results could not be systematically related to liquid fill formulation. There seemed to be other factors involved in color degradation such as formaldehyde formation.

It was shown that the brilliant blue content in the shell was not always related to the delta E value ( $R^2 = 0.1307$ ,  $p$ -value = 0.339, Figure 4-22). This can be explained that the delta E value was influenced by yellow color of non colored capsules which was also changed during storage. However, the brilliant blue contents in capsule shell were fairly related to maximum remaining formaldehyde in the liquid fill during storage for 90 days, as shown in  $R^2 = 0.3055$  (Figure 4-23) but this correlation was not significant at  $p$ -value = 0.123. The color content was less when the maximum remaining formaldehyde was greater.

However, at the same level of remaining formaldehyde, the color content in the liquid fill was increased (Figure 4-24). This could be explained by color migration from the shell into the liquid fill. Brilliant blue is water soluble dye so it can migrate together with water. Water soluble dye migration is commonly found when water migration due to evaporation of water from the surface during drying of granules or coating (103). In this study, the increased color contents in the liquid fill were significantly related to a decrease in color content in the shell (Figure 4-25) with  $p$ -value = 0.001) and corresponded to an increase in water content (Figure 4-26) with significant correlation with  $p$ -value = 0.012.

Color migration could also result in color fading of the capsule shell and it may provide more significant effect than color oxidation. The migrating color was predominantly greater than the color oxidized in the liquid fill.

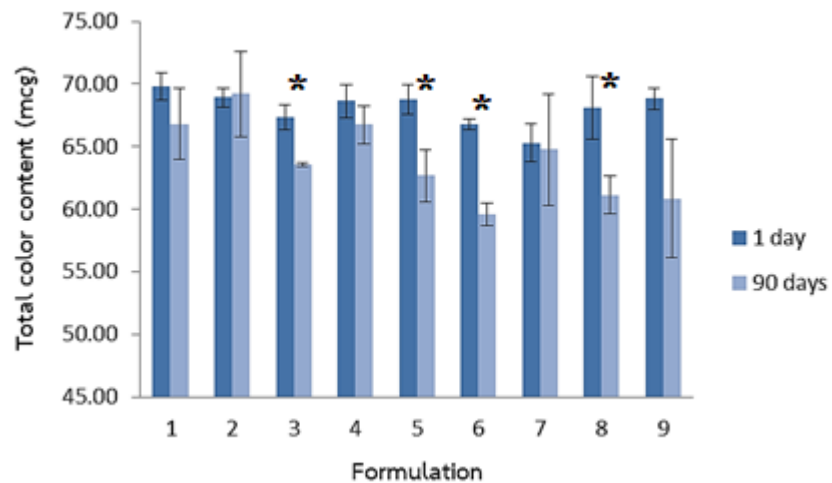


Figure 4- 21 Total color content of each formulation capsules at 1 and 90 days

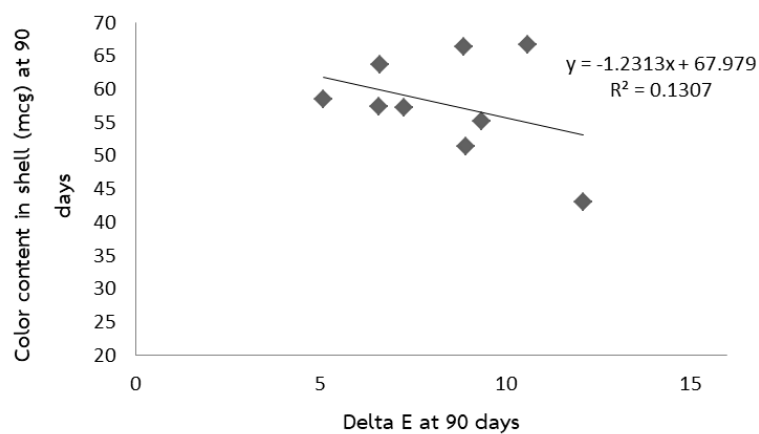


Figure 4- 22 Scatter plot between brilliant blue content in capsule shell and delta E at 90 days of colored capsules

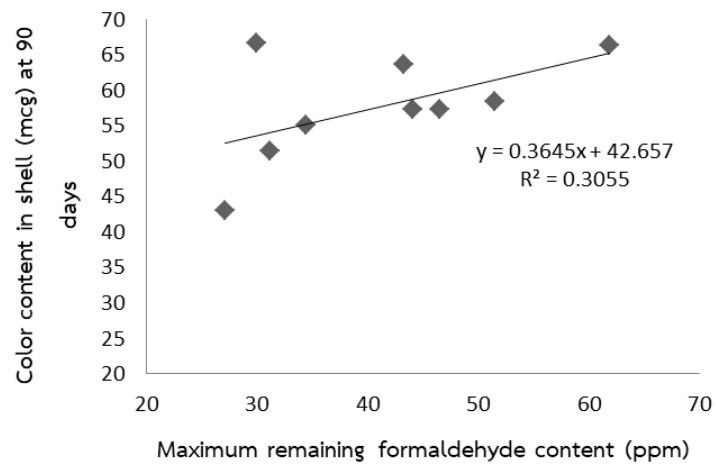


Figure 4- 23 Scatter plot between brilliant blue content in capsule shell at 90 days and maximum remaining formaldehyde in liquid fill during storage of colored capsules

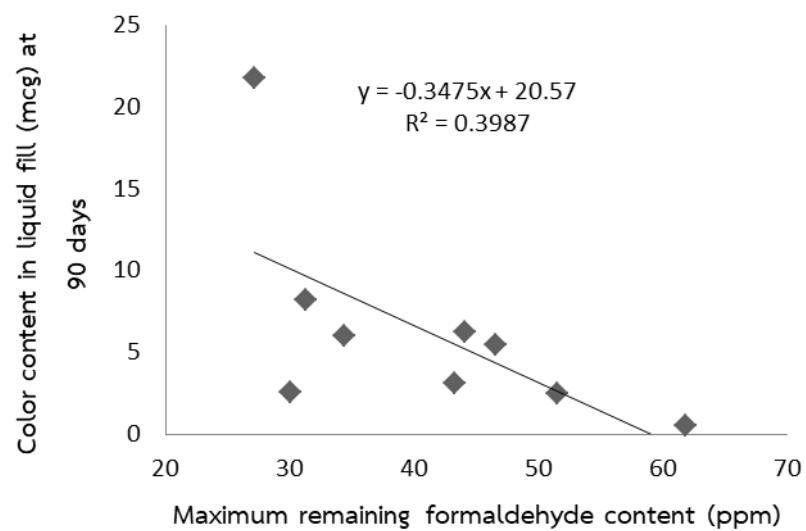


Figure 4- 24 Scatter plot between brilliant blue content in liquid fill and maximum remaining formaldehyde during storage of colored capsules

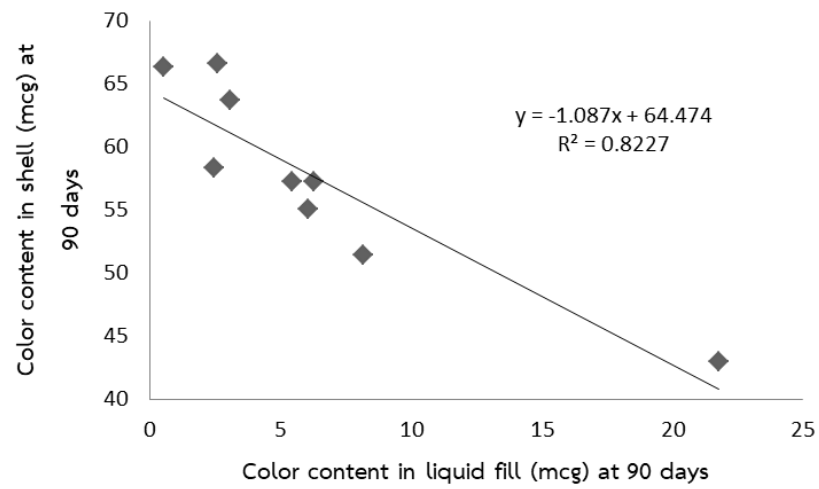


Figure 4- 25 Scatter plot between brilliant blue contents in the liquid fill and shell during storage of colored capsules

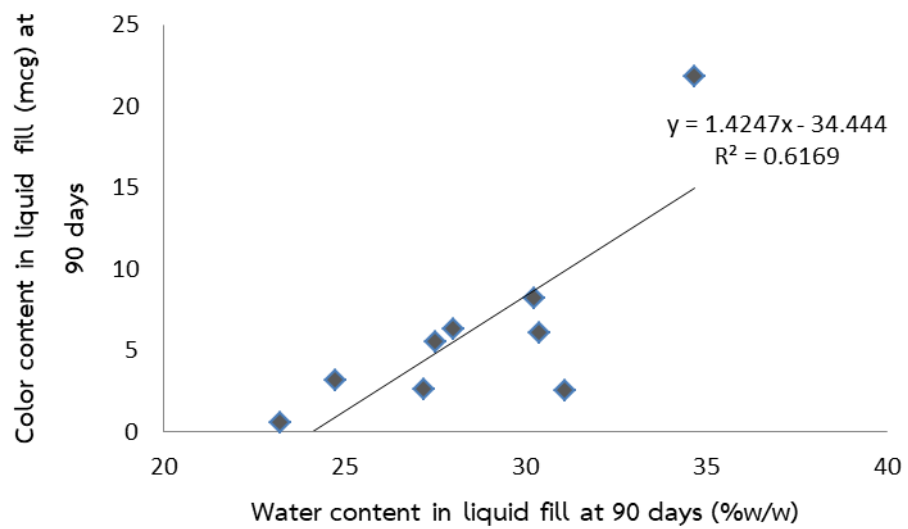


Figure 4- 26 Scatter plot between water contents and brilliant blue contents in liquid fill of colored capsules at 90 days

### 1.8 Investigation of molecular interaction in gelatin shell by Fourier transform infrared spectroscopy (FT-IR)

Gelatin can be cross-linked when exposed to aldehydes and/or stored under stressed conditions of high humidity, temperature and light for a period of time (11, 66).

Spectroscopic techniques such as NIR (74) and FT-IR (73) can be used to investigate gelatin crosslinking. However, the NIR spectrum/ peaks at 1780 and 2200 nm around indicating gelatin cross-linking as reported by Gold et al. was not observed in this study.

Alternatively, the gelatin capsule shells were examined by FT-IR; and the spectrum of freshly prepared soft gelatin capsules, i.e. 1 day after preparation, is shown in Figure 4-27. There was a major peak at  $1632\text{ cm}^{-1}$  of carbonyl stretching for amide I and  $1548\text{ cm}^{-1}$  of C-N stretching vibration and N-H bending for amide II. The peak around  $1033\text{ cm}^{-1}$  was caused by glycerol. The bands at  $3288\text{ cm}^{-1}$  could be due to free water or amide III which has vibrations in plane of C-N and N-H group of bound amide. This results corresponded to that was reported by Tengroth et al.(73).

Gelatin crosslinking caused by formaldehyde could be detected by intensity change at the peak position around 1030 and  $1080\text{ cm}^{-1}$  (73).

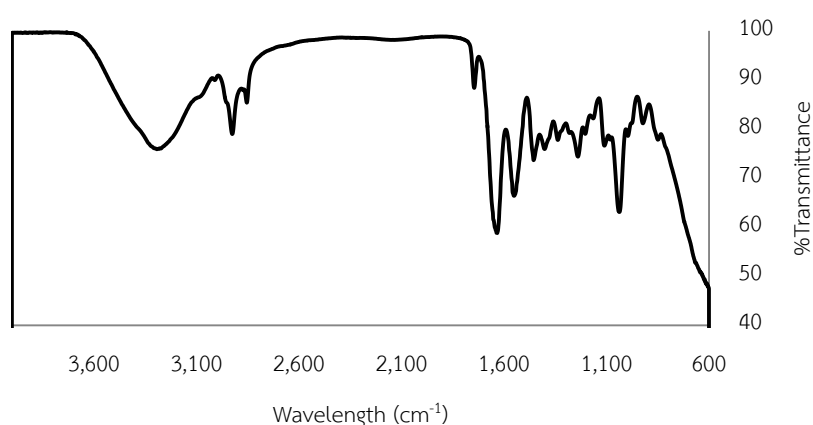


Figure 4- 27 FTIR spectrum of freshly prepared soft gelatin capsule shell

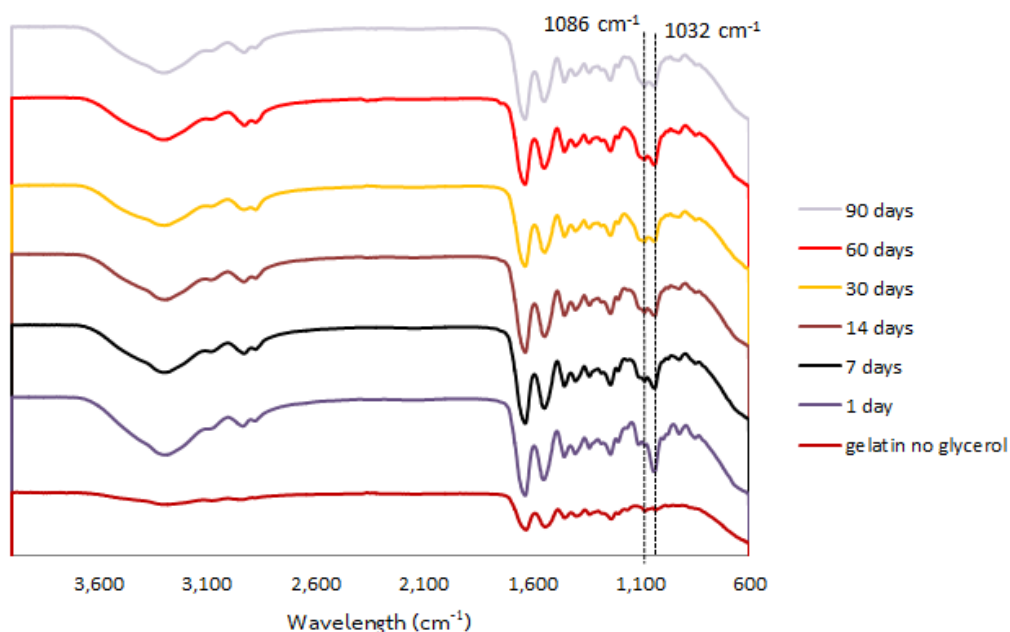


Figure 4- 28 FT-IR spectra of of gelatin capsule shell of non colored formulation 2 containing no ibuprofen at different time points

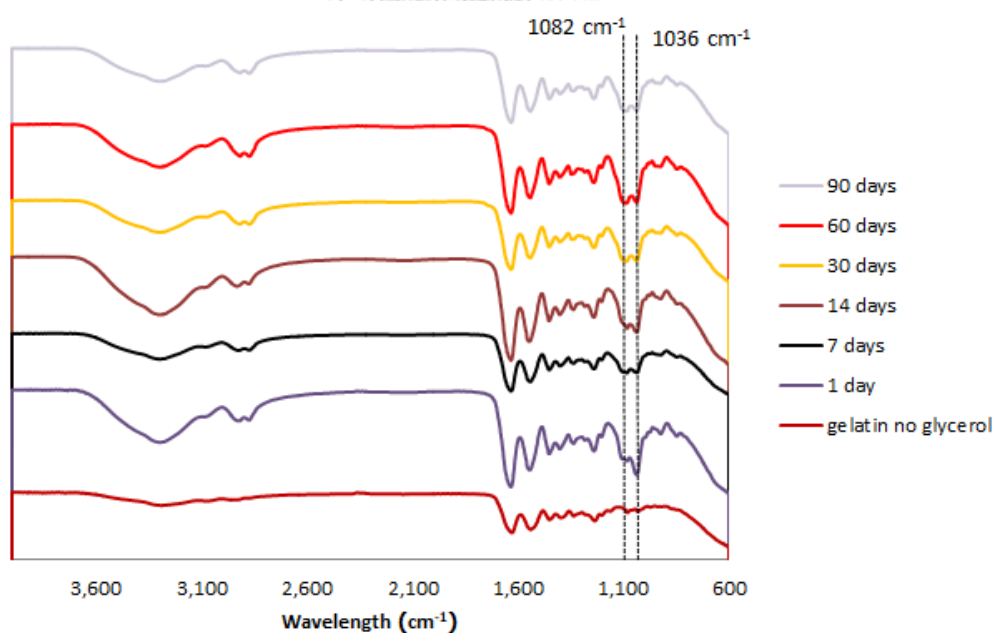


Figure 4- 29 FT-IR spectra of gelatin capsule shell of colored formulation 2 containing no ibuprofen at different time points

All FT-IR spectra of non-colored and colored gelatin shells of different fill formulations are presented in Figure V-1 – Figure V-8 (Appendix V). It was shown that

at 90 days all gelatin shells were crosslinked as the relative intensity between peak 1036 and 1082  $\text{cm}^{-1}$  was changed. However, crosslinking began to occur at different time points for studied fill formulations and the beginning time was also varied between non colored and colored formulations. The beginning of crosslinking in the non colored shells was likely to be different from that in the colored shell as shown in Figure 4-28 – Figure 4-29. The relative intensity between two interested peaks began to change at 14 days for SG-2 and 7 days for CSG-2.

The earliest beginning of crosslinking for non colored (formulation SG-4, SG-6 and SG-9) and colored formulation (formulation CSG-2, CSG-6, CSG-7 and CSG-8), was shown at 7 days. It was hardly related to the fill formulations. It may be caused by other factors such as variation in formaldehyde content and absorbed water. When the maximum remaining formaldehyde was greater, or less consumed formaldehyde, crosslinking began to occur later (Figure 4-30) with significant correlation with p-value = 0.003. While moisture content in capsule shell was higher, beginning of crosslink occurred earlier but it not significant correlated (p-value = 0.103).

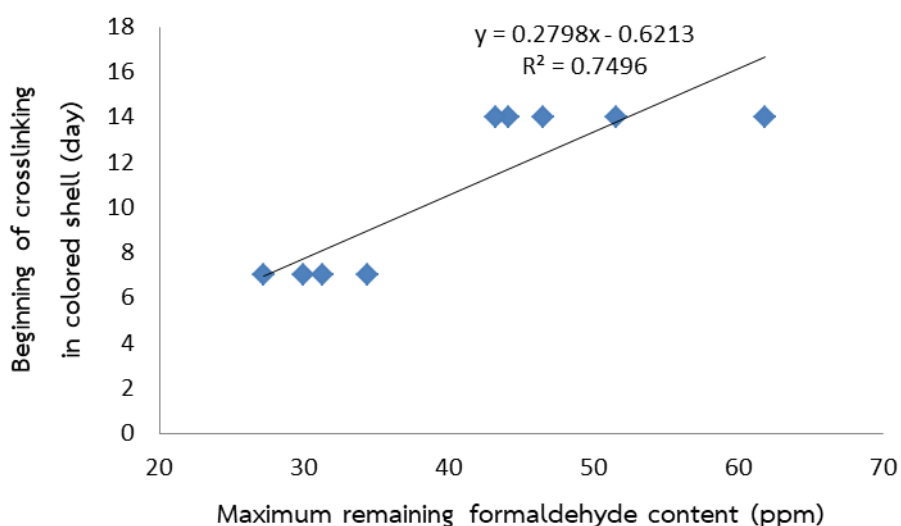


Figure 4- 30 Scatter plot between maximum remaining formaldehyde content during storage and beginning time of crosslinking

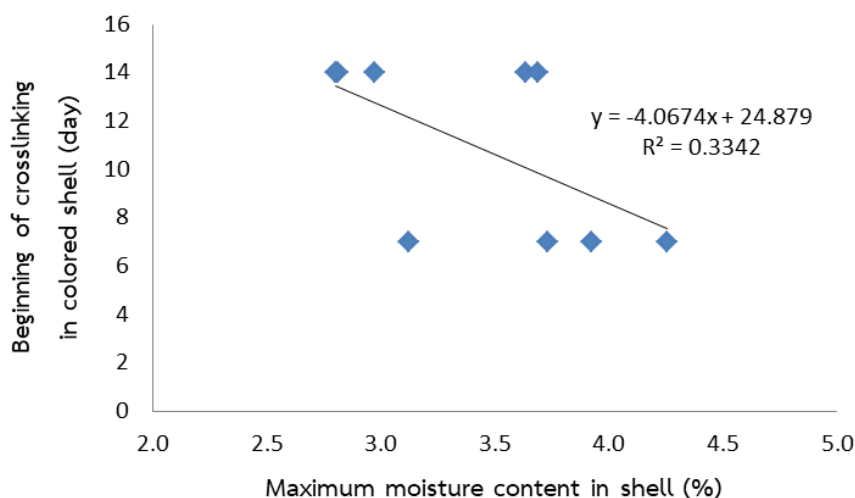


Figure 4- 31 Scatter plot between maximum moisture content in the shell during storage and beginning time of crosslinking

### 1.9 *In vitro* dissolution test

*In vitro* dissolution test can be an evidence to support presence of gelatin crosslinking (75, 104). It has been reported that gelatin crosslinking leads to retardation of *in vitro* dissolution. In this study, ibuprofen which could be dissolved in PEG 600 was chosen as model drug. The dissolution test was studied at 1, 30 and 90 days. The results are shown in Figure VI-1 – Figure VI-4 (Appendix VI). Ibuprofen was released not less than 90% in the pH 7.2 phosphate buffer after 60 min for all non colored and colored formulations after 1 day of preparation. After storage for 90 days, some capsule formulations, such as colored formulation 2 provided retardation of drug release as shown in Figure 4-32, while some capsule formulations such as colored formulation 9 did not (Figure 4-33). This corresponded to FT-IR spectra of formulation 2 and 9 as shown in Figure 4-34 and Figure 4-35, respectively. In addition, pellicle formation was observed for formulation 2 (Figure 4-36), which could explain retarded dissolution.

In general, the dissolution results corresponded to the gelatin crosslinking detected by FT-IR for capsule shells. However, in some formulations, crosslinking started to occur before retardation of dissolution was observed. These formulations were formulation 2 and 8 in which crosslinking started to occur at 30 days but the



ibuprofen dissolution was not retarded. It was possible that crosslinking began only for some capsules; only 1 out of 3 capsules was detected. Also, it may be explained that crosslinking in these capsules occurred only for some parts or fragments of gelatin.

It is noted here that the inclusion of ibuprofen in the fill formulation was found to affect the lag time of gelatin crosslinking as summarized in Figure 4-37.

For example, crosslinking for formulation CSG-2 which contained no ibuprofen began to occur at 7 days (Figure 4-29), while it began to occur at 30 days for formulation CSG-2 which contained ibuprofen (Figure 4-32). In addition, at 90 days, for some colored capsules containing ibuprofen such as formulation 9, crosslinking was not detected due to no change in relative intensity between peak 1036 and 1082  $\text{cm}^{-1}$  and their dissolution profile were not retard as shown in Figure 4-33.

Overall FT-IR and dissolution results suggested that there was existence of gelatin crosslinking which could be caused by formaldehyde formation in the liquid fill and variation of moisture content during storage.

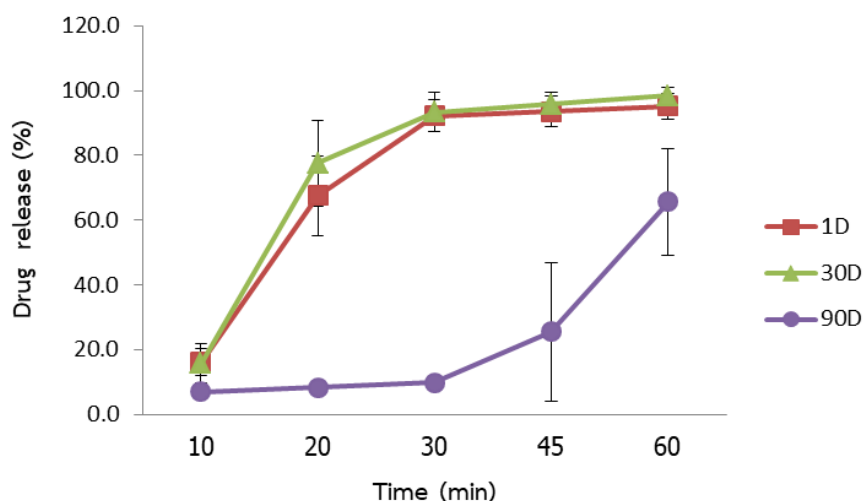


Figure 4- 32 Example of dissolution of cross-linked ibuprofen soft gelatin capsules for colored formulation (CSG-2) at 1 (1D), 30 (30D) and 90 (90D) days

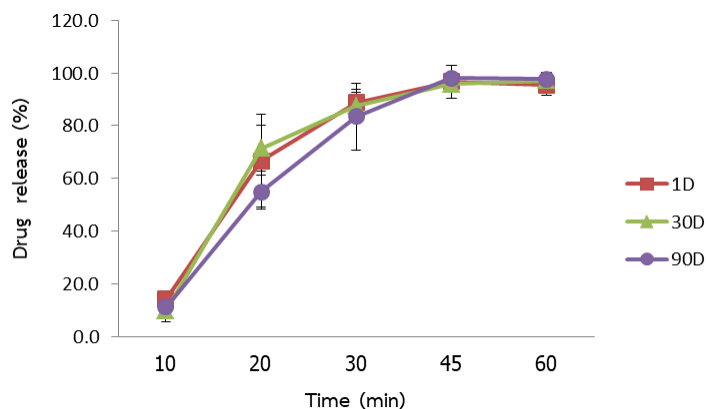


Figure 4- 33 Example of dissolution of cross-linked ibuprofen soft gelatin capsules for colored formulation CSG-9 at 1 (1D), 30 (30D) and 90 (90D) days

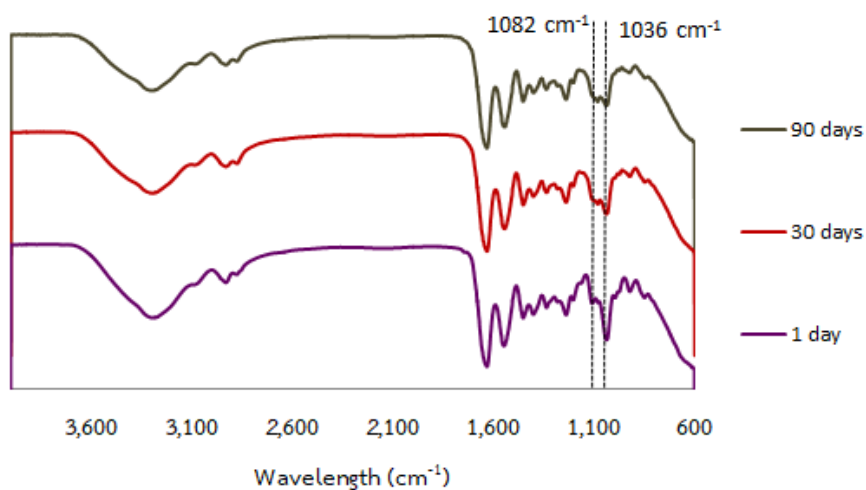


Figure 4- 34 FT-IR spectra of gelatin capsule shell of colored formulation CSG-2 containing ibuprofen at different time points

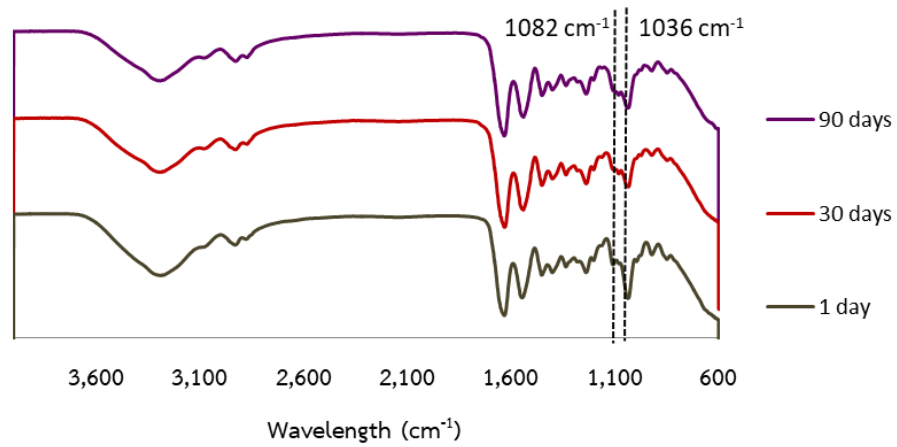


Figure 4- 35 FT-IR spectra of gelatin capsule shell of colored formulation CSG-9 containing ibuprofen at different time points



Figure 4- 36 Example of pellicle formed during dissolution test of colored ibuprofen soft gelatin capsule (CSG-2) at 90 days, after 30 min (a) and 60 min (b)

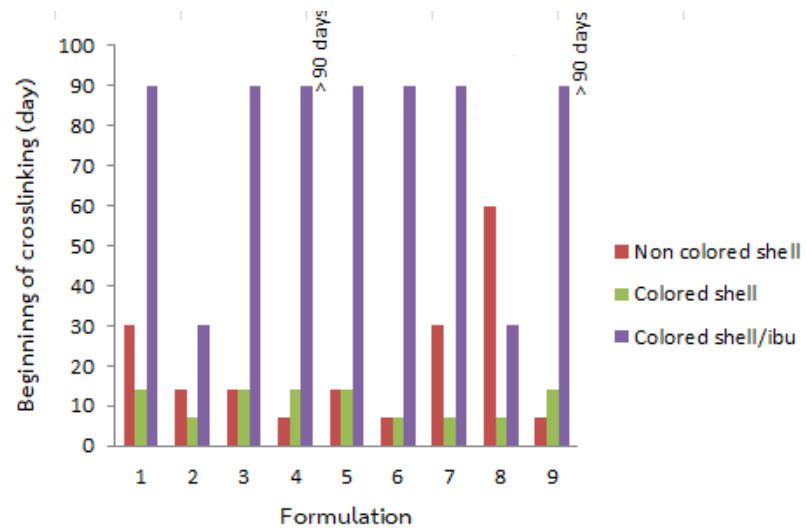


Figure 4- 37 Relative beginning time of gelatin crosslinking for studied formulations



## CHAPTER V

### CONCLUSIONS

In this study, the effect of degradation product of PEG 600 on color fading and crosslinking in soft gelatin capsule shells was investigated. The results could be concluded as the following:

- Under storage condition of 30°C/75%RH for 3 months, autoxidation of PEG 600 occurred in the fill formulations and gave formaldehyde to a certain level. The formation of formaldehyde was proved to be significantly affected by initial water content in the liquid fill. There was no evidence that a maximum level of d- $\alpha$ -tocopherol, i.e. 0.05% used in this study could inhibit autoxidation of PEG.
- The amount of formaldehyde formed could provide color fading and induce crosslinking. However, color fading was more affected by brilliant blue migration from the shell into the liquid fill.
- Water absorbed into the gelatin shell also showed a relation with the presence of crosslinking.

In addition, chemical migration could cause variation in physical and chemical properties, such as hardness and crosslinking, of the soft gelatin capsule studied. Some effects, i.e. the effect of moisture content in the shell on capsule hardness, were more prominent for the non-colored capsules which were less complicated system.

## REFERENCES

1. Gullapalli, R.P. Soft gelatin capsules (softgels). *Journal of Pharmaceutical Sciences*. 2010;99:4107-48.
2. Habiba I. Benza, Munyendo, W.L.L. A review of progress and challenges in soft gelatin capsules formulations for oral administration. *International Journal of Pharmaceutical Sciences Review and Research*. 2011;10:20-4.
3. Cao, N., Yang, X., et al. Effects of various plasticizers on mechanical and water vapor barrier properties of gelatin films. *Food Hydrocolloids*. 2009;23(3):729-35.
4. Glastrup, J. Degradation of polyethylene glycol. A study of the reaction mechanism in a model molecule: Tetraethylene glycol. *Polymer Degradation and Stability*. 1996;52:217-22.
5. Frontini, R., and Mielck, J.B. Formation of formaldehyde in polyethylene glycol and in poloxamer under stress conditions. *International Journal of Pharmaceutics*. 1995;114:121-3.
6. Hemenway, J.N., Carvalho, T.C., et al. Formation of reactive impurities in aqueous and neat polyethylene glycol 400 and effects of antioxidants and oxidation inducers. *Journal of Pharmaceutical Sciences*. 2012;101:3305-18.
7. Bindra, D.S., Williams, T.D., et al. Degradation of O<sup>6</sup>-benzylguanine in aqueous polyethylene glycol 400 (PEG 400) solutions: Concerns with formaldehyde in PEG 400. *Pharmaceutical Research*. 1994;11:1060-4.
8. Johnson, D.M., and Taylor, W.F. Degradation of fenprostalene in polyethylene glycol 400 solution. *Journal of Pharmaceutical Sciences*. 1984;73:1414-7.
9. Meyer, M.C., Straughn, A.B., et al. The effect of gelatin cross-linking on the bioequivalence of hard and soft gelatin acetaminophen capsules. *Pharmaceutical Research*. 2000;17:962-6.
10. Ofner, C.M., Zhang, Y.E., et al. Crosslinking studies in gelatin capsules treated with formaldehyde and in capsules exposed to elevated temperature and humidity. *Journal of Pharmaceutical Sciences*. 2001;90(1):79-88.

11. Venugopal, K., Singh, S. Evaluation of gelatins for cross-linking potential. *Pharmaceutical Technology*. 2001;25:32-4, 6-7.
12. Stability studies of a PEG-free, PVA-based film coating system [Internet]. 2012 [cited 8 December 2015]. Available from: [http://www.colorcon.com/literature/marketing/fc/Opadry%20200/pr\\_aaps2012\\_tecko\\_e\\_opadry200\\_stability.pdf](http://www.colorcon.com/literature/marketing/fc/Opadry%20200/pr_aaps2012_tecko_e_opadry200_stability.pdf).
13. Kolska, Z., Valha, P., et al. Refractometric study of systems water-poly(ethylene glycol) for preparation and characterization of Au nanoparticles dispersion. *Arabian Journal of Chemistry*. 2016;23:1-9.
14. Nassar, M.N., Nesarikar, V.N., et al. Influence of formaldehyde impurity in polysorbate 80 and PEG-300 on the stability of a parenteral formulation of BMS-204352: Identification and control of the degradation product. *Pharmaceutical Development and Technology*. 2004;9:189-95.
15. Waterman, K.C., Arikpo, W.B., et al. N-methylation and N-formylation of a secondary amine drug (varenicline) in an osmotic tablet. *Journal of Pharmaceutical Sciences*. 2008;97:1499-507.
16. Wang, G., Fiske, J.D., et al. Identification and control of a degradation product in Avapro film-coated tablet: Low dose formulation. *Pharmaceutical Development and Technology*. 2008;13:393-9.
17. Hovorka, S.W.a., Neich, C.S. Oxidative degradation of pharmaceuticals : theory, mechanisms and inhibition. *Journal of Pharmaceutical Sciences*. 2000;90:253-69.
18. Wasylaschuk, W.R., Harmon, P.A., et al. Evaluation of hydroperoxides in common pharmaceutical excipients. *Journal of Pharmaceutical Sciences*. 2007;96:106-16.
19. Waterman, K.C., Adami, R.C., et al. Handbook of Isolation and Characterization of Impurities in Pharmaceuticals. Ahuja S, editor. California: Academic Press; 2003.
20. Waterman, K.C., Adami, R.C., et al. Stabilization of pharmaceuticals to oxidative degradation. *Pharmaceutical Development and Technology*. 2002;7:1-32.
21. Walling, C. Some properties of radical reactions important in synthesis. *Tetrahedron*. 1985;41(19):3887-900.

22. Han, S., Kim, C., et al. Thermal/oxidative degradation and stabilization of polyethylene glycol. *Polymer* 1997;38:317-23.
23. McGinity, J.W., Patel, T.R., et al. Implications of peroxide formation in lotion and ointment dosage forms containing polyethylene glycols. *Drug Development Communications*. 1976;2:505-19.
24. Bottom, C.B., Clark, M., et al. Dissolution testing of soft shell capsules—Acetaminophen and nifedipine. *Journal of Pharmaceutical Sciences*. 1997;86:1057-61.
25. Hom, F.S., Veresh, S.A., et al. Soft gelatin capsules II: Oxygen permeability study of capsule shells. *Journal of Pharmaceutical Sciences*. 1975;64:851-7.
26. Li, Z., Kozłowski, B.M., et al. Analysis of aldehydes in excipients used in liquid/semi-solid formulations by gas chromatography-negative chemical ionization mass spectrometry. *Journal of Chromatography A*. 2007;1160:299-305.
27. McGinity, J.W., and Hill, J.A. Influence of peroxide impurities in polyethylene glycols on drug stability. *Journal of Pharmaceutical Sciences*. 1975;64:356-7.
28. Puz, M.J., Johnson, B.A., et al. Use of the antioxidant BHT in asymmetric membrane tablet coatings to stabilize the core to the acid catalyzed peroxide oxidation of a thioether drug. *Pharmaceutical Development and Technology*. 2005;1:115-25.
29. Byun, Y., Kim, Y.T., et al. Characterization of an antioxidant polylactic acid (PLA) film prepared with  $\alpha$ -tocopherol, BHT and polyethylene glycol using film cast extruder. *Journal of Food Engineering*. 2010;100:239-44.
30. Stein, D., and Bindra, D.S. Stabilization of hard gelatin capsule shells filled with polyethylene glycol matrices. *Pharmaceutical Development and Technology*. 2007;12:71-7.
31. Coppola, M., Djabourov, M., et al. Phase diagram of gelatin plasticized by water and glycerol. *Macromolecular Symposia*. 2008;273:56-65.
32. Thomazine, M., Carvalho, R.A., et al. Physical properties of gelatin films plasticized by blends of glycerol and sorbitol. *Journal of Food Science*. 2005;70:172-6.



33. Duconseille, A., Astruc, T., et al. Gelatin structure and composition linked to hard capsule dissolution: A review. *Food Hydrocolloids*. 2015;43:360-76.
34. Hakata, T., Sato, H., et al. Effect of storage temperature on the physicochemical properties of soft gelatin capsule shells. *Chemical & Pharmaceutical Bulletin*. 1994;42:1496-500.
35. Cristea, D., Vilarem, G. Improving light fastness of natural dyes on cotton yarn. *Dyes and Pigments*. 2006;70:238-45.
36. Mroz, C. Coloring agent. In: Rowe RC, Sheskey PJ, editors. *Handbook of Pharmaceutical Excipients*. 7 ed. London: Pharmaceutical Press; 2012. p. 189-96.
37. Nalliah, R.E. Oxone/ $\text{Fe}^{2+}$  degradation of food dyes: demonstration of catalyst-like behavior and kinetic separation of color. *Journal of Chemical Education*. 2015;92:1681-3.
38. Garrett, E.R., Carper, R.F. Prediction of stability in pharmaceutical preparations. I. Color stability in a liquid multisulfa preparation. *Journal of the American Pharmaceutical Association American Pharmaceutical Association*. 1955;44:515-8.
39. Lachman, L., Swartz, C.J., et al. Color stability of tablet formulations. II. Influence of light intensity on the fading of several water-soluble dyes. *Journal of the American Pharmaceutical Association*. 1960;49:165-9.
40. Lachman, L., Weinstein, S., et al. Color stability of tablet formulations. III. Comparative light fastness of several water-soluble dyes and their corresponding lakes. *Journal of Pharmaceutical Sciences*. 1961;50:141-4.
41. Lachman, L., Swartz, C.J., et al. A comprehensive pharmaceutical stability testing laboratory III. A light stability cabinet for evaluating the photosensitivity of pharmaceuticals. *Journal of the American Pharmaceutical Association American Pharmaceutical Association*. 1960;49:213-8.
42. Everhard EM, Goodhart, F.W. Fading of FD&C Red No. 3 in tablets as a function of concentration, time, and light intensity. *Journal of Pharmaceutical Sciences*. 1963;52:281-3.
43. Swartz, C.J., Lachman, L., et al. Color stability of tablet formulations. IV. Protective influence of various colored glasses on the fading of tablets. *Journal of Pharmaceutical Sciences*. 1961;50:145-8.

44. Lachman, L., Urbanyi, T., et al. Color stability of tablet formulations. V. Effect of ultraviolet absorbers on the photostability of colored tablets. *Journal of Pharmaceutical Sciences*. 1962;51:321-6.
45. Hajratwala, B.R. Influence of sunscreens on color stability of tablets coated with certified dyes II: FD & C blue no. 1. *Journal of Pharmaceutical Sciences*. 1974;63:1927-30.
46. Hajratwala, B.R., Hennig, A.J. Influence of sunscreens on color stability of tablets coated with certified dyes III: FD&C yellow no.6. *Journal of Pharmaceutical Sciences*. 1977;66:107-9.
47. Swartz, C.J., Lachman, L., et al. Color stability of tablet formulations. VI. Preliminary study of temperature dependence of colorant loss in tablets at various pH levels. *Journal of Pharmaceutical Sciences*. 1962;51:326-9.
48. Brownley, C.A., and Lachman, L. Preliminary report on the comparative stability of certified colorants with lactose in aqueous solution. *Journal of Pharmaceutical Sciences*. 1963;52:86-93.
49. Kuramoto, R., Lachman, L., et al. A study of the effect of certain pharmaceutical materials on color stability. *Journal of the American Pharmaceutical Association American Pharmaceutical Association*. 1958;47:175-80.
50. Brown, S.R., Haywood, E.A., et al. Factors that affect the discoloration and fading of film coated tablets. Pfizer Global Research & Development.
51. Gosetti, F., Gianotti, V., et al. Oxidative degradation of food dye E133 brilliant blue FCF liquid chromatography–electrospray mass spectrometry identification of the degradation pathway. *Journal of Chromatography A*. 2004;1054:379-87.
52. Nadupalli, S., Dasireddy, V.D.B.C., et al. Kinetics and mechanism of the oxidation of coomassie brilliant blue-R dye by hypochlorite and role of acid therein. *South African Journal of Chemistry*. 2015;68:85-106.
53. Cooper, J.W., Ansel, H.C., et al. Liquid and solid solution interactions of primary certified colorants with pharmaceutical gelatins. *Journal of Pharmaceutical Sciences*. 1973;62:1156-64.

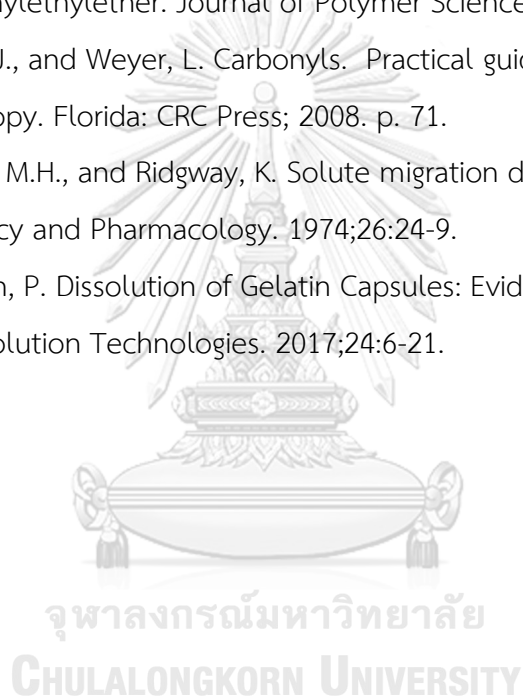
54. Putt, K.S., Kernick, E.R., et al. The use of chromophore and fluorophore degradation to quantitate UV dose: FD&C dyes as chemical identifiers for UV sterilization. *Journal of Microbiological Methods*. 2012;91:215-21.
55. Yasri, N.G., Seddik, H., et al. Spectrophotometric determination of formaldehyde based on the telomerization reaction of tryptamine. *Arabian Journal of Chemistry*. 2015;8:487-94.
56. Liang, C., Huang, C.F., et al. A rapid spectrophotometric determination of persulfate anion in ISCO. *Chemosphere*. 2008;73:1540-3.
57. Turi, P., Brusco, D., et al. Rapid determination of color stability of tablet formulations. *Journal of Pharmaceutical Sciences*. 1972;61:1811-4.
58. Turi, P., Tausendfreund, R.A., et al. Rapid evaluation of effect of excipients on color fading II. *Journal of Pharmaceutical Sciences*. 1974;63:1309-11.
59. Urbanyi, T., Swartz, C.J., et al. Color Stability of Tablet Formulations I\* Measurement of Changes in Individual Tablet Reflectance. *Journal of the American Pharmaceutical Association*. 1960;49:163-4.
60. Colour Measurements and Modeling. 2010. In: *Nondestructive Evaluation of Food Quality* [Internet]. Springer-Verlag Berlin Heidelberg; [17-40].
61. Dey, M., Enever, R., et al. The dissolution and bioavailability of etodolac from capsules exposed to conditions of high relative humidity and temperatures. *Pharmaceutical Research*. 1993;10:1295-300.
62. Chafetz, L., Hong, W.H., et al. Decrease in the rate of capsule dissolution due to formaldehyde from polysorbate 80 autoxidation. *Journal of Pharmaceutical Sciences*. 1984;73:1186-8.
63. Chafetz, L., Hong, W.-H., et al. Decrease in the rate of capsule dissolution due to formaldehyde from polysorbate 80 autoxidation. *Journal of Pharmaceutical Sciences*. 1984;73:1186-8.
64. Han, S., Kim, C., et al. Thermal degradation of poly(ethyleneglycol). *Polymer Degradation and Stability*. 1995;47:203-8.
65. Boughen, L., Liggat, J., et al. Thermal degradation of polyethylene glycol 6000 and its effect on the assay of macroprolactin. *Clinical Biochemistry*. 2010;43:750-3.

66. Digenis, G.A., Gold, T.B., et al. Cross-linking of gelatin capsules and its relevance to their in vitro-in vivo performance. *Journal of Pharmaceutical Sciences*. 1994;83:915-21.
67. Desai, D.S., Rubitski, B.A., et al. Effect of formaldehyde formation on dissolution stability of hydrochlorothiazide bead formulations. *International Journal of Pharmaceutic*. 1994;107:141-7.
68. Ofner, C.M., Zhang, Y.E., et al. Crosslinking studies in gelatin capsules treated with formaldehyde and in capsules exposed to elevated temperature and humidity. *Journal of Pharmaceutical Sciences*. 2001;90:79-88.
69. Albert, K., Peter, B., et al. Crosslinking of Gelatin with Formaldehyde; a  $^{13}\text{C}$  NMR Study. *A Journal of Chemical Sciences*. 1986:351-8.
70. Albert, K., and Bayer, E. Investigation of the hardening reaction of gelatin with  $^{13}\text{C}$  labeled formaldehyde by solution and solid state  $^{13}\text{C}$  NMR spectroscopy. *Zeitschrift für Naturforschung*. 1991;46:385-90.
71. Salsa, T., Pina, M.E., et al. Crosslinking of gelatin in the reaction with formaldehyde: An FT-IR spectroscopic study. *Applied Spectroscopy*. 1996;50:1314-8.
72. Hakata, T., Sato, H., et al. Effect of formaldehyde on the physicochemical properties of soft gelatin capsule shells. *Chemical & Pharmaceutical Bulletin*. 1994;42:1138-42.
73. Tengroth, C., Gasslander U., et al. Cross-linking of gelatin capsules with formaldehyde and other aldehydes: an FTIR spectroscopy study. *Pharmaceutical Development and Technology*. 2005;10:405-12.
74. Gold, T.B., Buice, R.G., et al. Detection of formaldehyde-induced crosslinking in soft elastic gelatin capsules using near-infrared spectrophotometry. *Pharmaceutical Development and Technology*. 1998;3:209-14.
75. Johnson, B.F., Mcauley, P.V., et al. The effects of storage upon in vitro and in vivo characteristics of soft gelatin capsules containing digoxin. *Journal of Pharmacy and Pharmacology*. 1977;29:576-8.
76. Reich, G. Near-infrared spectroscopy and imaging: basic principles and pharmaceutical applications. *Advanced Drug Delivery Reviews*. 2005;57:1109-43.

77. Rinnan, Å., Nørgaard, L., et al. Data Pre-processing. In: Sun D-W, editor. Infrared spectroscopy for food quality analysis and control. London: Academic Press 2009. p. 29-50.
78. Rinnan, S., Berg, F.V.D., et al. Review of the most common pre-processing techniques for near-infrared spectra. *TrAC Trends in Analytical Chemistry*. 2009;28:1201-22.
79. Tong, P., Du, Y., et al. Improvement of NIR model by fractional order Savitzky–Golay derivation (FOSGD) coupled with wavelength selection. *Chemometrics and Intelligent Laboratory Systems*. 2015;143:40-8.
80. Owen, A.J. Uses of derivative spectroscopy. In: Technologies A, editor. 1995.
81. Broad, N., Graham, P., et al. Guidelines for the Development and Validation of Near-infrared Spectroscopic Methods in the Pharmaceutical Industry. In: Chalmers JM, and Griffiths PR, editors. *Handbook of Vibrational Spectroscopy*. Chichester: John Wiley & Sons Ltd; 2002. p. 1-21.
82. Li, X., Fang, D., et al. Application of Fourier Transform near-infrared spectroscopy combined with high-performance liquid chromatography in rapid and simultaneous determination of essential components in crude radix scrophulariae. *American Association of Pharmaceutical Scientists*. 2012;13(4):1428-35.
83. Water. In: Workman J, Weyer L, editors. *Practical guide to interpretive near-infrared spectroscopy*. Florida: CRC Press; 2008. p. 63.
84. Cho, S., Chung, H., et al. Determination of water content in ethanol by miniaturized near-infrared (NIR) system. *Bulletin of the Korean Chemical Society*. 2005;26:115-8.
85. Zhou, X., Hines, P., et al. Moisture determination in hygroscopic drug substances by near infrared spectroscopy. *Journal of Pharmaceutical and Biomedical Analysis*. 1998;17:219-25.
86. Mantanus, J., Ziemons, E., et al. Moisture content determination of pharmaceutical pellets by near infrared spectroscopy: method development and validation. *Analytica Chimica Acta*. 2009;642:186-92.

87. Potthast, H., Dressman, J.B., et al. Biowaiver monographs for immediate release solid oral dosage forms: Ibuprofen. *Journal of Pharmaceutical Sciences*. 2005;94:2121-31.
88. Patel, M.S., Morton, F.S.S., et al. Factors affecting the chemical stability of carboxylic acid drugs in enhanced solubility system (ESS) softgel formulations based on polyethylene glycol (PEG). *Drug Development and Industrial Pharmacy*. 2008;18(1):1-19.
89. Quinn, M. Alpha Tocopherol. In: Rowe RC, Sheskey PJ, editors. *Handbook of Pharmaceutical Excipients*. 7 ed. London: Pharmaceutical Press; 2012. p. 210.
90. Barrio, M.A., Hu, J., et al. Simultaneous determination of formic acid and formaldehyde in pharmaceutical excipients using headspace GC/MS. *Journal of Pharmaceutical and Biomedical Analysis*. 2006;41:738-43.
91. Pleass, W.B. The absorption of water by gelatin: Part VII. The influence of temperature on swelling in acid solutions and the combination of gelatin with hydrochloric, nitric or sulphuric acid. *Biochemical Journal*. 1931;25:1943-8.
92. Serajuddin, T.M., Chshaeng, P., et al. Water migration from soft gelatin capsule shell to fill material and its effect on drug solubility. *Journal of Pharmaceutical Sciences*. 1986;75:62-4.
93. Armstrong, N.A., Pugh, W.K., et al. Drug migration into soft gelatin capsule shells and its effect on in-vitro availability. *Journal of Pharmacy and Pharmacology* 1984;36:361-5.
94. Bhunia, K., Sablani, S.S., et al. Migration of chemical compounds from packaging polymers during microwave, Conventional Heat Treatment, and Storage. *Comprehensive Reviews in Food Science and Food Safety*. 2013;12:523-45.
95. Reich, G. Formulation and physical properties of soft capsules. In: Podczek F, and Jones BE, editors. *Pharmaceutical Capsules*. London, UK Pharmaceutical Press; 2004.
96. Nazzal, S., and Wang, Y. Characterization of soft gelatin capsules by thermal analysis. *International Journal of Pharmaceutics*. 2001;230:35-45.
97. Cantor, S.L. In: Augsburger LL, and Hoag SW, editors. *Pharmaceutical Dosage Forms - Tablets*. 3<sup>th</sup> ed. Florida: CRC Press; 2008. p. 285.

98. Bista, R.K., Bruch, R.F. Near-infrared spectroscopy of newly developed PEGylated lipids. *Spectrochimica Acta Part A: Molecular and Biomolecular Spectroscopy*. 2008;71:410-6.
99. Macrogols. *European Pharmacopoeia 8.0*. Strasbourg July 2016. p. 2665-7.
100. Shelley, R., Bush, D., et al. Effect of aldehyde-induced crosslinking on the molecular weight of the softgel shell and on the disintegration time for placebo softgels stored at accelerated stability conditions. 2015.
101. Snavely, D.L., and Dubsy, J. Near-IR spectra of polyethylene, polyethylene glycol, and polyvinylethylether. *Journal of Polymer Sciences*. 1996;34:2575-9.
102. Workman, J., and Weyer, L. *Carbonyls. Practical guide to interpretive near-infrared spectroscopy*. Florida: CRC Press; 2008. p. 71.
103. Rubinstein, M.H., and Ridgway, K. Solute migration during granule drying. *Journal of Pharmacy and Pharmacology*. 1974;26:24-9.
104. Lu, X., Shah, P. Dissolution of Gelatin Capsules: Evidence and Confirmation of Cross-Linking. *Dissolution Technologies*. 2017;24:6-21.





APPENDICES

จุฬาลงกรณ์มหาวิทยาลัย  
CHULALONGKORN UNIVERSITY



### Appendix I: Physicochemical properties of soft gelatin capsules

Table I- 1 Average thickness (mm, n = 3) of non colored gelatin capsule shells

TIME (DAY)	SG-1	SG-2	SG-3	SG-4	SG-5	SG-6	SG-7	SG-8	SG-9
1	0.53	0.76	0.77	0.54	0.72	0.63	0.79	0.60	0.96
7	0.73	0.63	0.78	0.79	0.66	0.67	0.65	0.92	0.79
14	0.82	0.61	0.56	0.85	0.64	0.72	0.73	0.86	0.66
30	0.78	0.64	0.98	0.65	0.77	0.79	0.79	0.65	0.58
60	0.84	0.69	0.74	0.82	0.61	0.83	0.69	0.77	0.68
90	0.67	0.77	0.75	0.65	0.87	0.79	0.82	0.76	0.73

Table I- 2 Average thickness (mm, n = 3) of colored gelatin capsule shells

TIME (DAY)	CSG-1	CSG-2	CSG-3	CSG-4	CSG-5	CSG-6	CSG-7	CSG-8	CSG-9
1	0.80	0.80	0.70	0.85	0.68	0.73	0.78	0.79	0.71
7	0.45	0.37	0.64	0.43	0.43	0.60	0.41	0.64	0.58
14	0.49	0.47	0.46	0.46	0.48	0.44	0.45	0.58	0.55
30	0.78	0.85	0.71	0.71	0.57	0.77	0.77	0.74	0.76
60	0.80	0.78	0.80	0.89	0.82	0.92	0.90	0.75	0.92
90	0.65	0.77	0.78	0.88	0.83	0.92	0.85	0.82	0.66

Table I- 3 Formaldehyde content (n=2, ppm) in the liquid fill of colored capsules determined by GC-MS and model M36-2 of NIR technique

Formulation	1 day		14 days		30 days		90 days	
	GC-MS	NIR	GC-MS	NIR	GC-MS	NIR	GC-MS	NIR
CSG-1	36.18	988.85	61.87	2357.89	26.74	4599.13	4.84	3595.14
CSG-2	25.72	2144.37	30.01	4582.40	15.82	3737.32	5.84	4421.21
CSG-3	44.10	985.34	35.58	3759.70	21.41	3618.93	7.15	4583.16
CSG-4	34.21	765.70	43.28	1417.13	22.61	2508.89	5.96	3968.19
CSG-5	37.80	421.05	46.53	1398.39	18.77	2508.84	6.44	4449.07
CSG-6	29.68	2702.04	31.26	3083.68	24.58	4449.85	6.29	4828.88
CSG-7	23.95	2233.91	27.18	2855.03	18.65	4400.00	5.37	5374.75
CSG-8	32.20	1713.63	34.42	1904.88	13.54	4238.99	6.10	4859.92
CSG-9	51.56	1908.53	28.99	1816.87	19.94	2514.99	14.25	4888.26

## Appendix II: Statistical analysis

Table II- 1 ANOVA results for capsule hardness at 90 days

Measured response	df	Adj SS	Adj MS	F-value	R <sup>2</sup>	Adj-R <sup>2</sup>	Pred-R <sup>2</sup>	P-value
Hardness	9	1578752	175417	2.11	70.3%	36.92%	0.00%	0.154
Block	1	433660	433660	5.20	-	-	-	0.052
Water	2	559922	279961	3.36	-	-	-	0.087
d- $\alpha$ -tocopherol	2	365758	182879	2.19	-	-	-	0.174
Water* d- $\alpha$ -tocopherol	4	219412	54853	0.66	-	-	-	0.638

SS = sum of squares; df = degree of freedom; MS = mean of squares; Adj-R<sup>2</sup> = adjusted R<sup>2</sup>; Pred-R<sup>2</sup> = predicted R<sup>2</sup>

Table II- 2 ANOVA results for % moisture content in capsule shells at 90 days

Measured response	df	Adj SS	Adj MS	F-value	R <sup>2</sup>	Adj-R <sup>2</sup>	Pred-R <sup>2</sup>	P-value
Moisture content	9	7.4917	0.8324	2.17	70.90	38.16%	0.00%	0.145
Block	1	2.8032	2.8032	7.29	%	-	-	0.027
Water	2	0.9628	0.4814	1.25	-	-	-	0.336
d- $\alpha$ -tocopherol	2	2.9144	1.4572	3.79	-	-	-	0.069
Water* d- $\alpha$ -tocopherol	4	0.8113	0.2028	0.53	-	-	-	0.719

SS = sum of squares; df = degree of freedom; MS = mean of squares; Adj-R<sup>2</sup> = adjusted R<sup>2</sup>; Pred-R<sup>2</sup> = predicted R<sup>2</sup>

Table II- 3 ANOVA results for formaldehyde content in liquid fill at 14 days

Measured response	df	Adj SS	Adj MS	F-value	R <sup>2</sup>	Adj-R <sup>2</sup>	Pred-R <sup>2</sup>	P-value
Formaldehyde content	8	1991.8	248.97	5.79	83.73 %	69.26%	34.91%	0.008
Water	2	1530.3	765.15	17.79	-	-	-	0.001
d- $\alpha$ -tocopherol	2	221.0	110.51	2.57	-	-	-	0.131
Water* d- $\alpha$ -tocopherol	4	240.5	60.12	1.40	-	-	-	0.310

SS = sum of squares; df = degree of freedom; MS = mean of squares; Adj-R<sup>2</sup> = adjusted R<sup>2</sup>; Pred-R<sup>2</sup> = predicted R<sup>2</sup>

Table II- 4 ANOVA results for % increase of formaldehyde at 14 days

Measured response	df	Adj SS	Adj MS	F-value	R <sup>2</sup>	Adj-R <sup>2</sup>	Pred-R <sup>2</sup>	P-value
%Increase of Formaldehyde	8	15992	1999.0	6.60	85.44 %	72.5%	41.76	0.005
Water	2	10428	5214.0	17.22	-	-	-	0.001
d- $\alpha$ -tocopherol	2	1932	966.2	3.19	-	-	-	0.090
Water* d- $\alpha$ -tocopherol	4	3631	907.8	3.00	-	-	-	0.079

SS = sum of squares; df = degree of freedom; MS = mean of squares; Adj-R<sup>2</sup> = adjusted R<sup>2</sup>; Pred-R<sup>2</sup> = predicted R<sup>2</sup>

Table II- 5 ANOVA results for delta E at 90 days

Measured response	df	Adj SS	Adj MS	F-value	R <sup>2</sup>	Adj-R <sup>2</sup>	Pred-R <sup>2</sup>	P-value
Delta E	9	73.310	8.146	3.21	78.30%	53.90%	0.00%	0.058
Block	1	44.347	44.347	17.47	-	-	-	0.003
Water	2	11.594	5.797	2.28	-	-	-	0.164
d- $\alpha$ -tocopherol	2	5.400	2.700	1.06	-	-	-	0.389
Water* d- $\alpha$ -tocopherol	4	11.969	2.992	1.18	-	-	-	0.389

SS = sum of squares; df = degree of freedom; MS = mean of squares; Adj-R<sup>2</sup> = adjusted R<sup>2</sup>; Pred-R<sup>2</sup> = predicted R<sup>2</sup>

Table II- 6 Two-sample independent t-test between total color contents in the capsules at 1 and 90 days

Formulation	df	Estimate for difference	P-value
CSG-1	2	2.99	0.234
CSG-2	2	-0.28	0.903
CSG-3	2	3.79	0.022*
CSG-4	2	1.88	0.200
CSG-5	2	6.11	0.021*
CSG-6	2	7.179	0.006*
CSG-7	2	0.53	0.865
CSG-8	2	6.96	0.027*
CSG-9	2	7.95	0.104

df = degree of freedom

Appendix III: Pretreatment of NIR spectra, and calibration and validation of PLS models for prediction of water in liquid fill

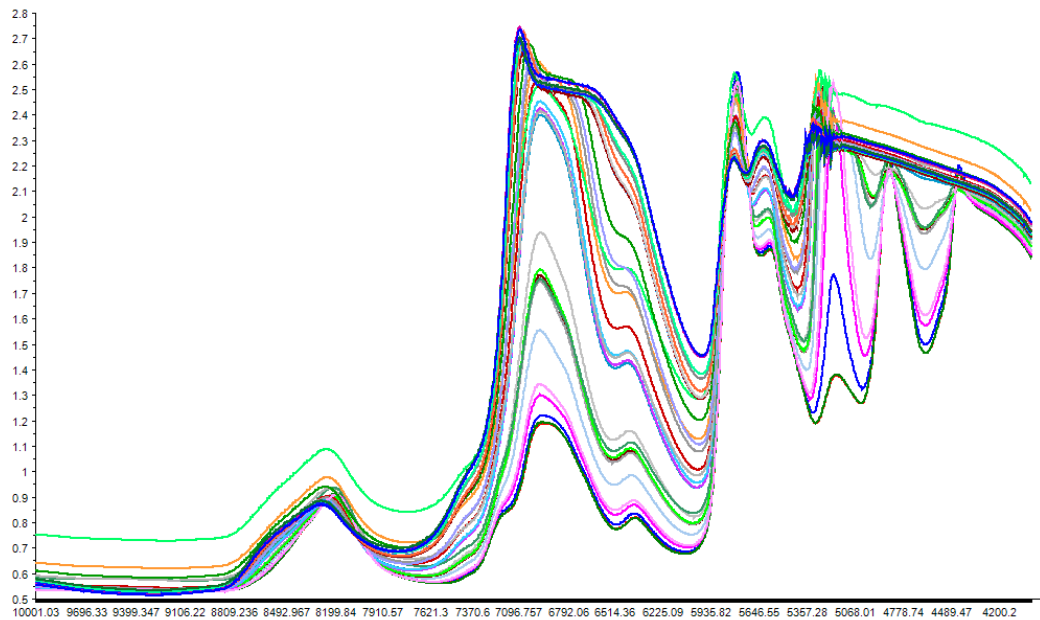


Figure III- 1 Pretreatment of NIR spectra for PLS model W1: No pretreatment

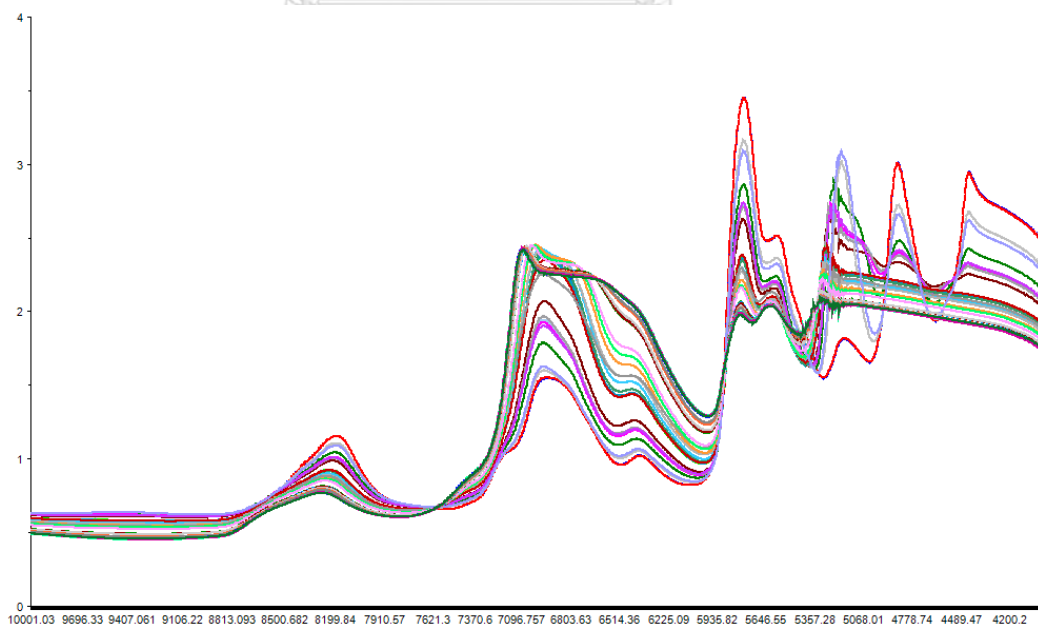


Figure III- 2 Pretreatment of NIR spectra for PLS model W2: MSC

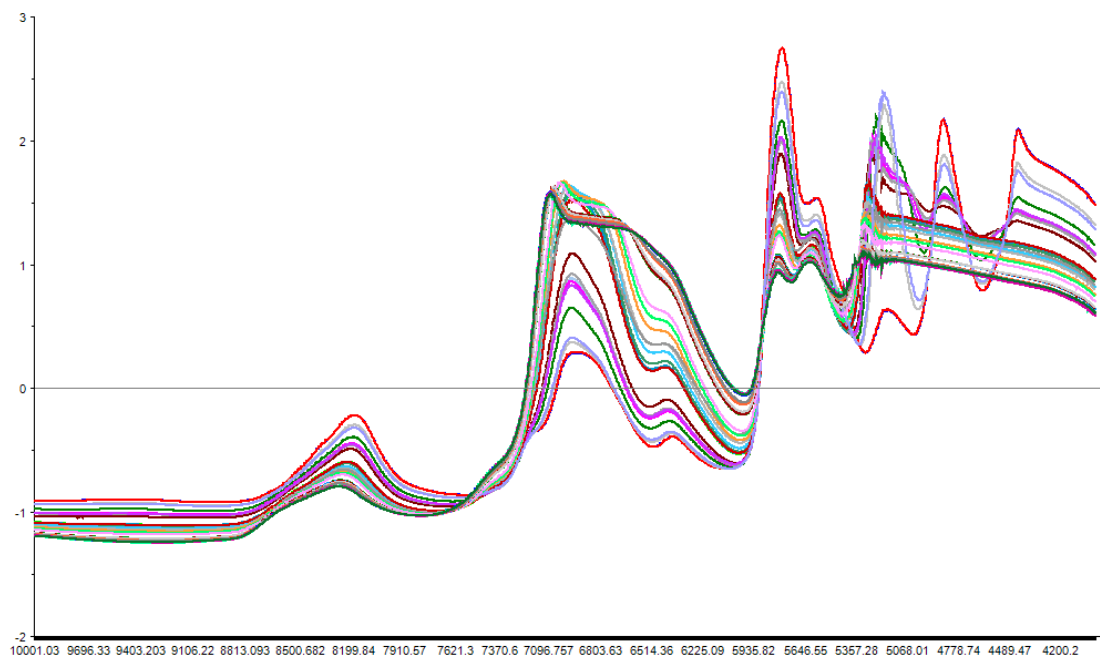


Figure III- 3 Pretreatment of NIR spectra for PLS model W3: SNV

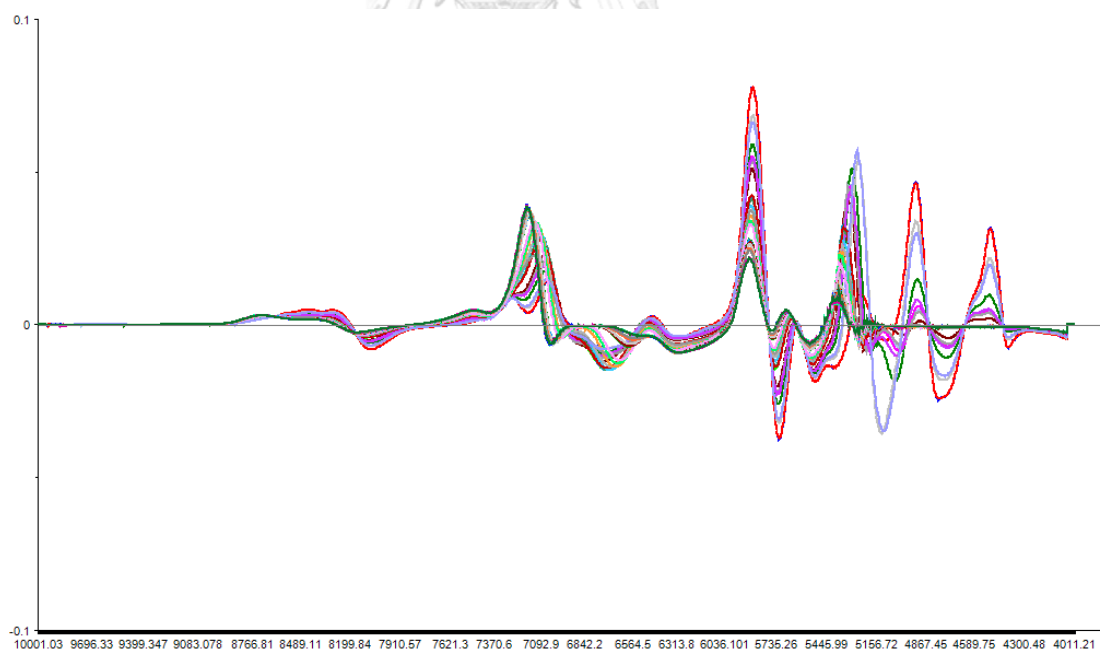


Figure III- 4 Pretreatment of NIR spectra for PLS model W4: MSC 1<sup>st</sup> derivative with Norris-Williams

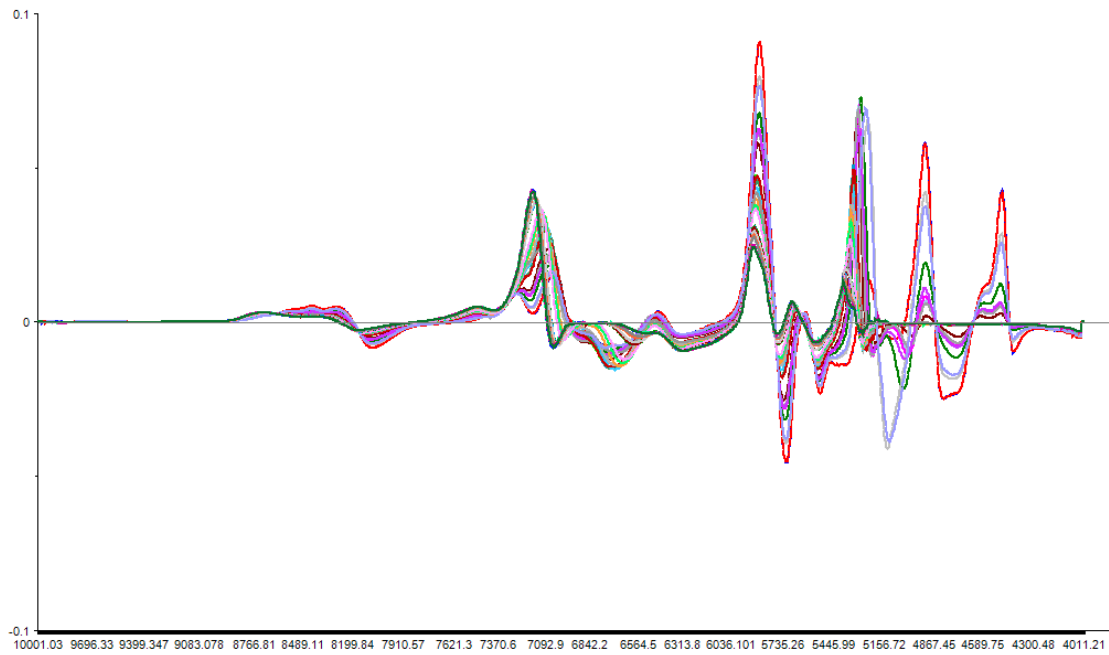


Figure III- 5 Pretreatment of NIR spectra for PLS model W5: MSC 1<sup>st</sup> derivative with Savitzky-Golay

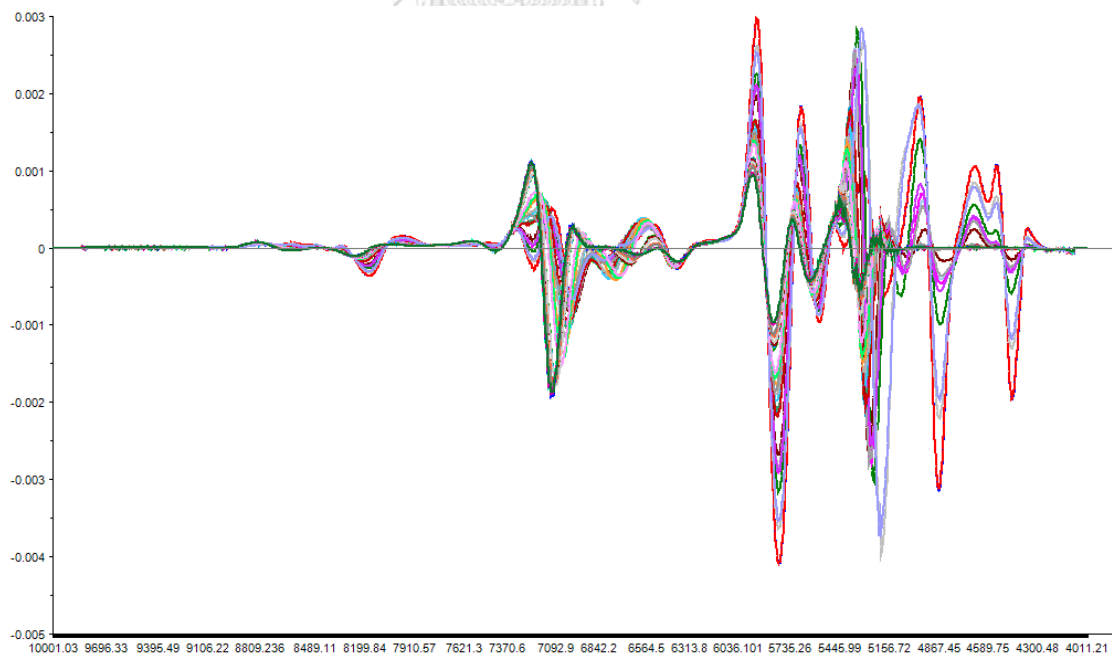


Figure III- 6 Pretreatment of NIR spectra for PLS model W6: MSC 2<sup>nd</sup> derivative with Norris-Williams



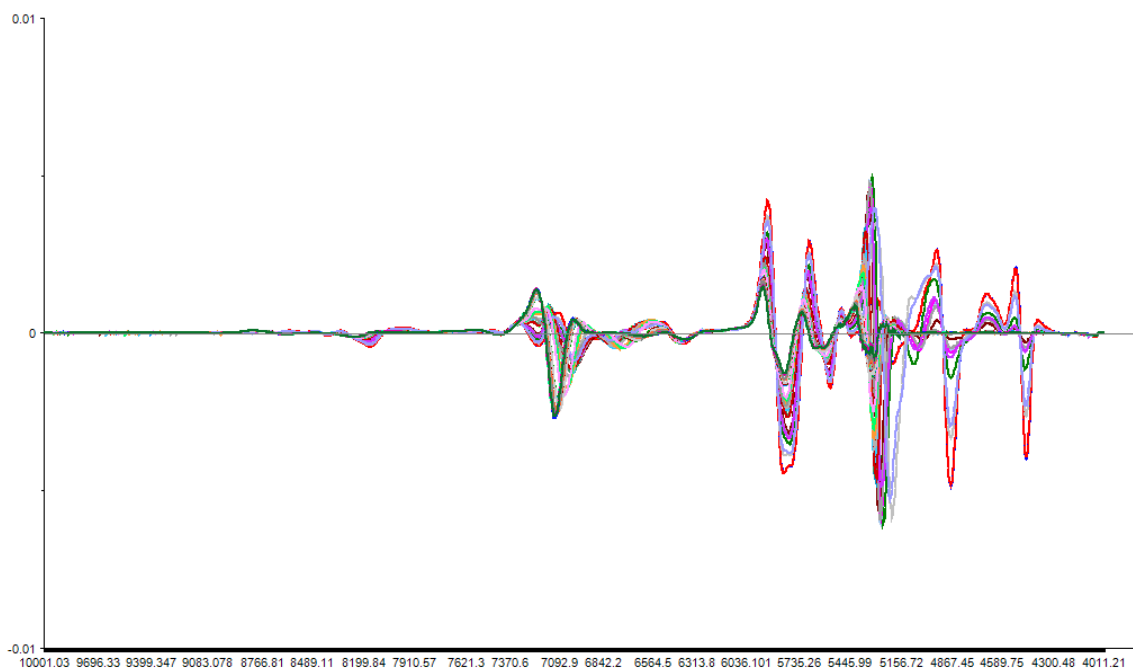


Figure III- 7 Pretreatment of NIR spectra for PLS model W7: MSC 2<sup>nd</sup> derivative with Savitzky-Golay

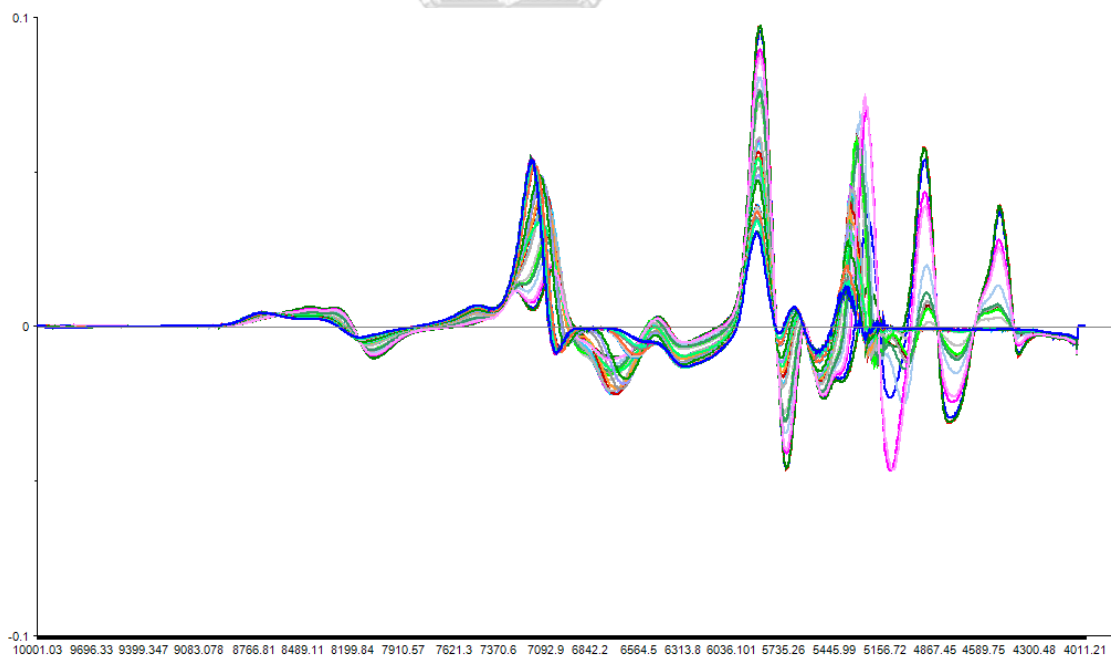


Figure III- 8 Pretreatment of NIR spectra for PLS model W8: SNV 1<sup>st</sup> derivative with Norris-Williams

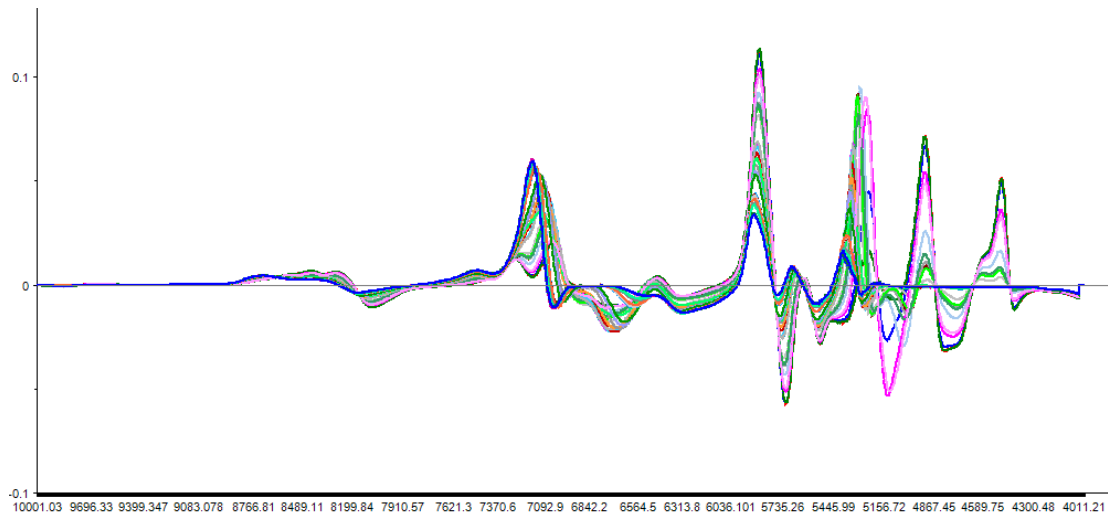


Figure III- 9 Pretreatment of NIR spectra for PLS model W9: SNV 1<sup>st</sup> derivative with Savitzky-Golay

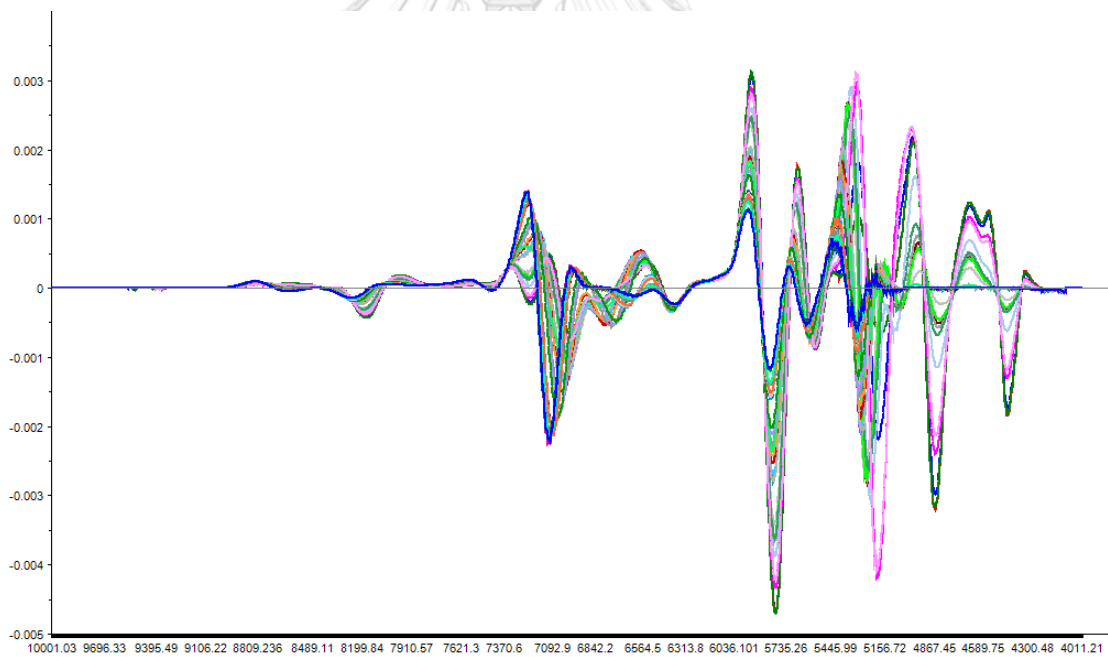


Figure III- 10 Pretreatment of NIR spectra for PLS model W10: SNV 2<sup>nd</sup> derivative with Norris-Williams

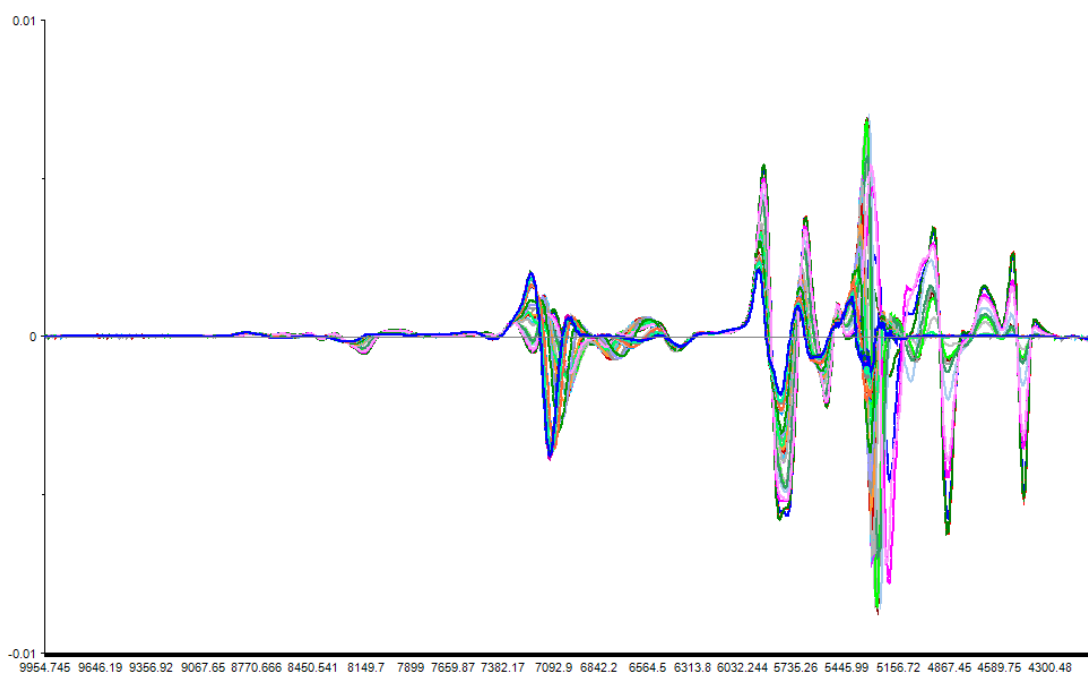


Figure III- 11 Pretreatment of NIR spectra for PLS model W11: SNV 2<sup>nd</sup> derivative with Savitzky-Golay

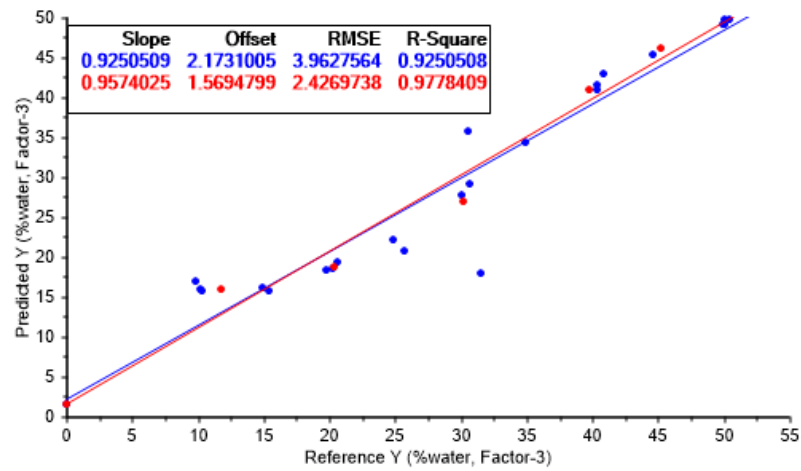


Figure III- 12 Calibration and validation of PLS model W1

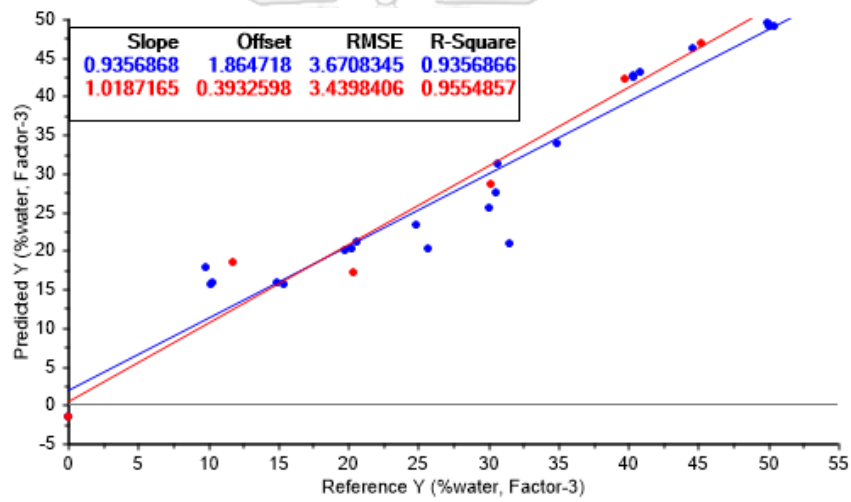


Figure III- 13 Calibration and validation of PLS model W2

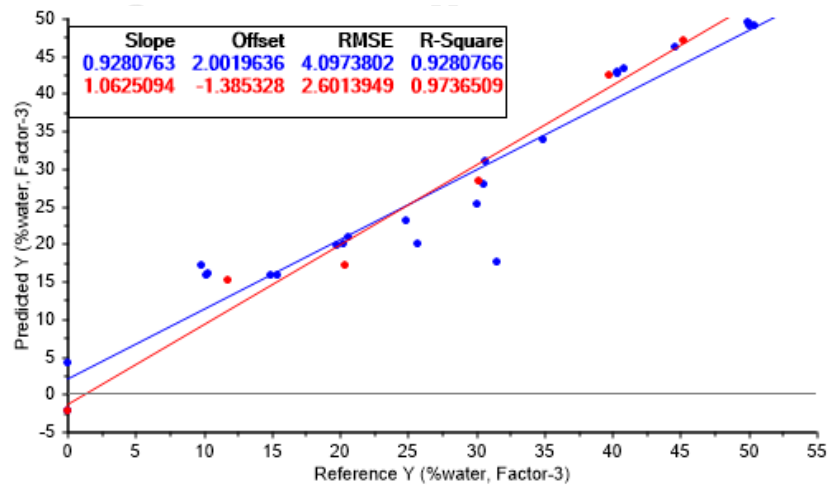


Figure III- 14 Calibration and validation of PLS model W3

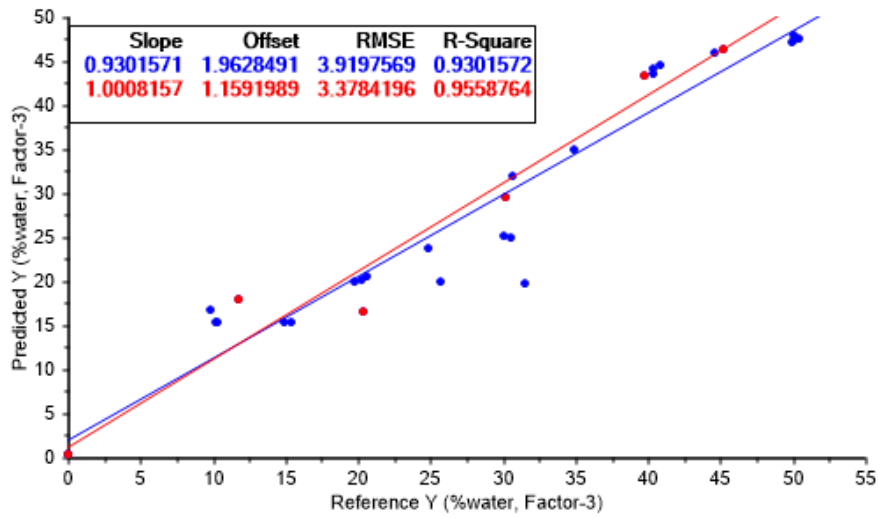


Figure III- 15 Calibration and validation of PLS model W4

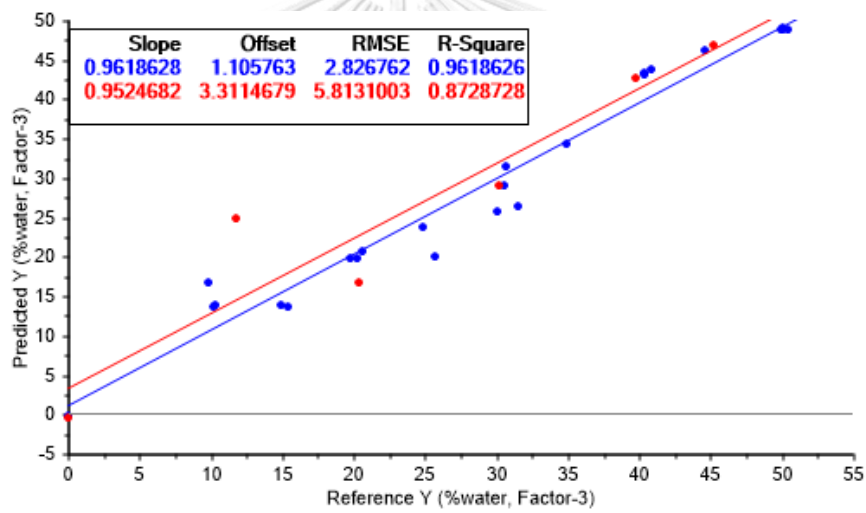


Figure III- 16 Calibration and validation of PLS model W5

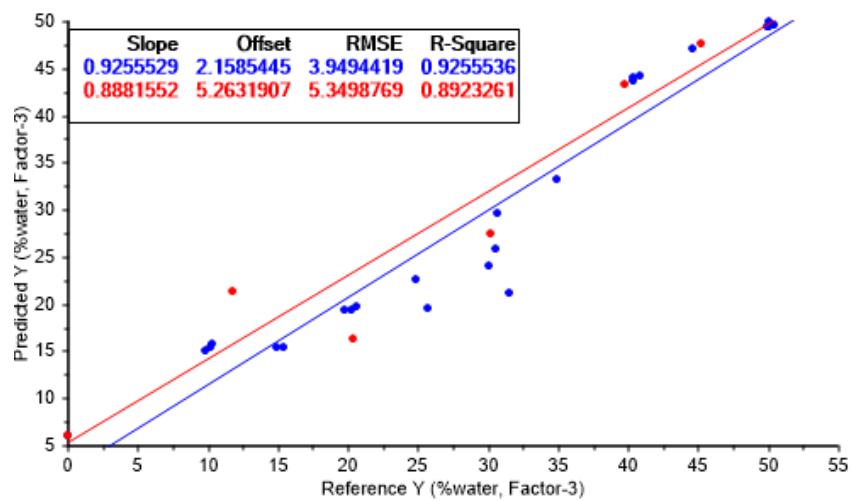


Figure III- 17 Calibration and validation of PLS model W6

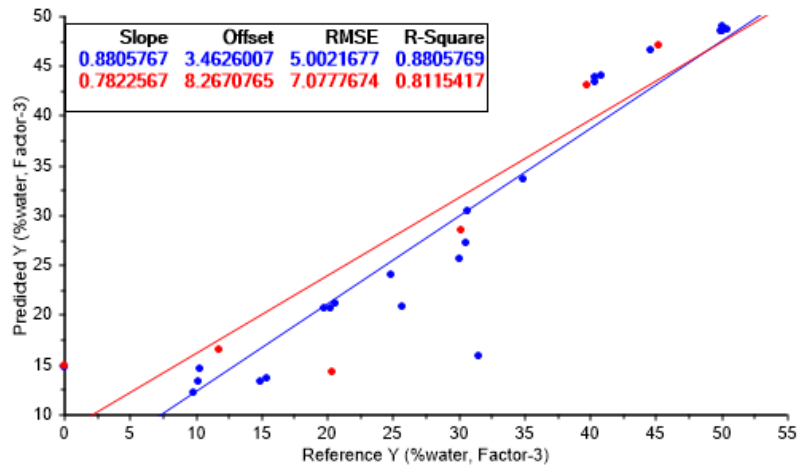


Figure III- 18 Calibration and validation of PLS model W7

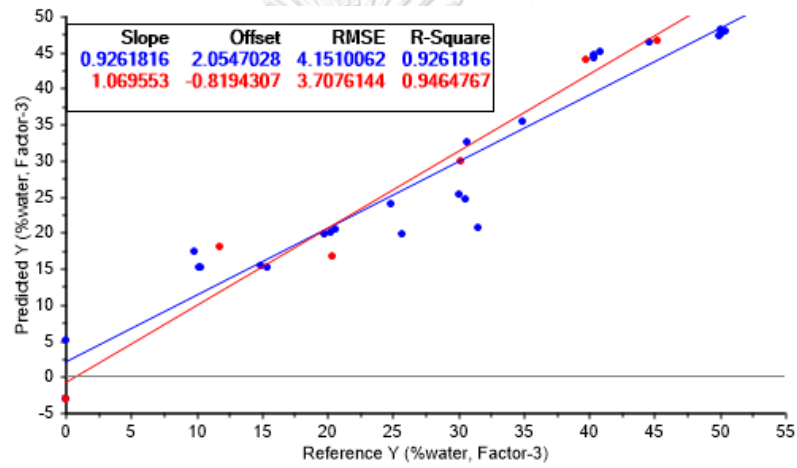


Figure III- 19 Calibration and validation of PLS model W8

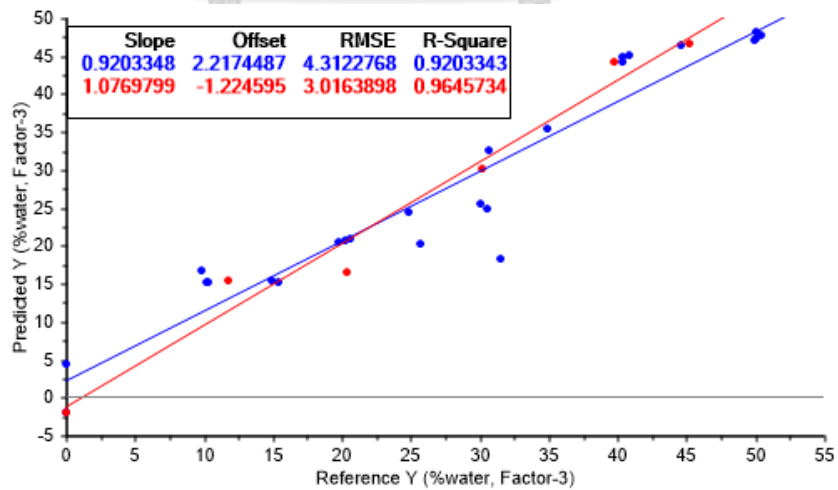


Figure III- 20 Calibration and validation of PLS model W9

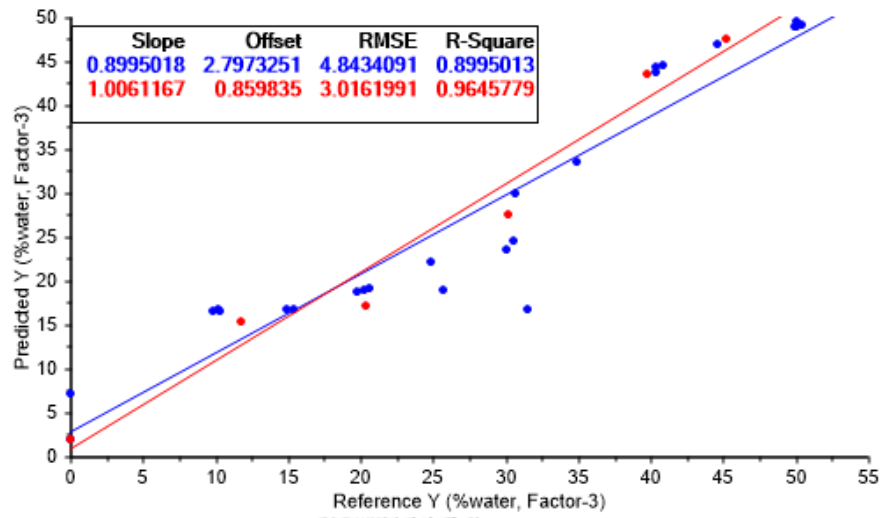


Figure III- 21 Calibration and validation of PLS model W10

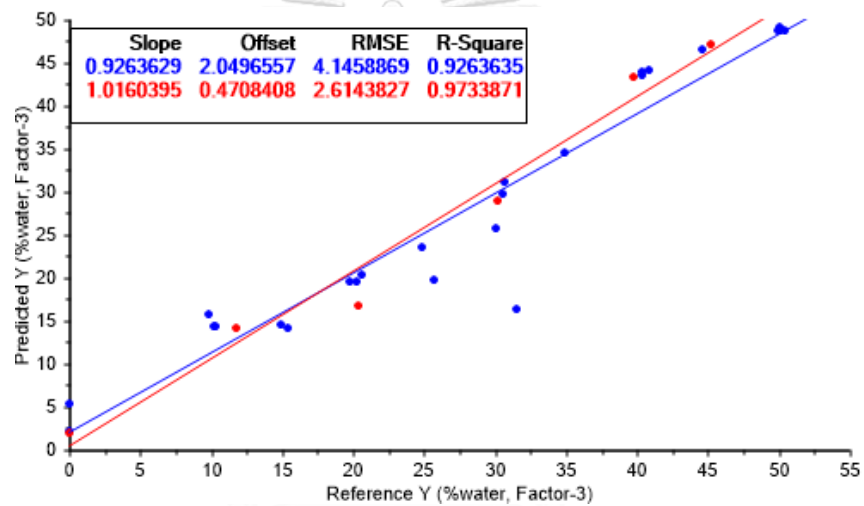


Figure III- 22 Calibration and validation of PLS model W11

Appendix IV: Pretreatment of NIR spectra and calibration and validation of the PLS models for prediction of formaldehyde in liquid fill

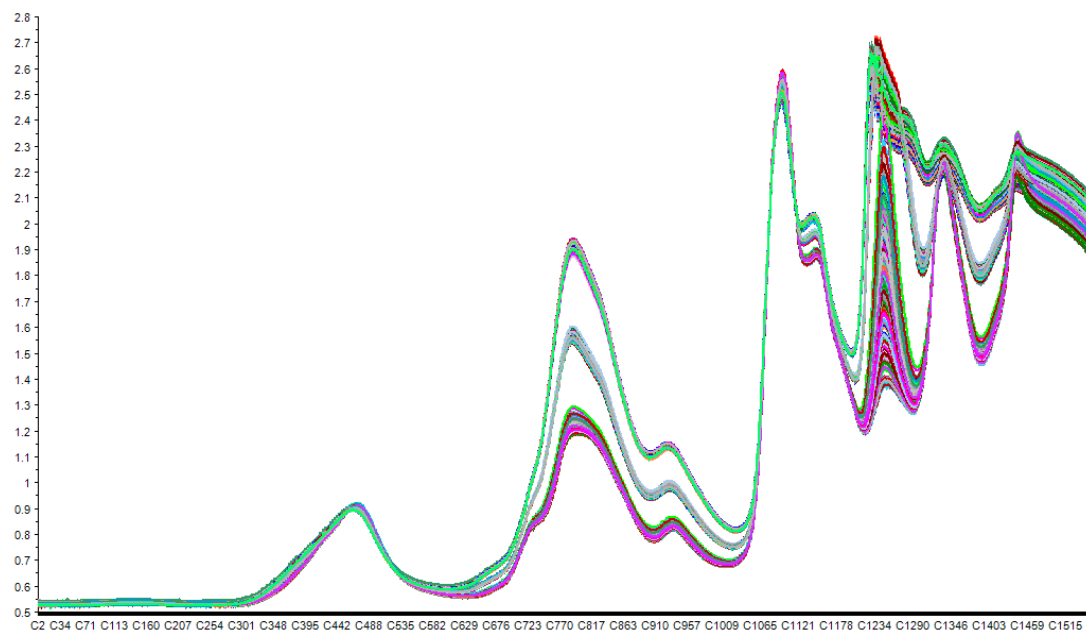


Figure IV- 1 Pretreatment of NIR spectra for PLS model M34: No pretreatment

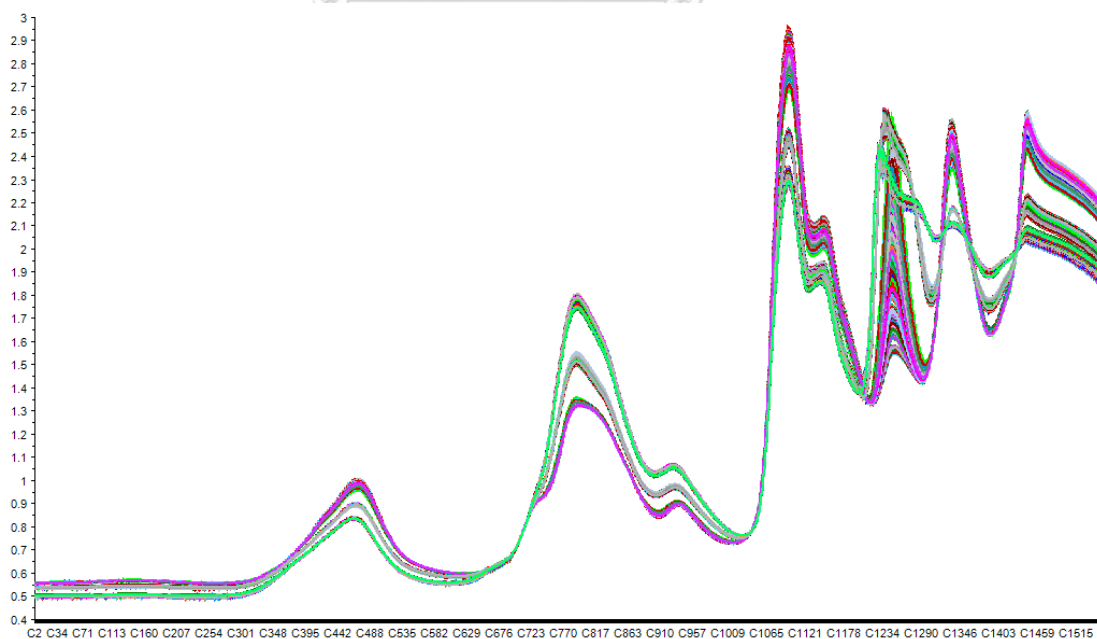


Figure IV- 2 Pretreatment of NIR spectra for PLS model M35: MSC



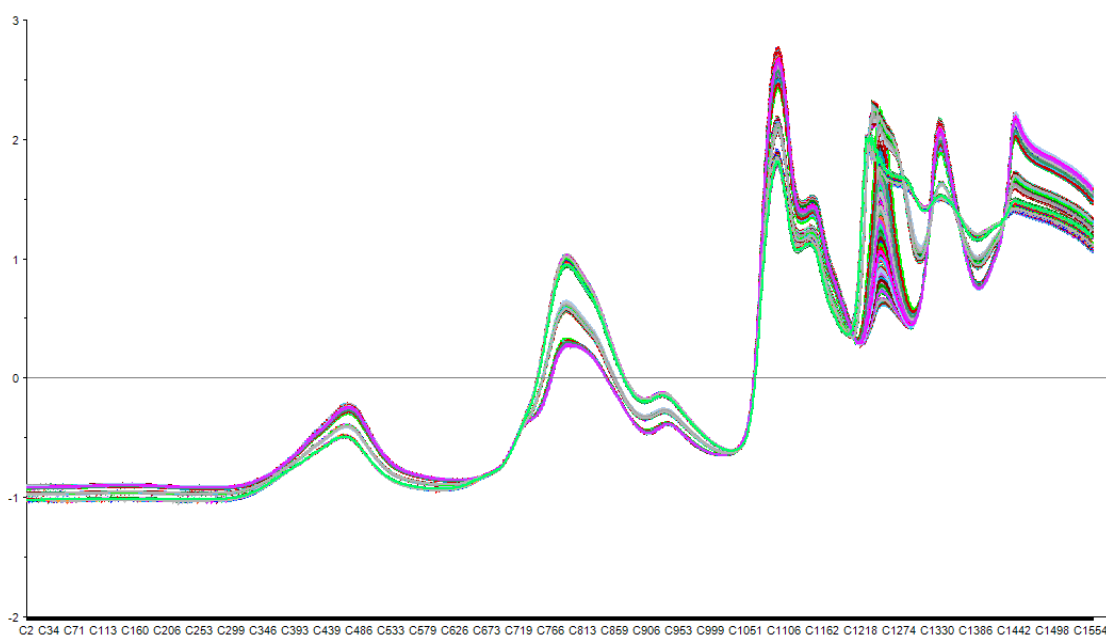


Figure IV- 3 Pretreatment of NIR spectra for PLS model M36: SNV

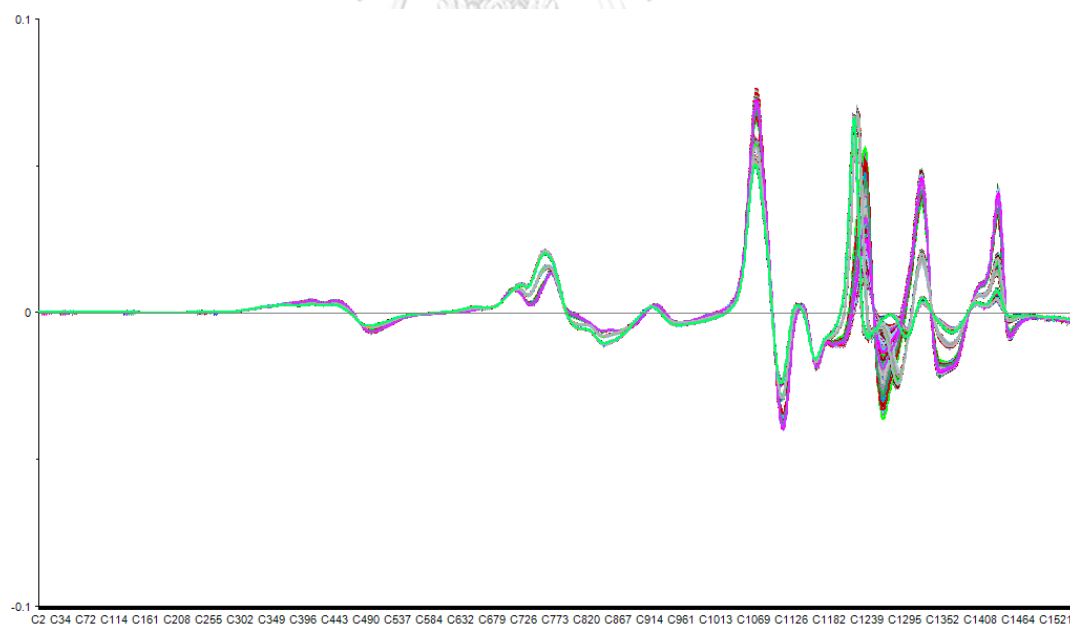


Figure IV- 4 Pretreatment of NIR spectra for PLS model M37: MSC 1<sup>st</sup> derivative with Norris-Williams

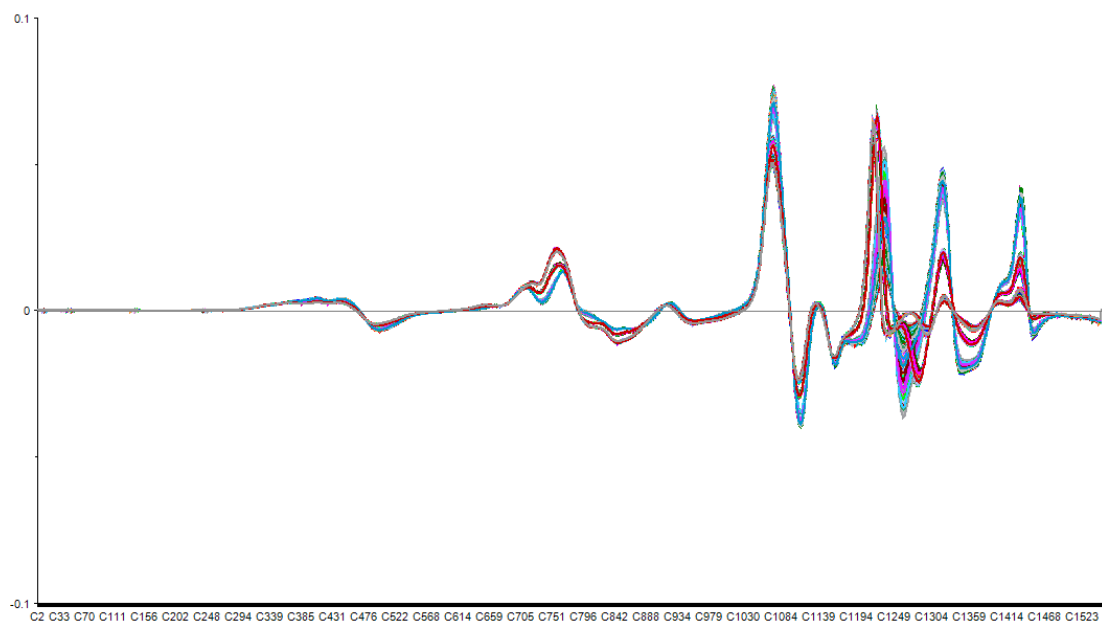


Figure IV- 5 Pretreatment of NIR spectra for PLS model M38: MSC 1<sup>st</sup> derivative with Savitzky-Golay

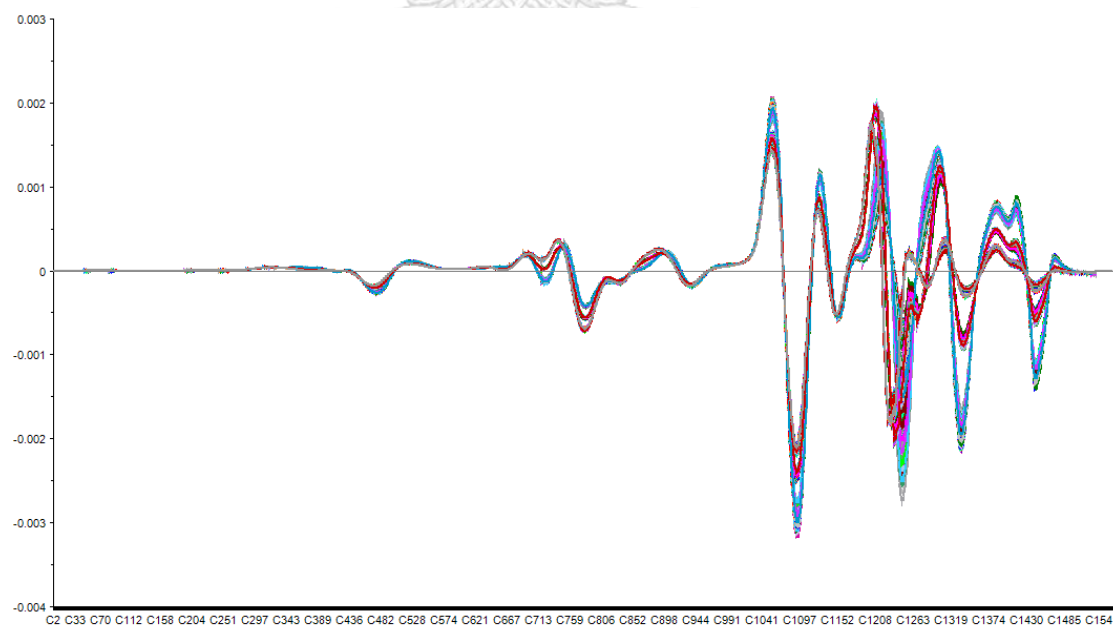


Figure IV- 6 Pretreatment of NIR spectra for PLS model M39: MSC 2<sup>nd</sup> derivative with Norris-Williams

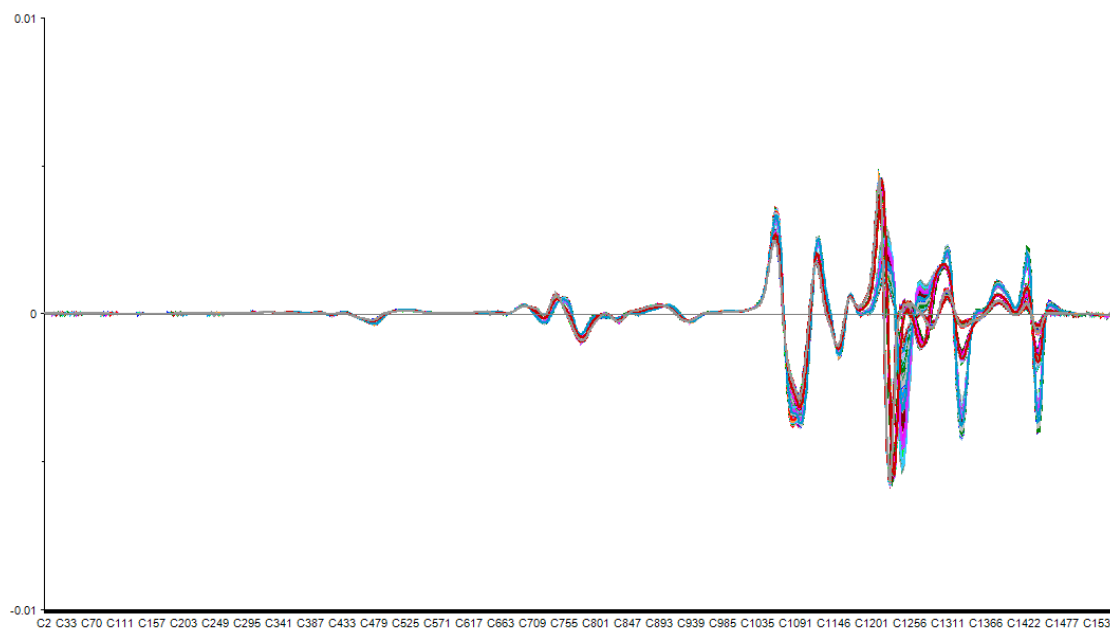


Figure IV- 7 Pretreatment of NIR spectra for PLS model M40: MSC 2<sup>nd</sup> derivative with Savitzky-Golay

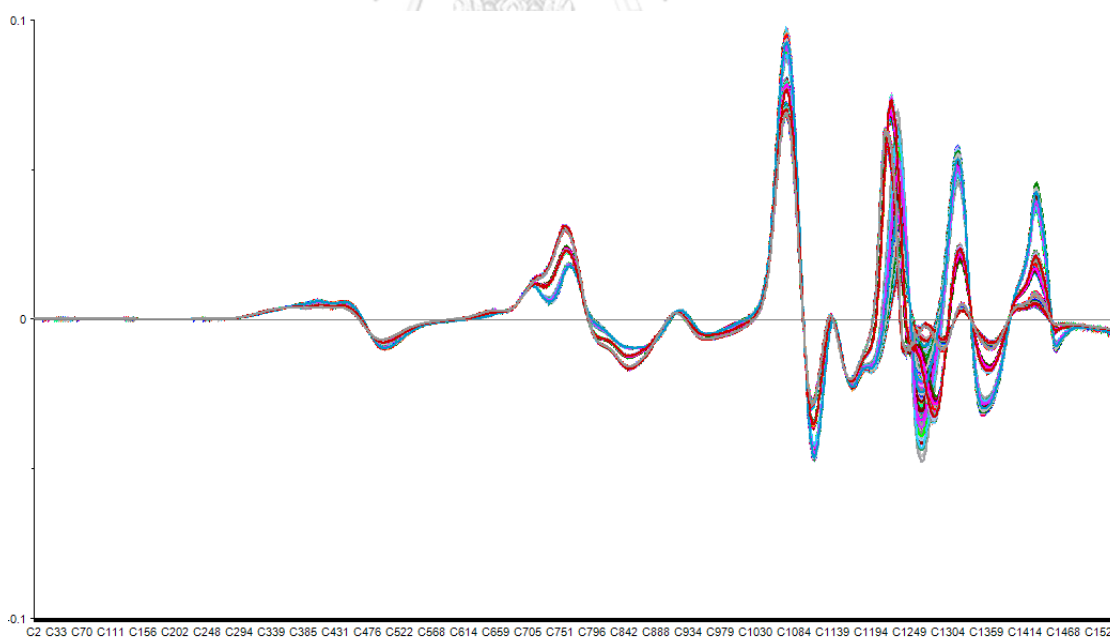


Figure IV- 8 Pretreatment of NIR spectra for PLS model M41: SNV 1<sup>st</sup> derivative with Norris-Williams

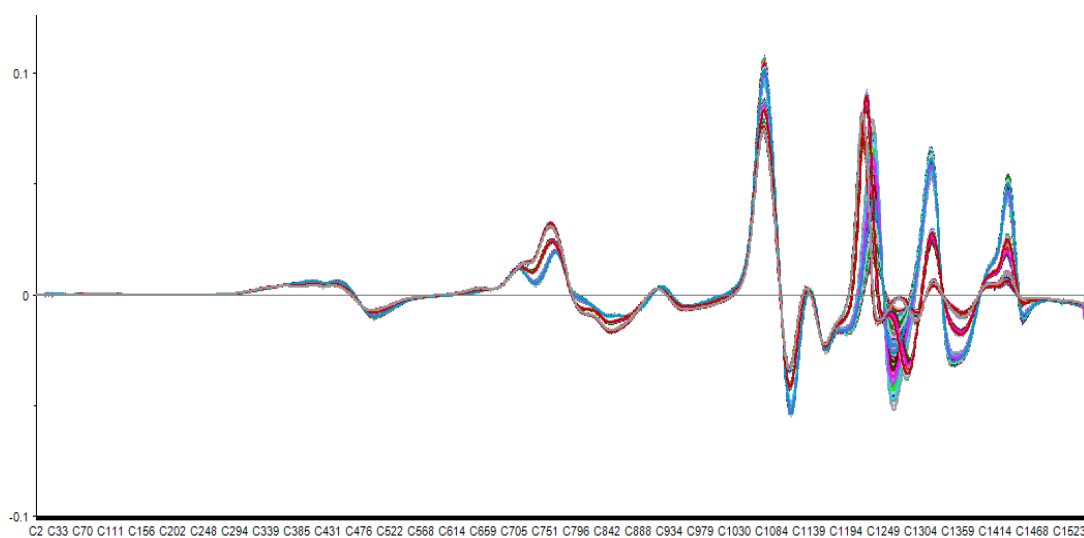


Figure IV- 9 Pretreatment of NIR spectra for PLS model M42: SNV 1<sup>st</sup> derivative with Savitzky-Golay

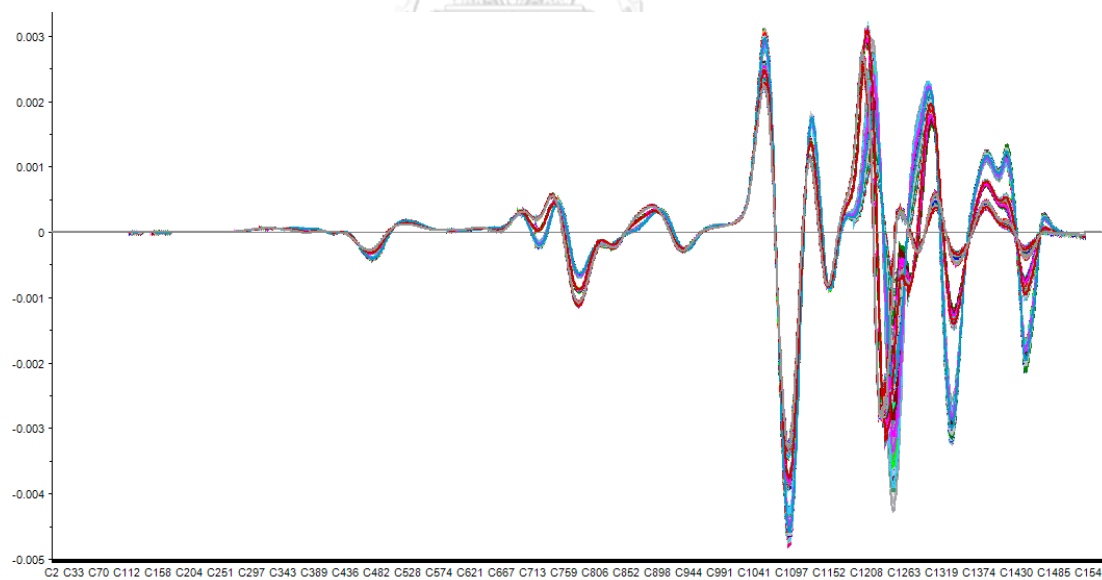


Figure IV- 10 Pretreatment of NIR spectra for PLS model M43: SNV 2<sup>nd</sup> derivative with Norris-Williams

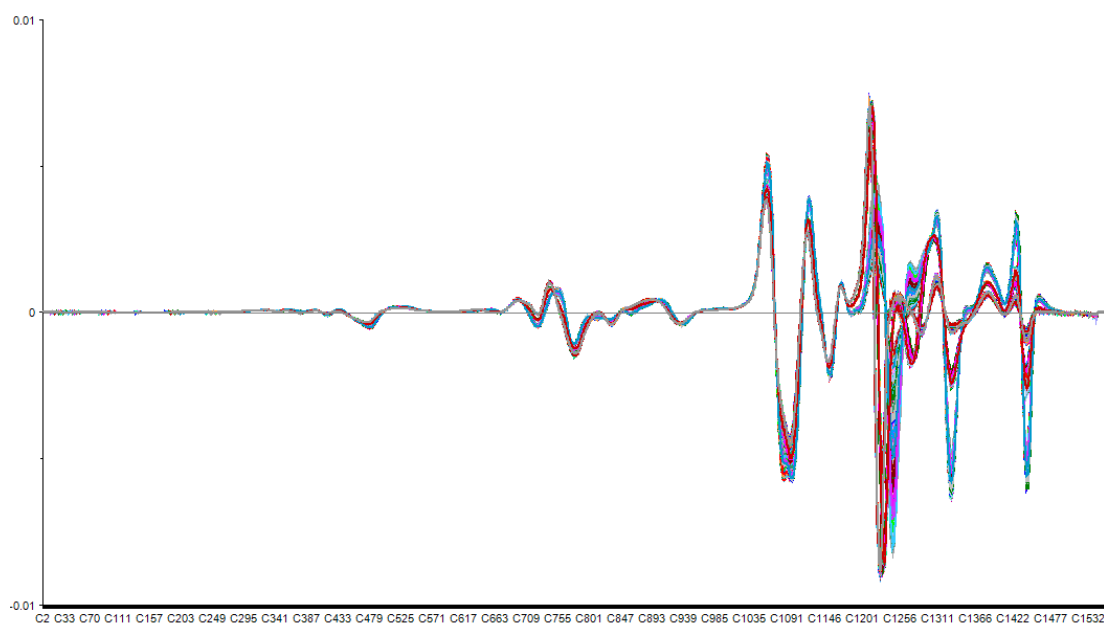


Figure IV- 11 Pretreatment of NIR spectra for PLS model M44: SNV 2<sup>nd</sup> derivative with Savitzky-Golay

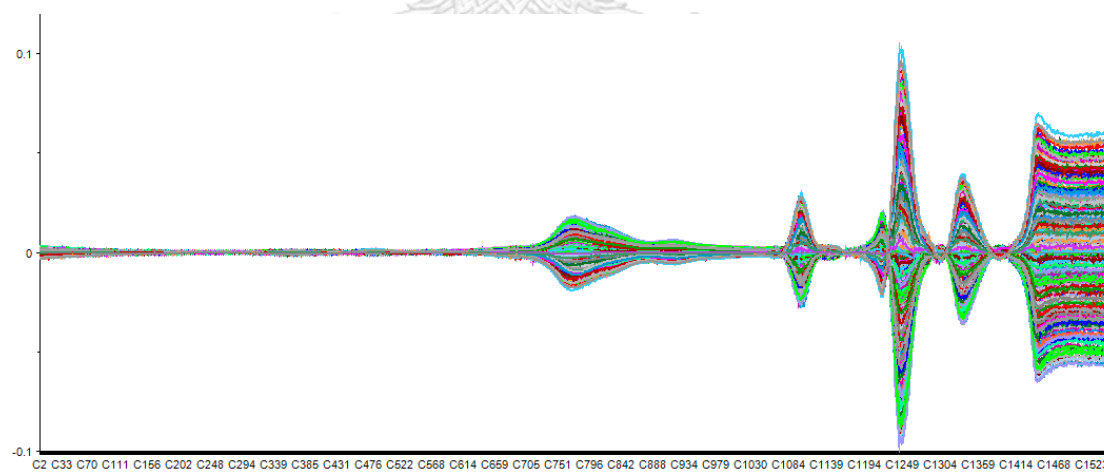


Figure IV- 12 Pretreatment of NIR spectra for PLS model M34-2: OSC

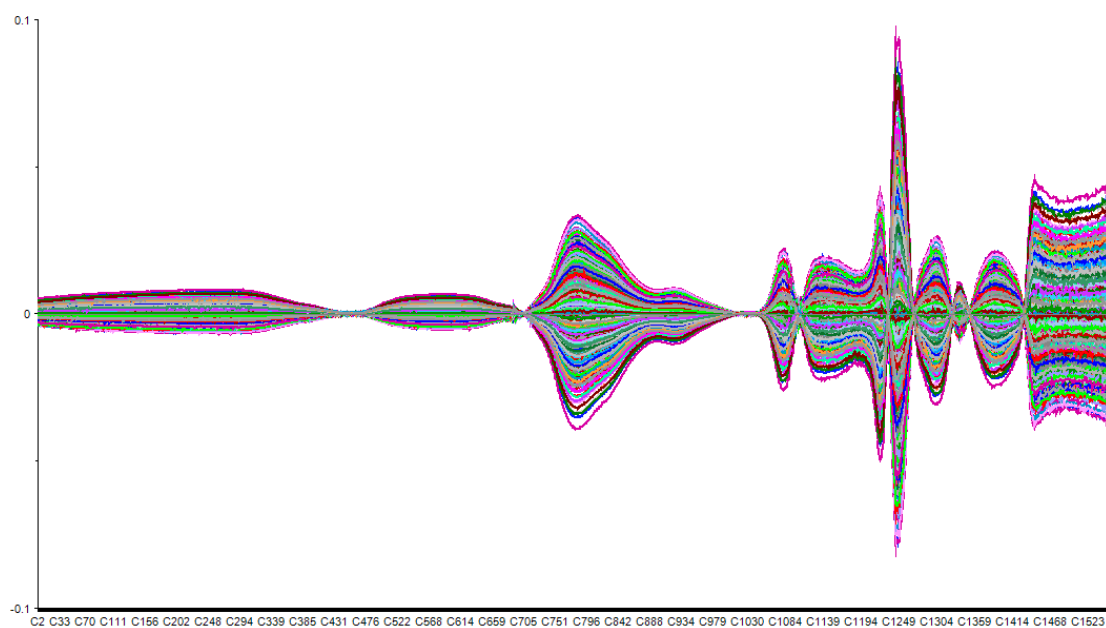


Figure IV- 13 Pretreatment of NIR spectra for PLS model M35-2: MSC-OSC

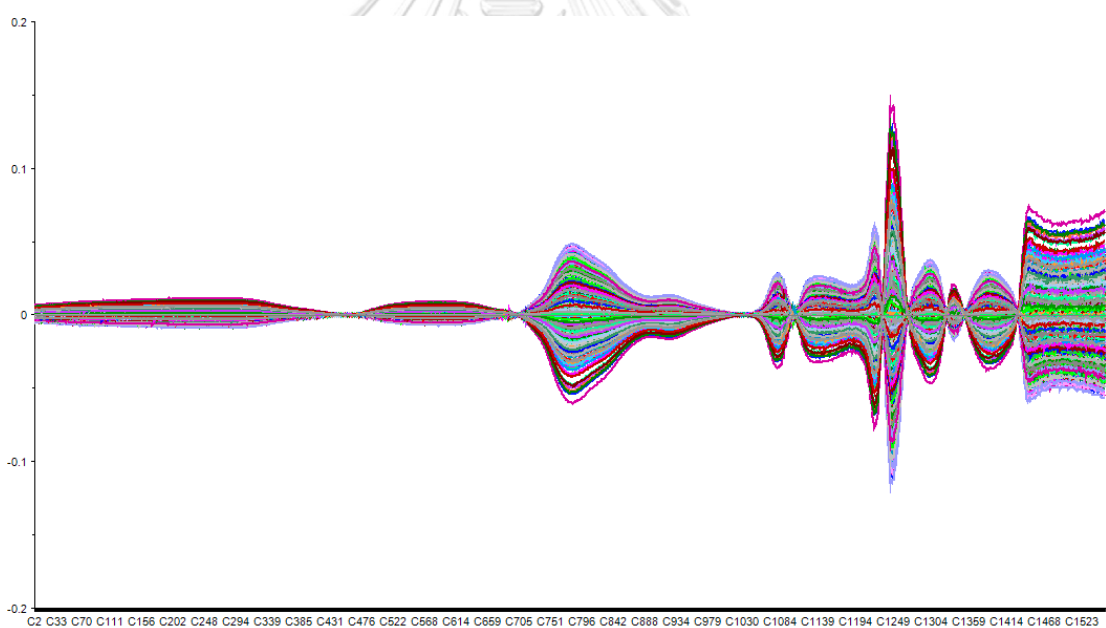


Figure IV- 14 Pretreatment of NIR spectra for PLS model M36-2: SNV-OSC

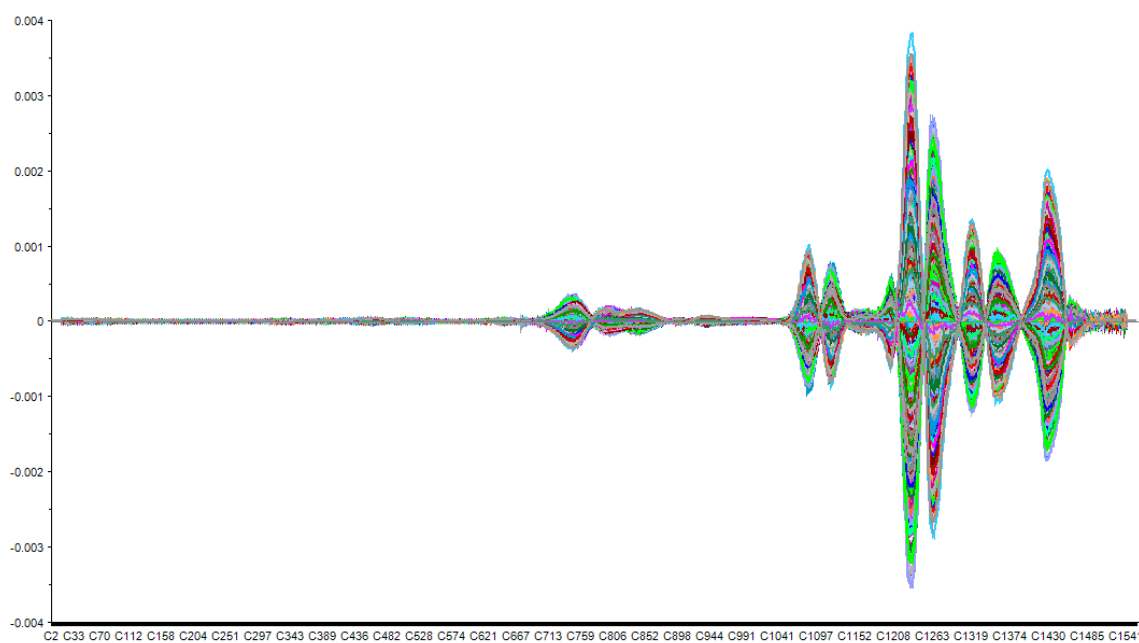


Figure IV- 15 Pretreatment of NIR spectra for PLS model M37-2: OSC-1<sup>st</sup> derivative with Norris-Williams

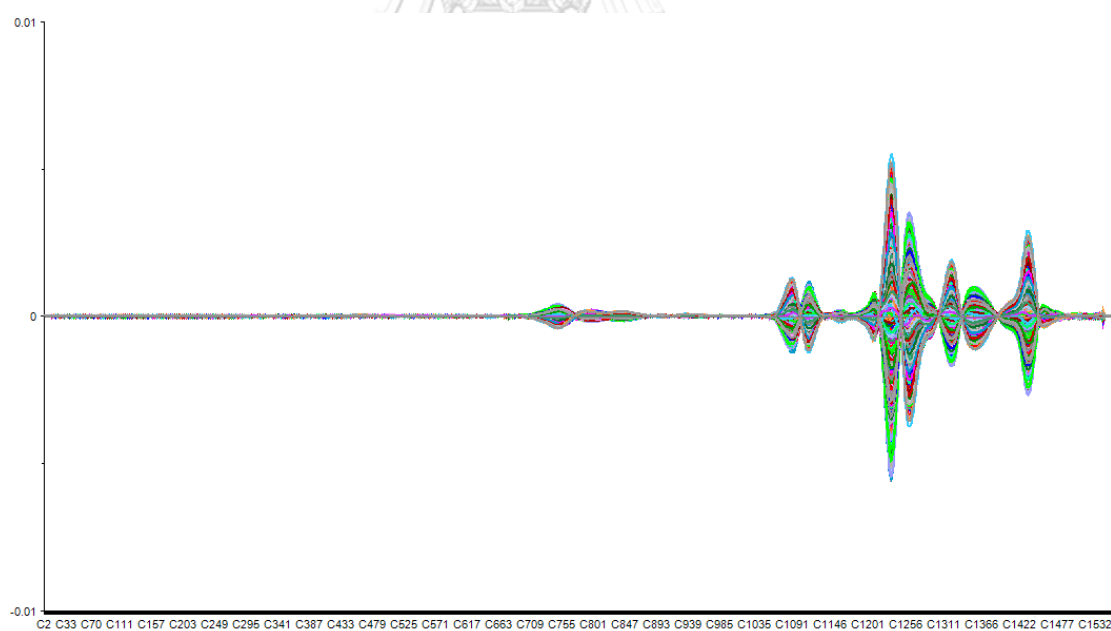


Figure IV- 16 Pretreatment of NIR spectra for PLS model M38-2: OSC 1<sup>st</sup> derivative with Savitzky-Golay

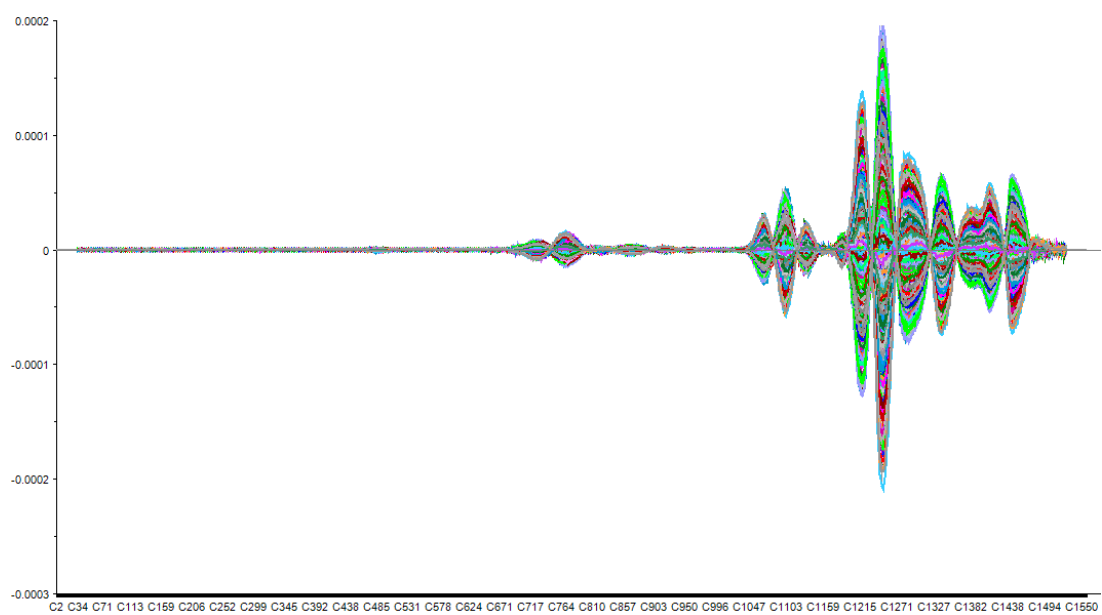


Figure IV- 17 Pretreatment of NIR spectra for PLS model M39-2: OSC 2<sup>nd</sup> derivative with Norris-Williams

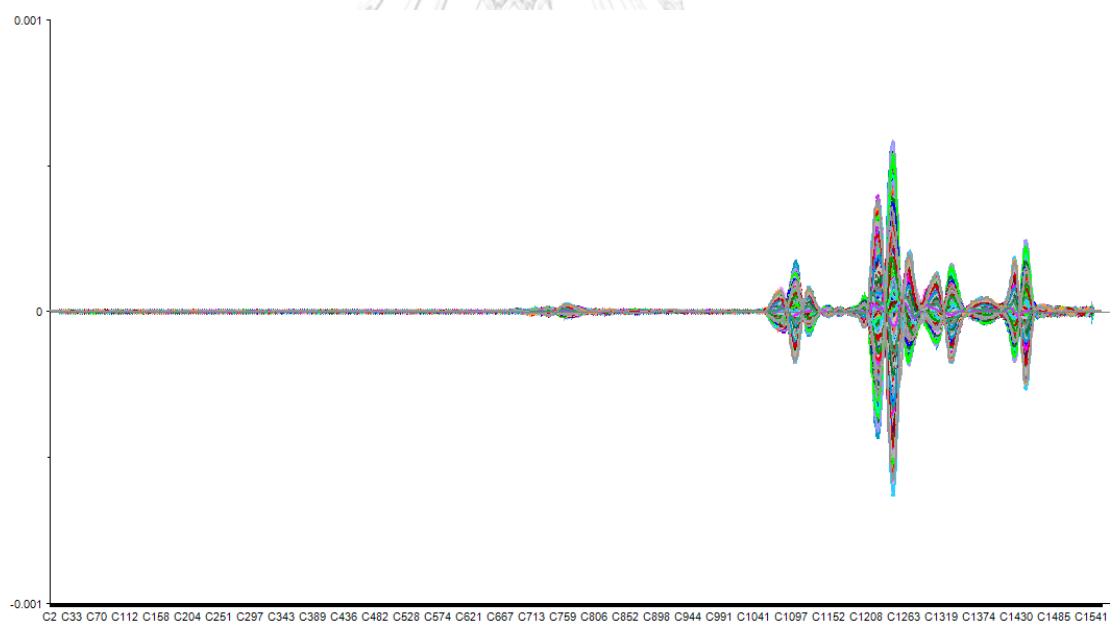


Figure IV- 18 Pretreatment of NIR spectra for PLS model M40-2: OSC 2<sup>nd</sup> derivative with Savitzky-Golay



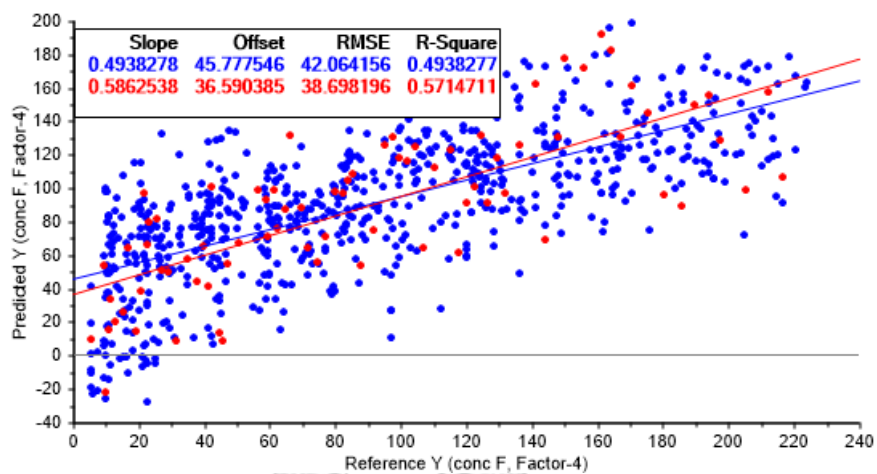


Figure IV- 19 Calibration and validation of PLS model M34

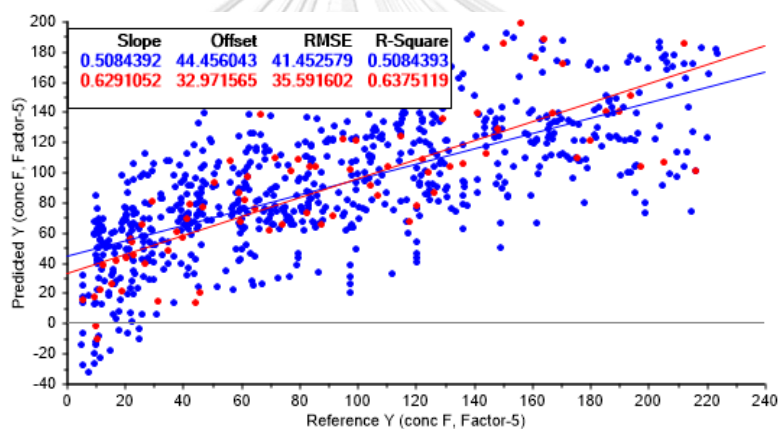


Figure IV- 20 Calibration and validation of PLS model M35

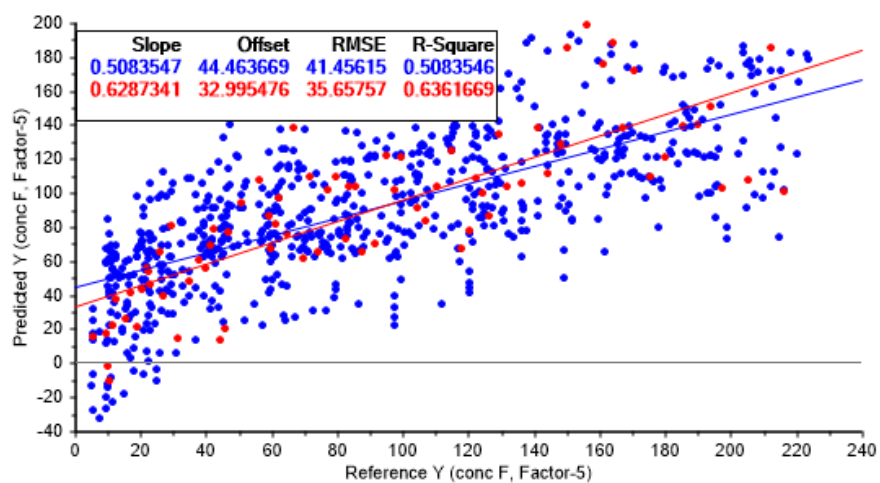


Figure IV- 21 Calibration and validation of PLS model M36

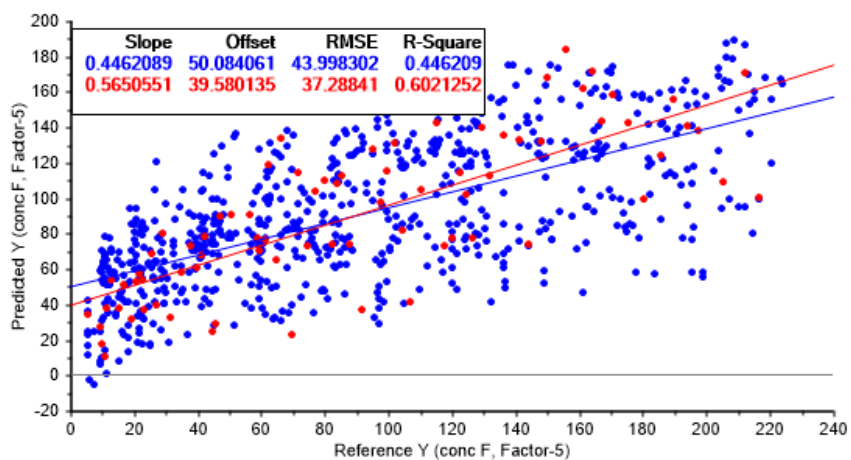


Figure IV- 22 Calibration and validation of PLS model M37

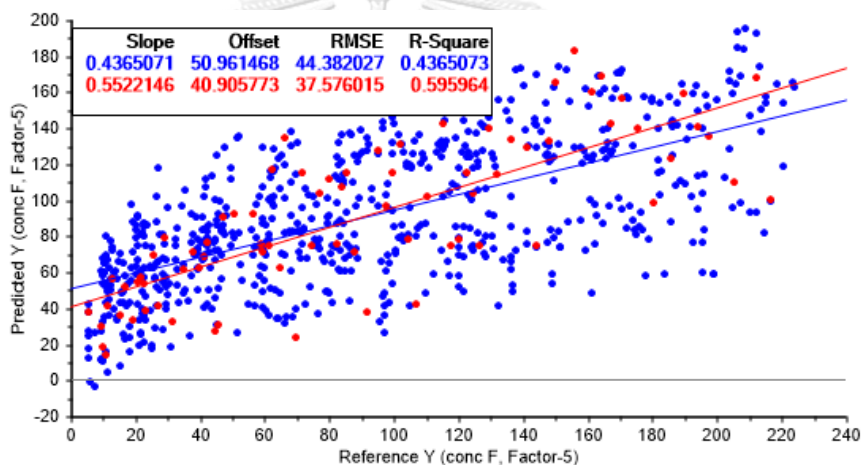


Figure IV- 23 Calibration and validation of PLS model M38

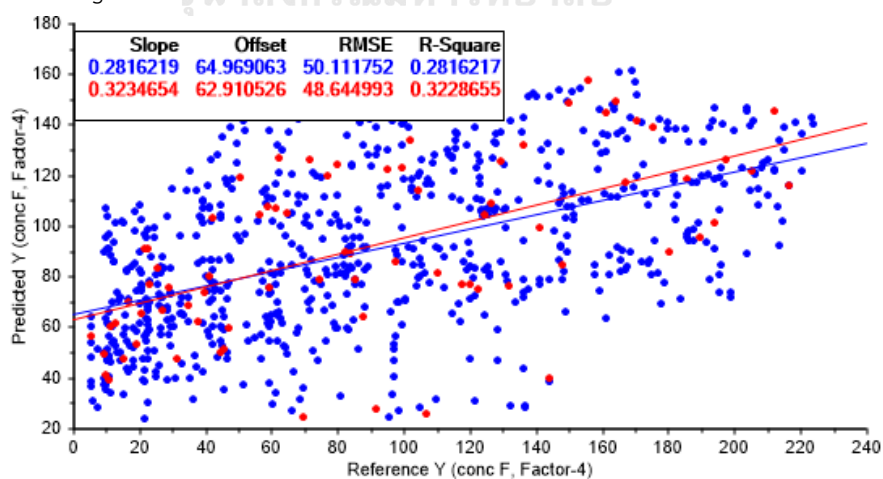


Figure IV- 24 Calibration and validation of PLS model M39

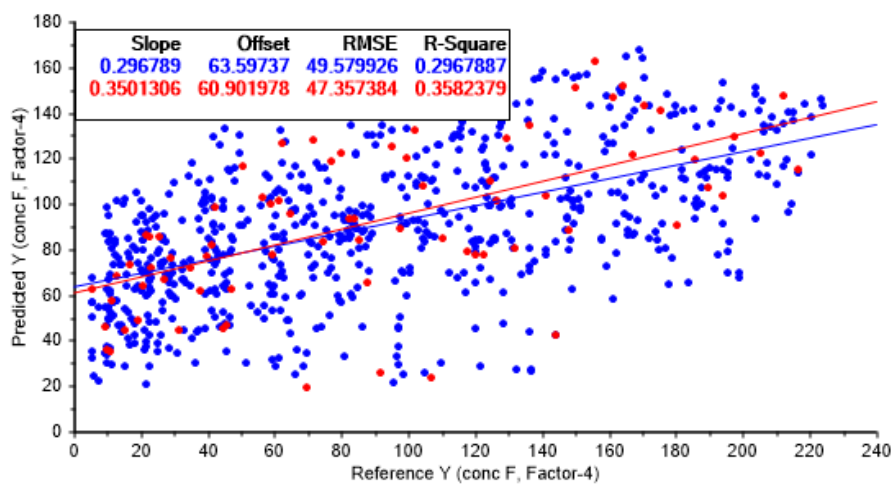


Figure IV- 25 Calibration and validation of PLS model M40

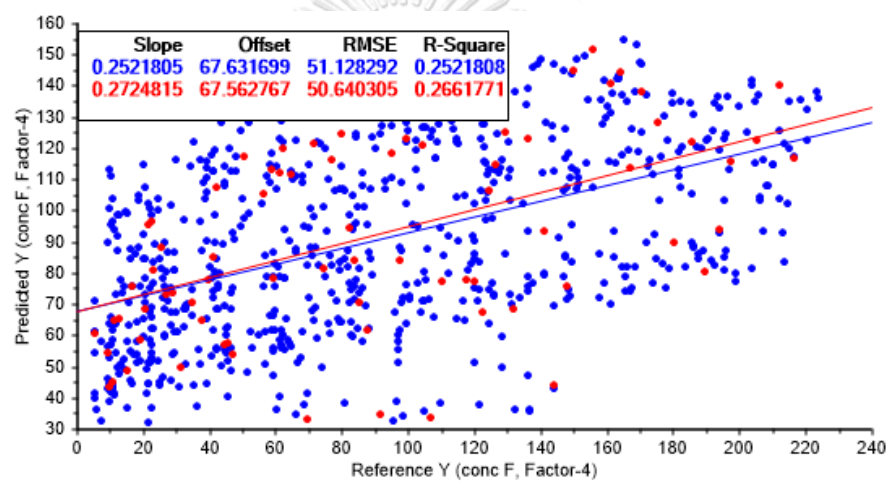


Figure IV- 26 Calibration and validation of PLS model M41

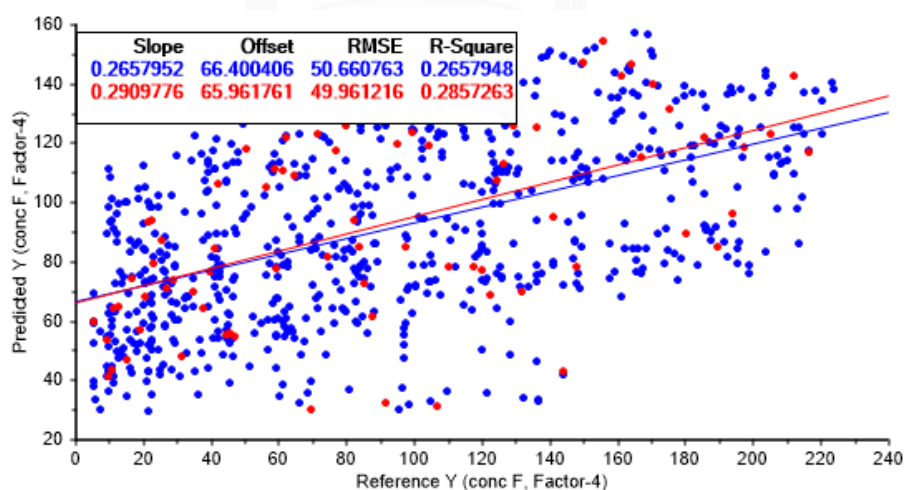


Figure IV- 27 Calibration and validation of PLS model M42

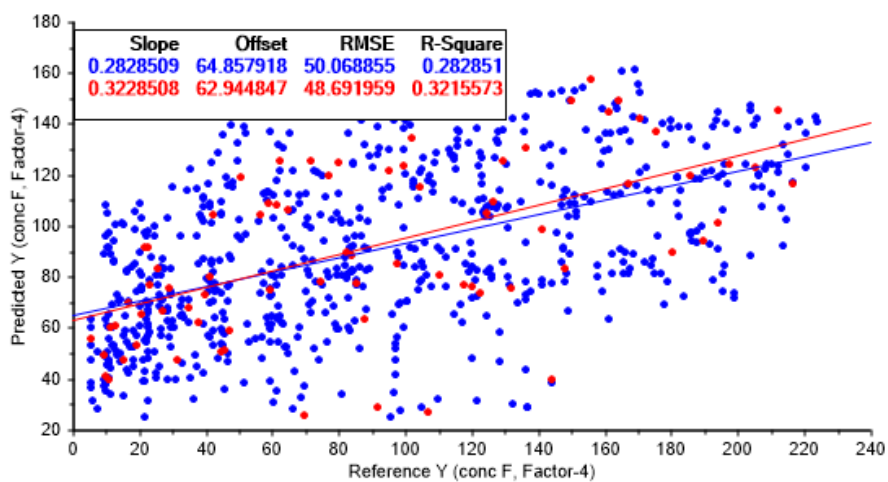


Figure IV- 28 Calibration and validation of PLS model M43

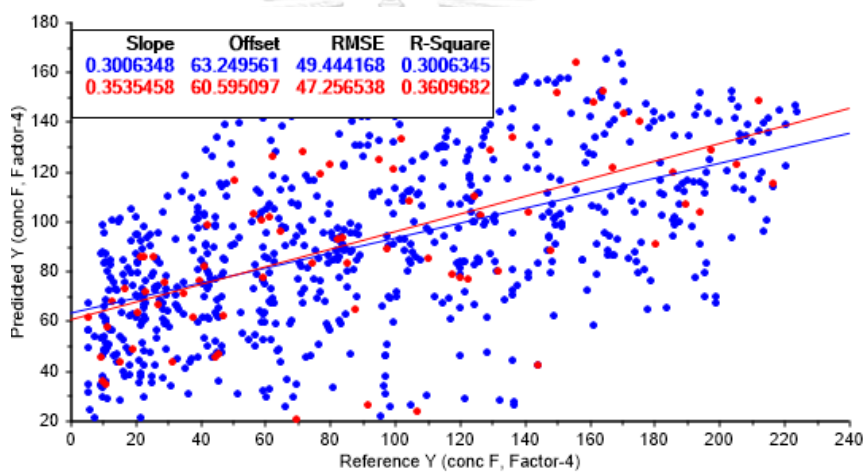


Figure IV- 29 Calibration and validation of PLS model M44

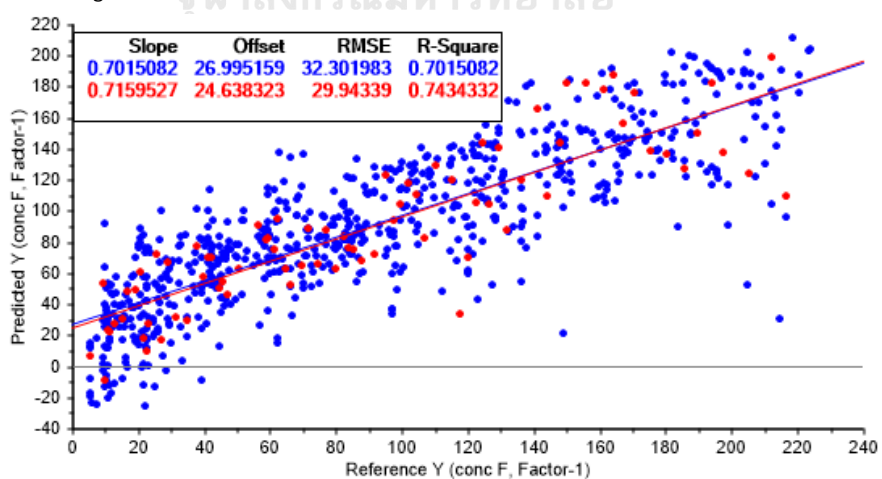


Figure IV- 30 Calibration and validation of PLS model M34-2

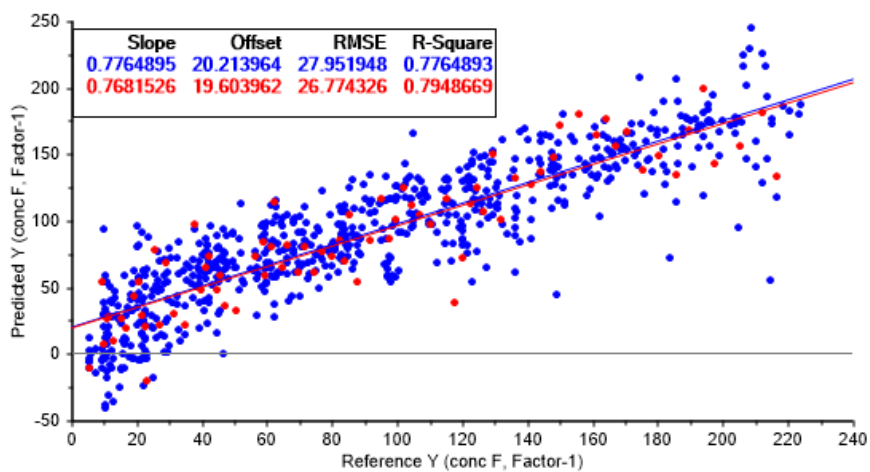


Figure IV- 31 Calibration and validation of PLS model M35-2

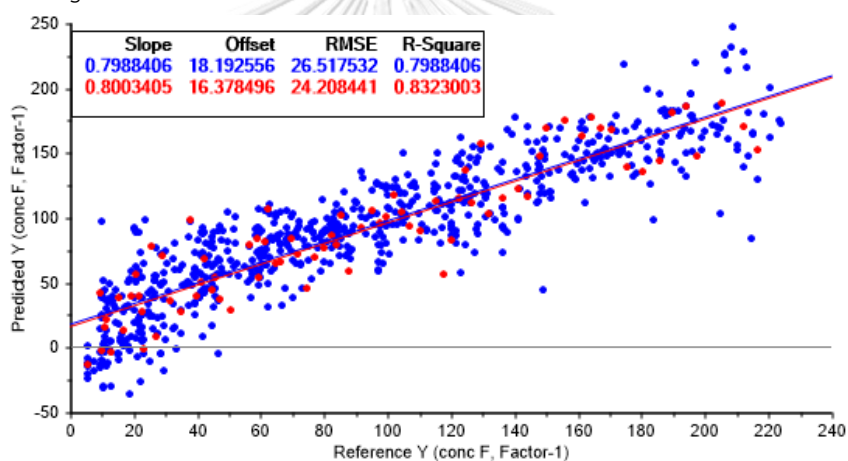


Figure IV- 32 Calibration and validation of PLS model M36-2

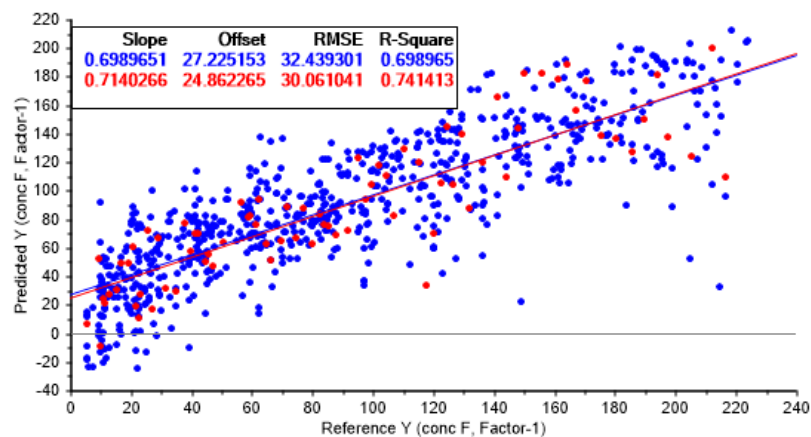


Figure IV- 33 Calibration and validation of PLS model M37-2

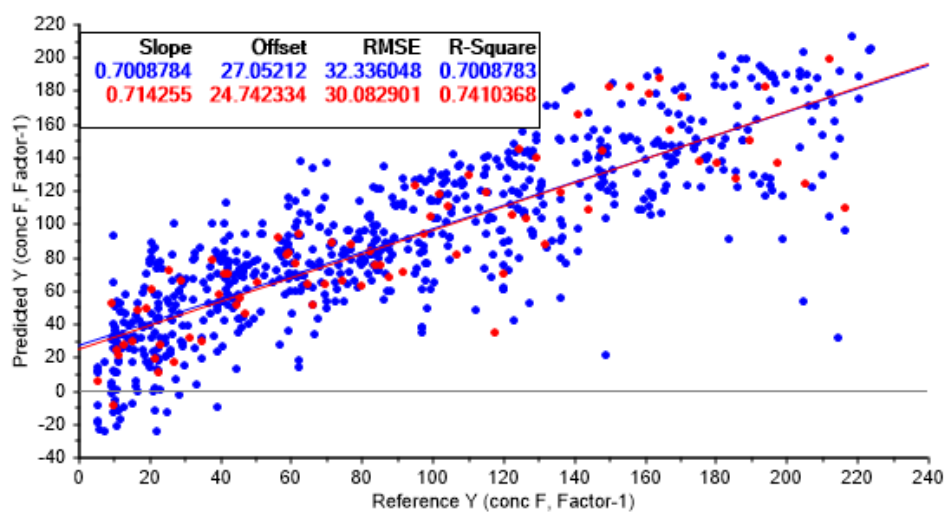


Figure IV- 34 Calibration and validation of PLS model M38-2

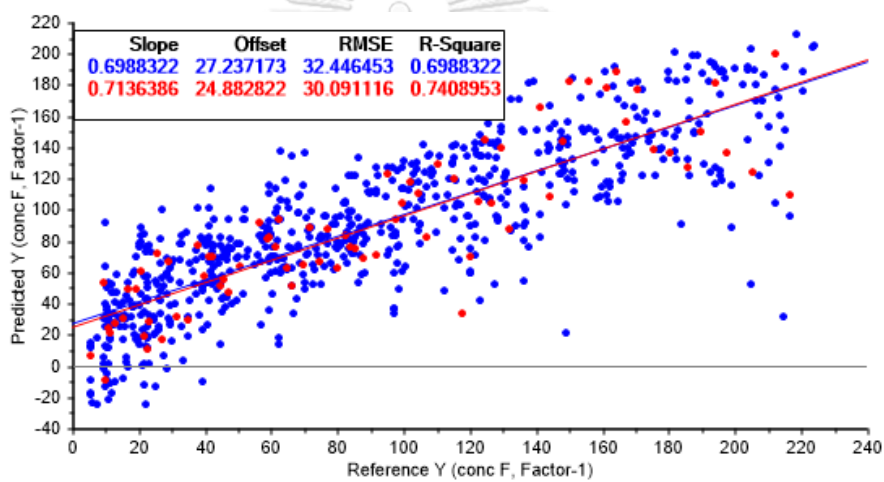


Figure IV- 35 Calibration and validation of PLS model M39-2

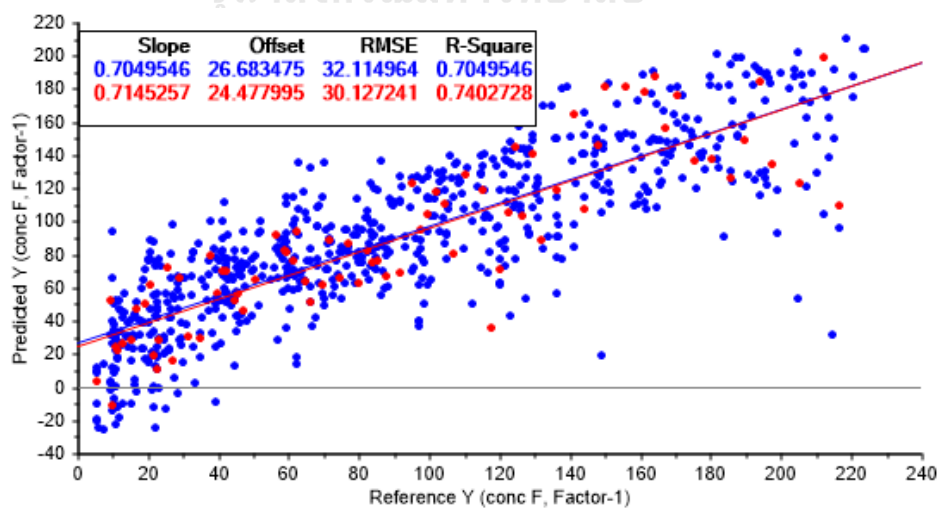
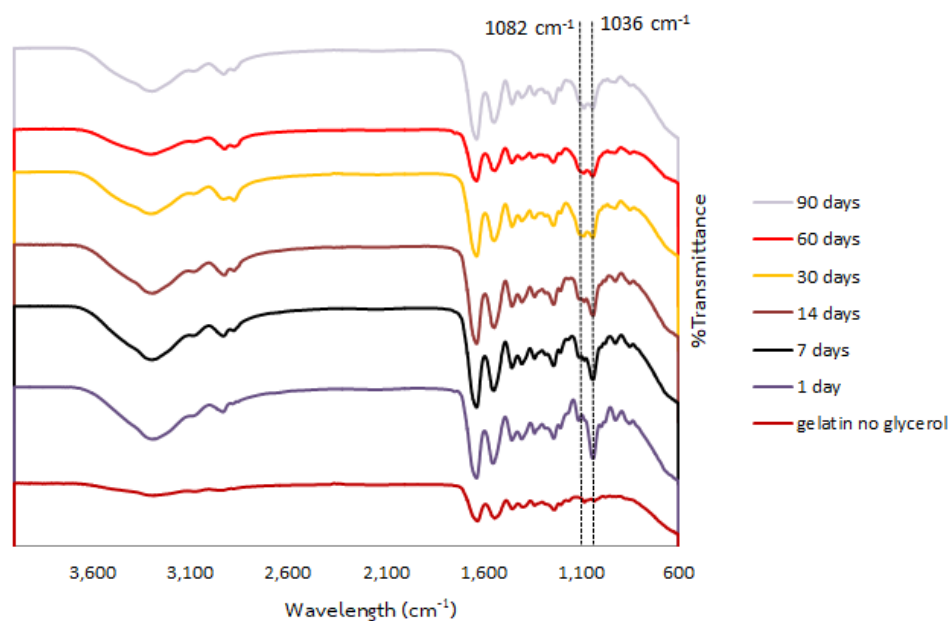


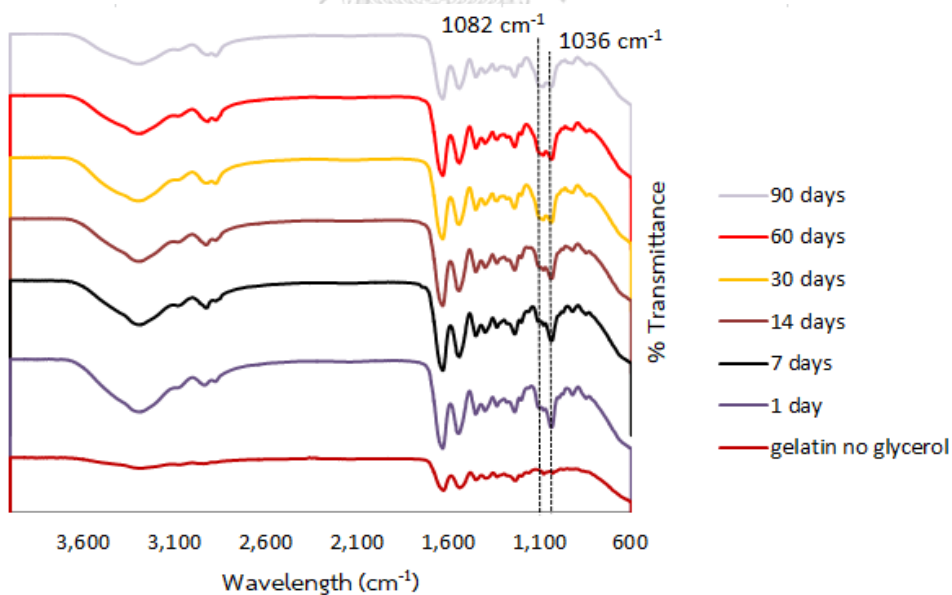
Figure IV- 36 Calibration and validation of PLS model M40-2



## Appendix V: IR spectra of gelatin capsule shell

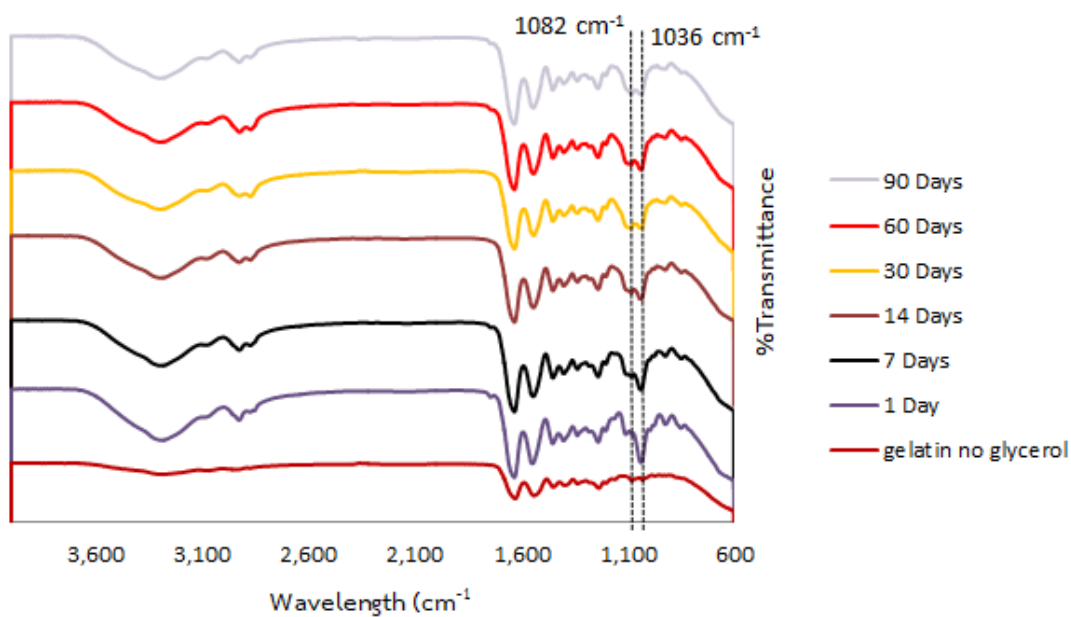


(a) SG-1

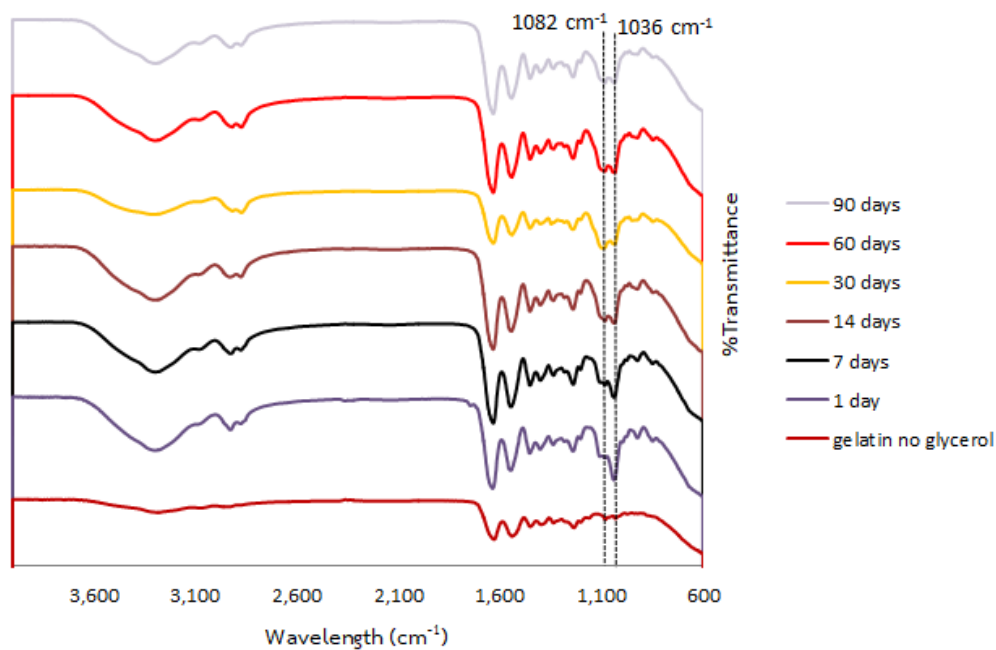


(b) CSG-1

Figure V- 1 FT-IR spectra of of gelatin capsule shell formulation 1; non colored (a) and colored (b) containing no ibuprofen at different time points



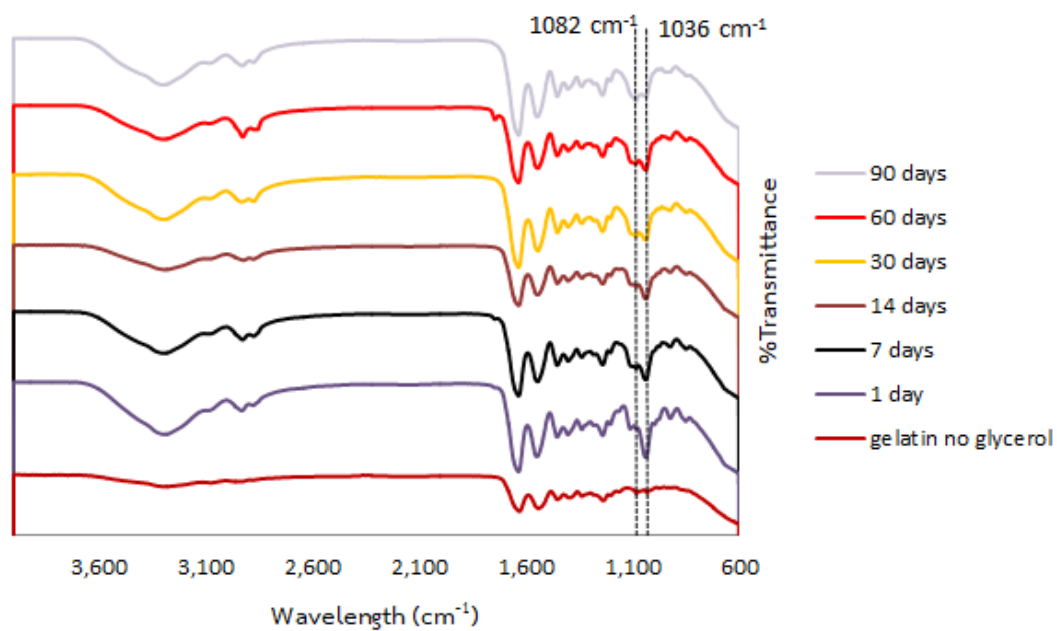
(a) SG-3



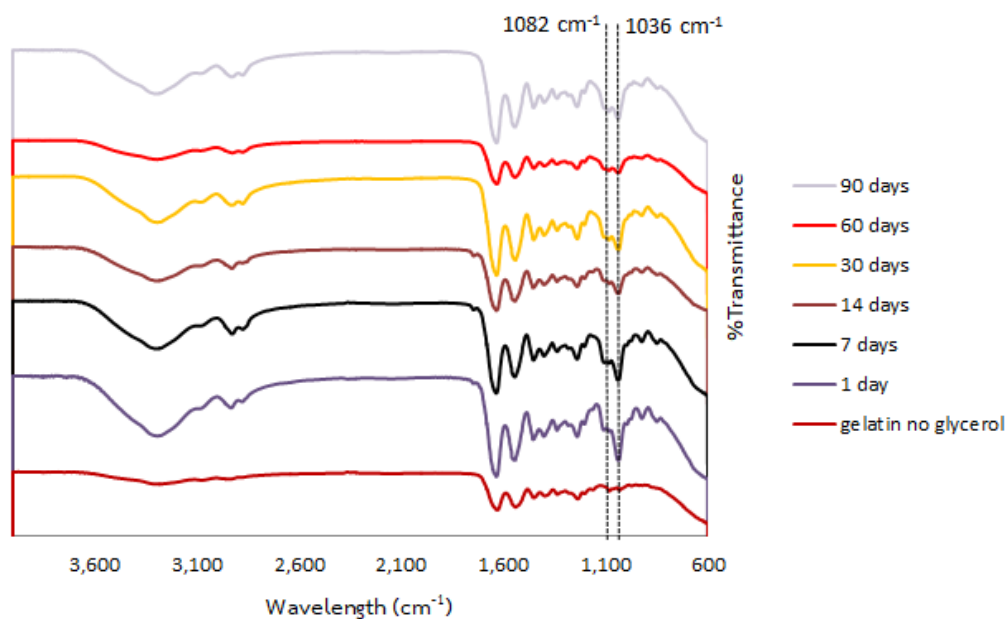
(b) CSG-3

Figure V- 2 FT-IR spectra of of gelatin capsule shell formulation 3; non colored (a) and colored (b) containing no ibuprofen at different time points



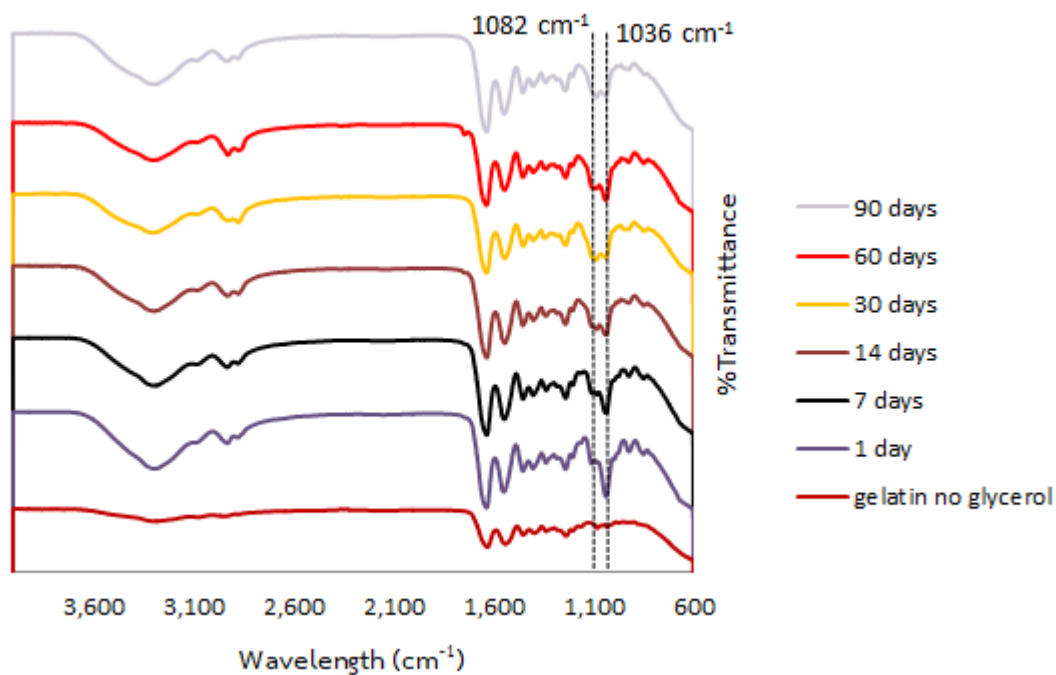


(a) SG-4

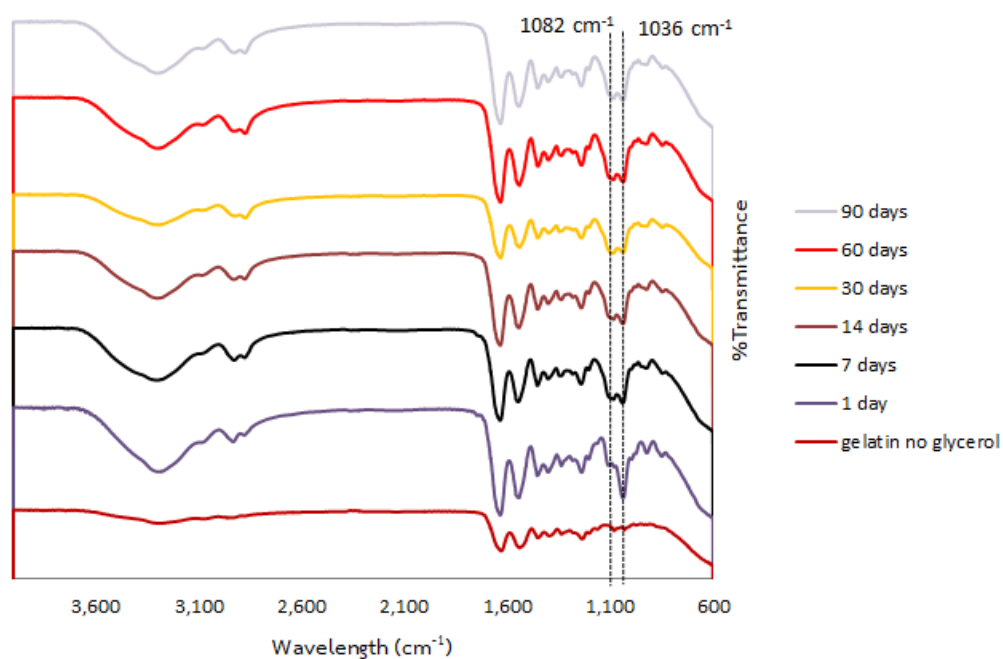


(b) CSG-4

Figure V- 3 FT-IR spectra of of gelatin capsule shell formulation 4; non colored (a) and colored (b) containing no ibuprofen at different time points

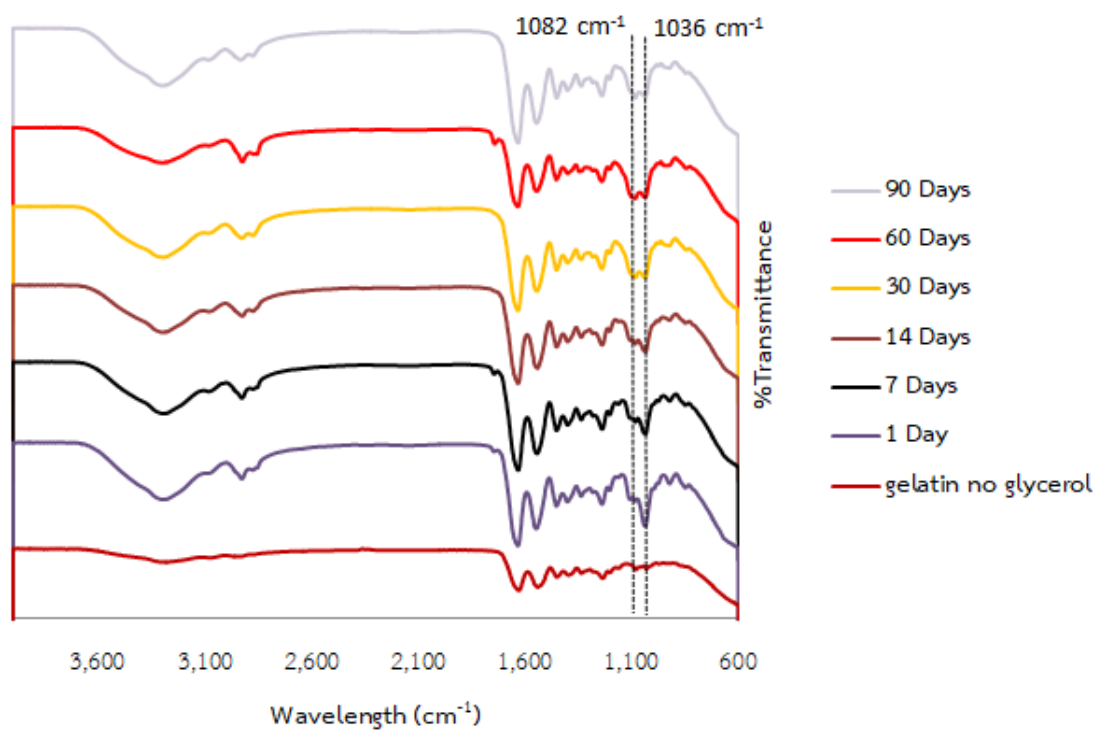


(a) SG-5

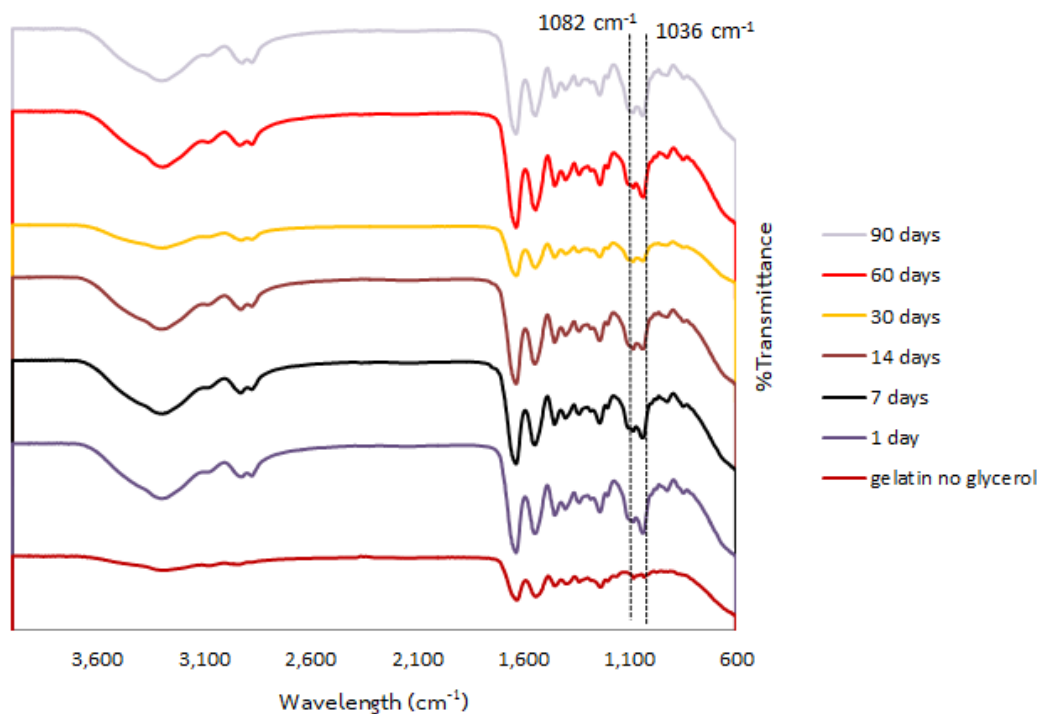


(b) CSG-5

Figure V- 4 FT-IR spectra of of gelatin capsule shell formulation 5; non colored (a) and colored (b) containing no ibuprofen at different time points

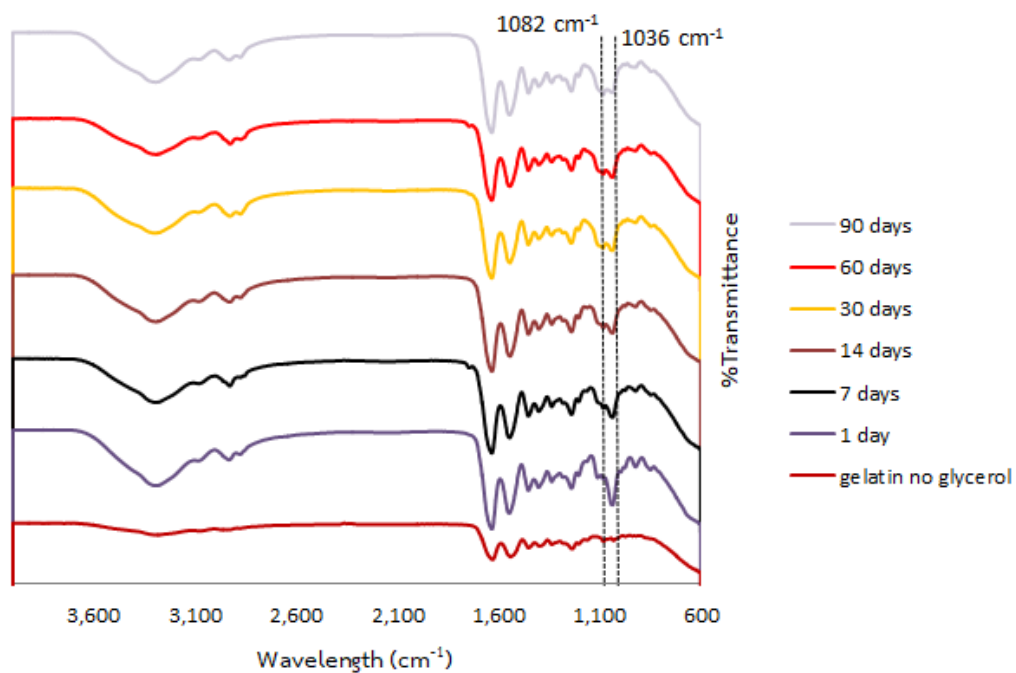


(a) SG-6

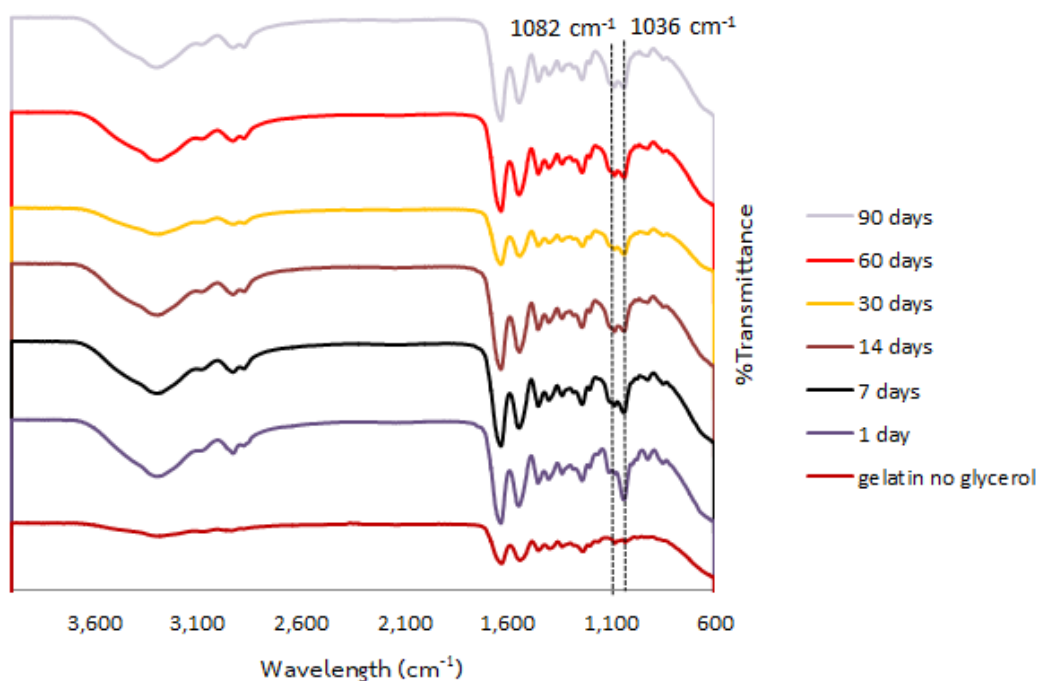


(c) CSG-6

Figure V- 5 FT-IR spectra of of gelatin capsule shell formulation 6; non colored (a) and colored (b) containing no ibuprofen at different time points

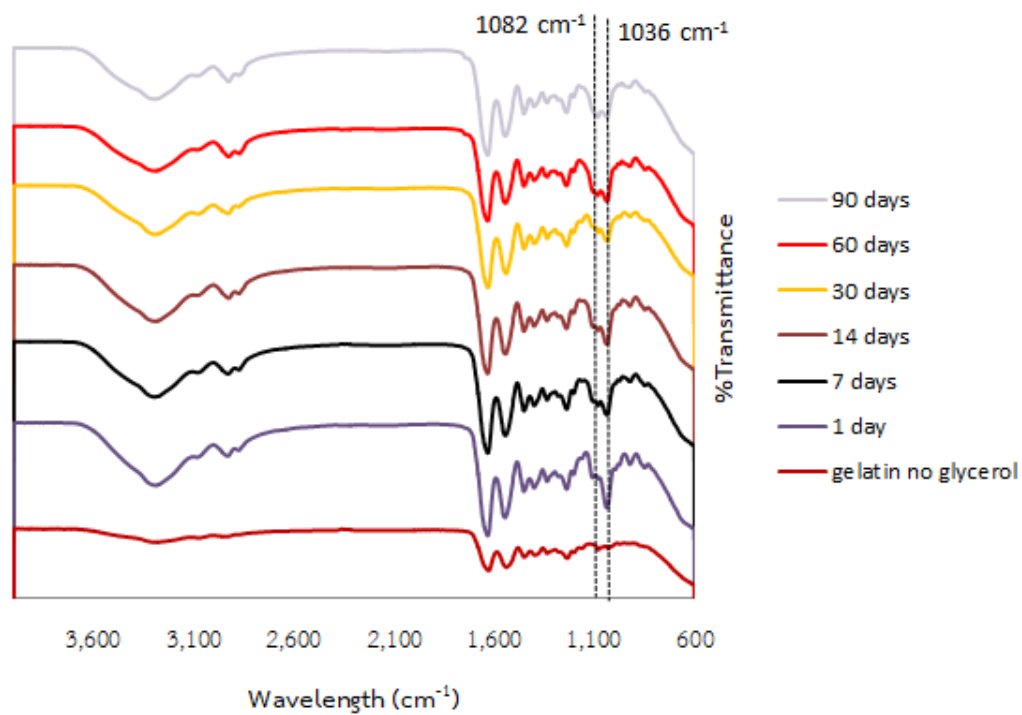


(a) SG-7

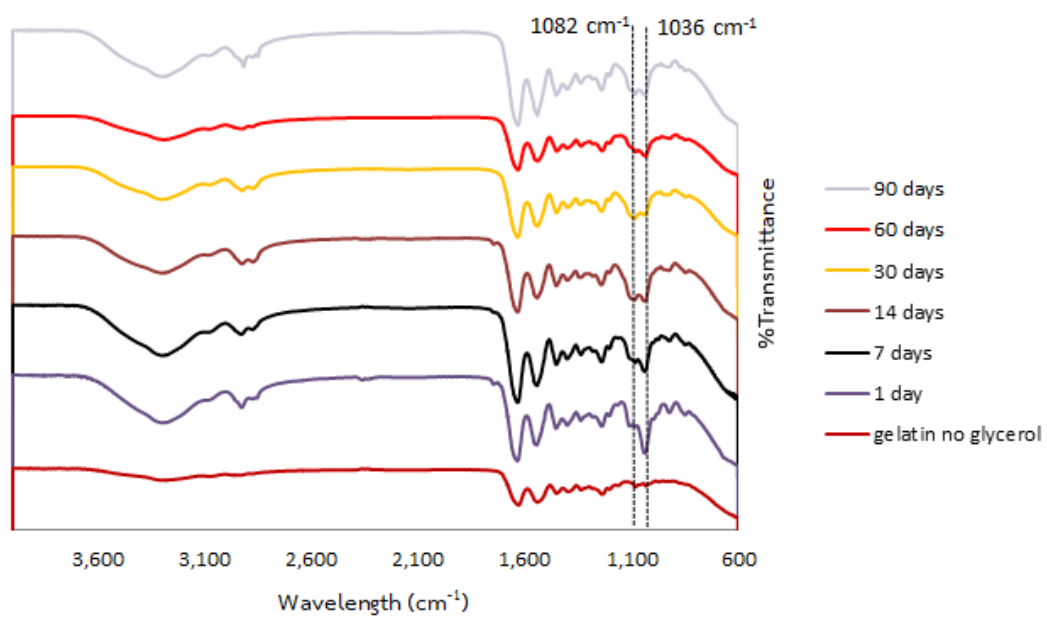


(b) CSG-7

Figure V- 6 FT-IR spectra of of gelatin capsule shell formulation 7; non colored (a) and colored (b) containing no ibuprofen at different time points

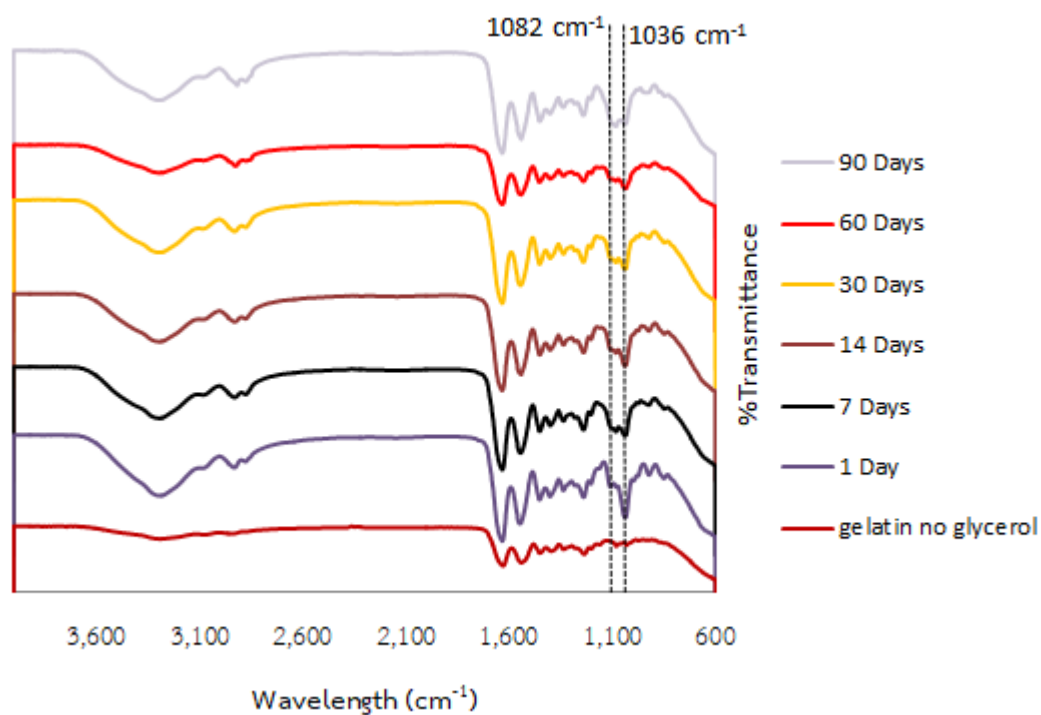


(a) SG-8

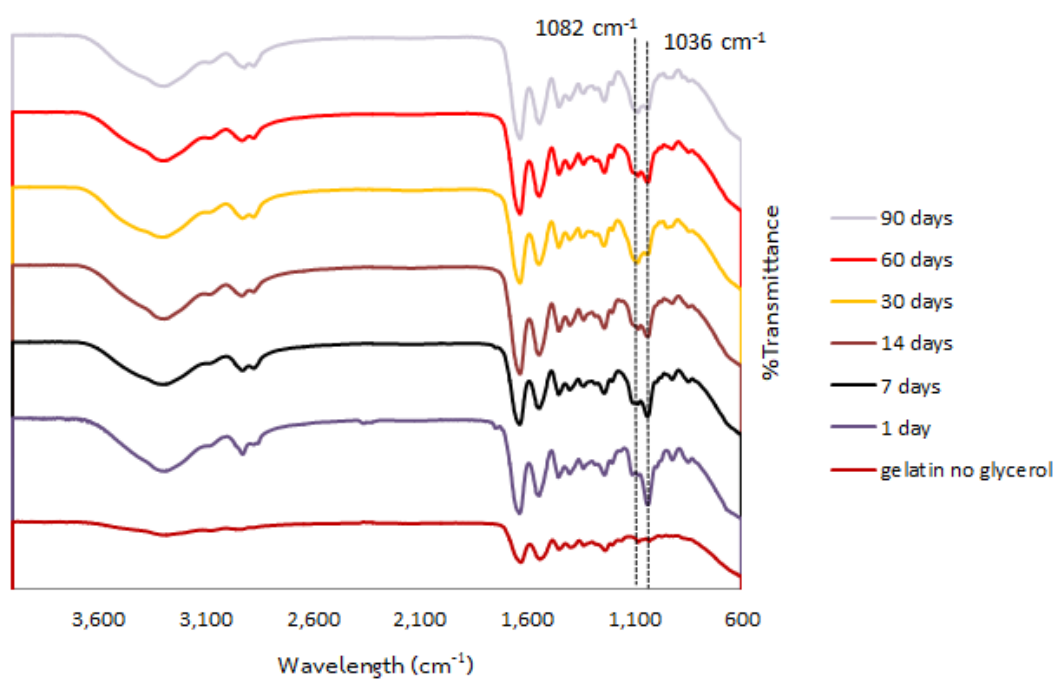


(b) CSG-8

Figure V- 7 FT-IR spectra of of gelatin capsule shell formulation 8; non colored (a) and colored (b) containing no ibuprofen at different time points

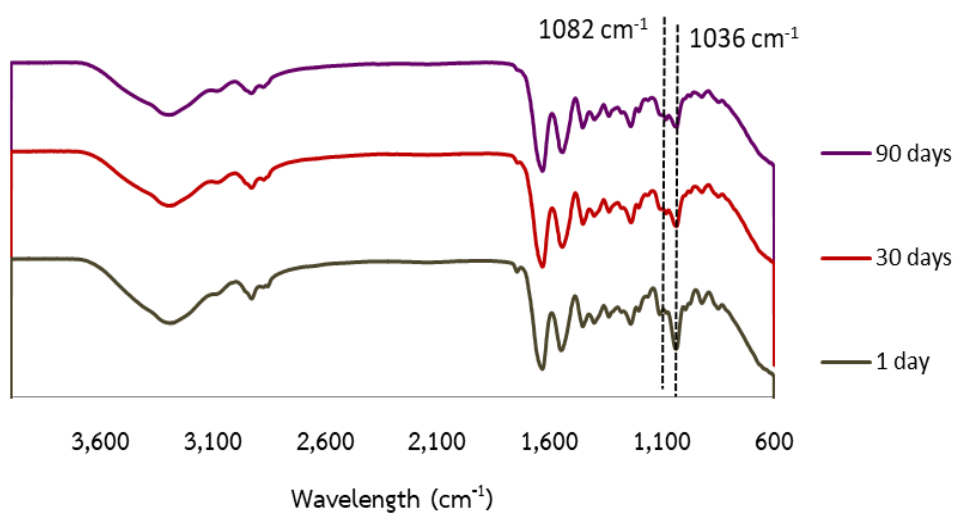
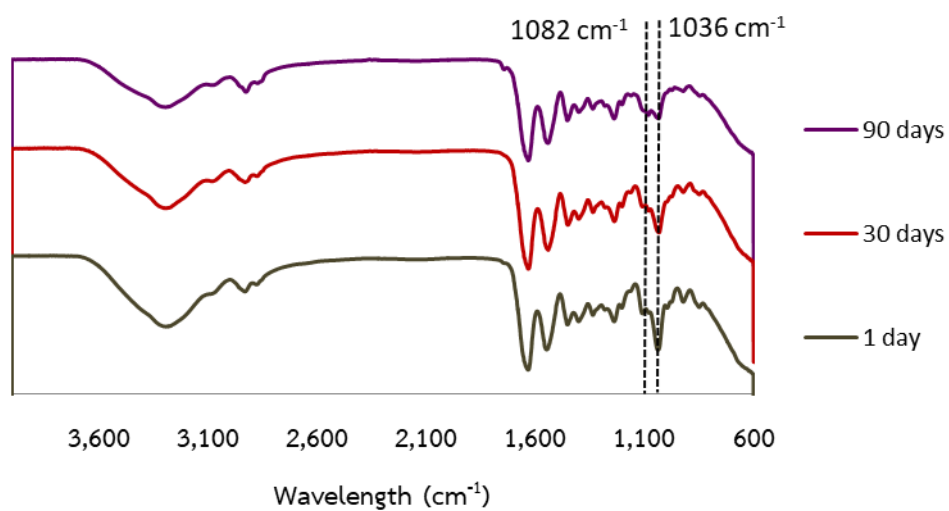


(a) SG-9



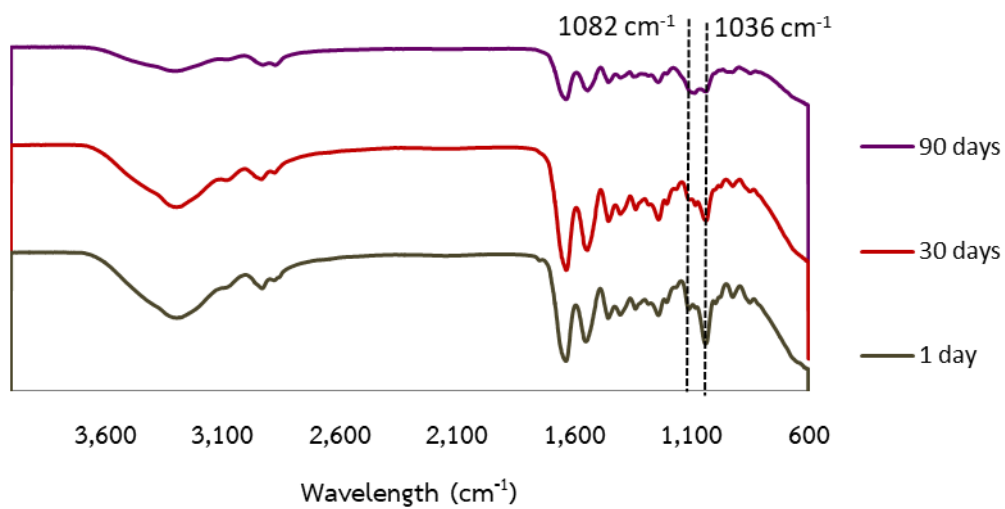
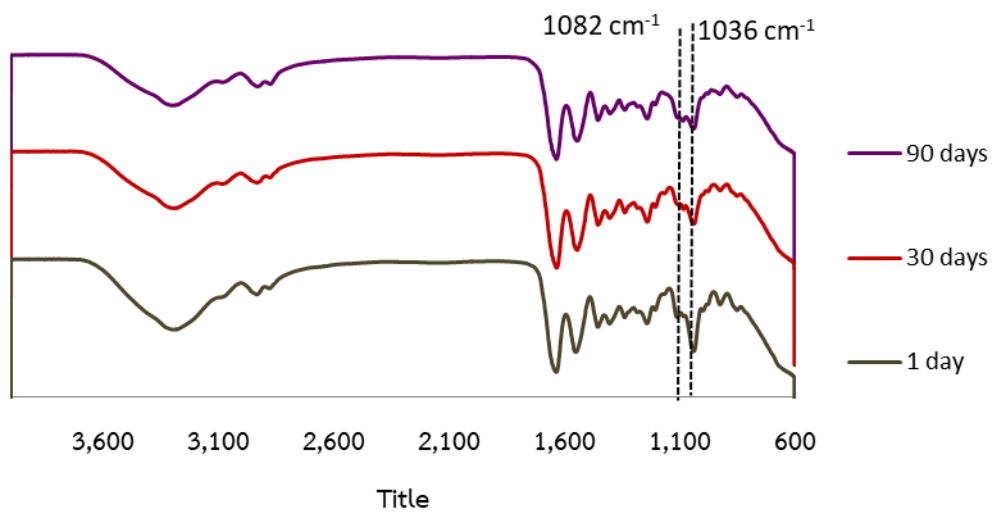
(b) CSG-9

Figure V- 8 FT-IR spectra of of gelatin capsule shell formulation 9; non colored (a) and colored (b) containing no ibuprofen at different time points



(b) CSG-3

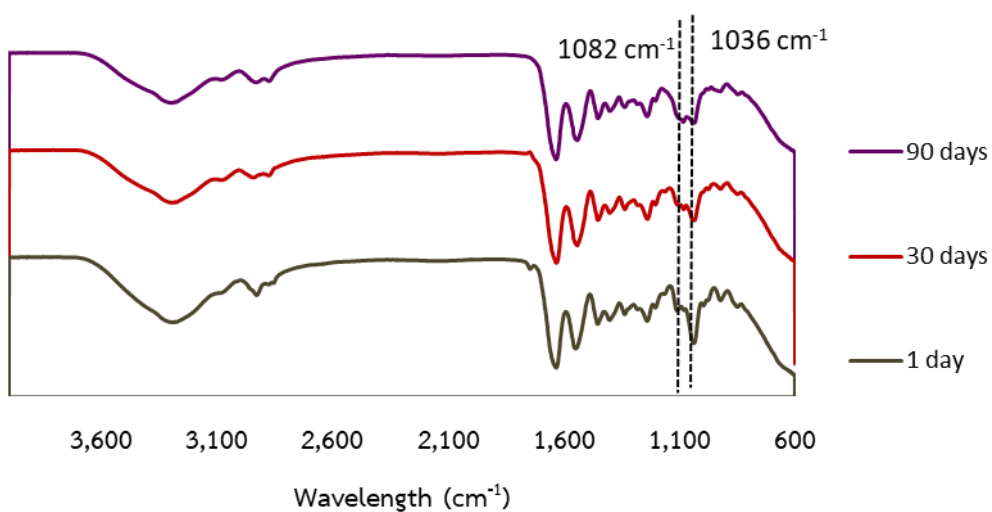
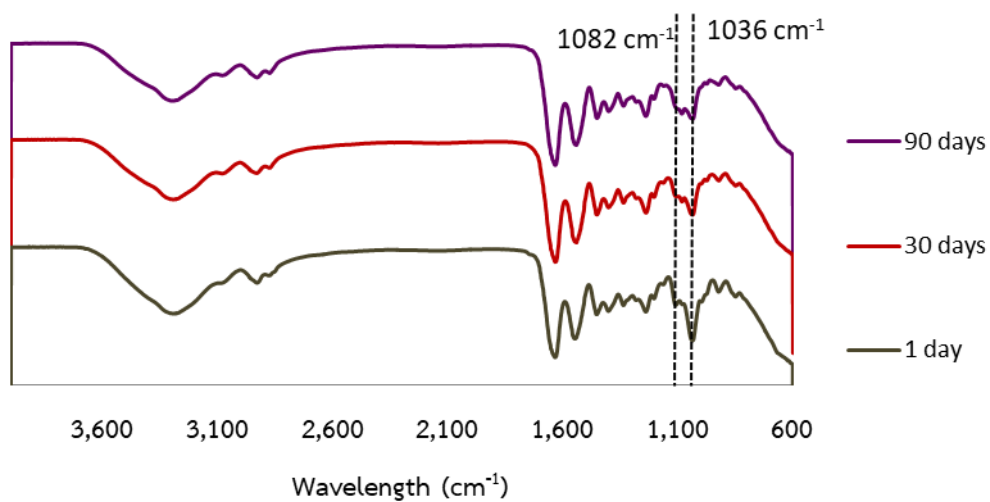
Figure V- 9 FT-IR spectra of gelatin capsule shell of colored formulation 1 (a) and colored formulation 3 (b) containing ibuprofen at different time points



(b) CSG-5

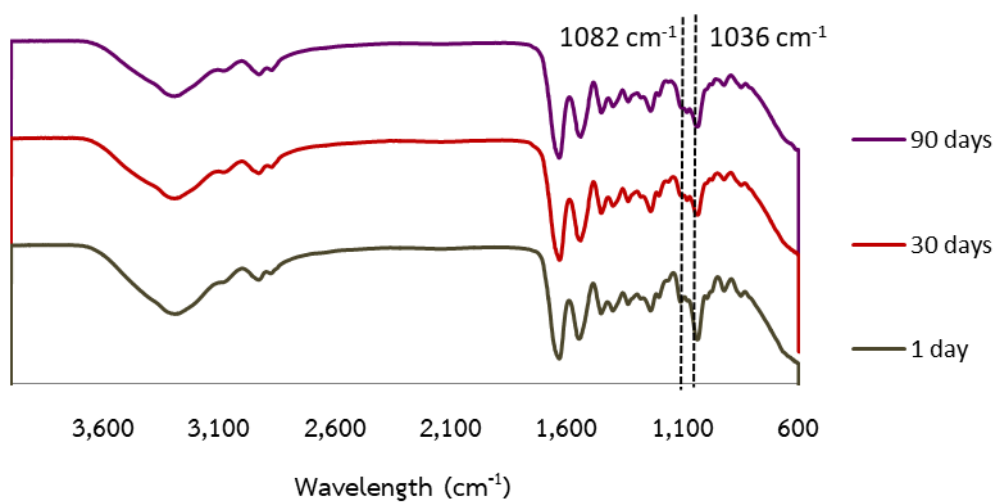
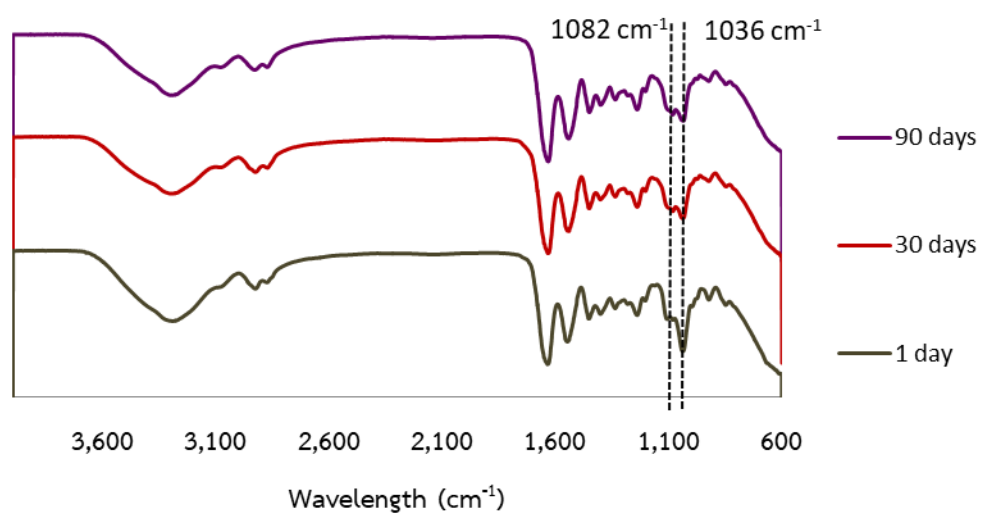
Figure V- 10 FT-IR spectra of gelatin capsule shell of colored formulation 4 (a) and colored formulation 5 (b) containing ibuprofen at different time points





(b) CSG-7

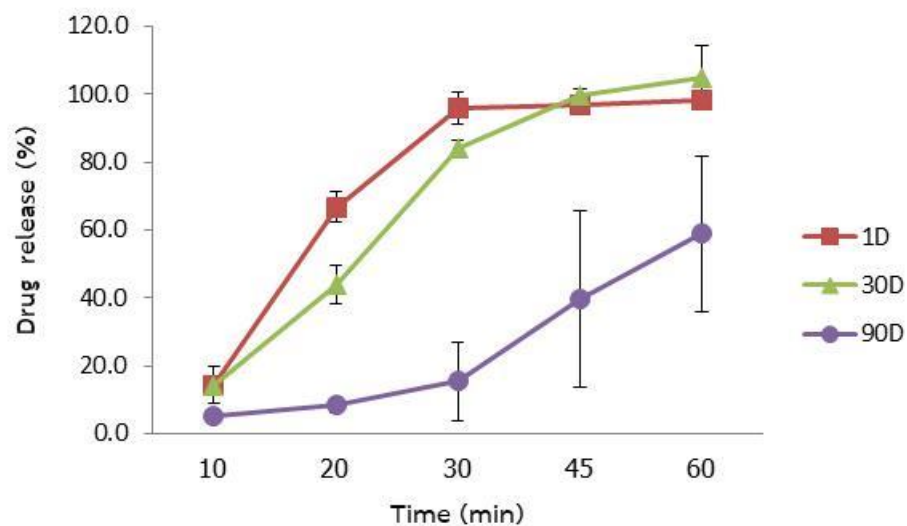
Figure V- 11 FT-IR spectra of gelatin capsule shell of colored formulation 6 (a) and colored formulation 7 (b) containing ibuprofen at different time points



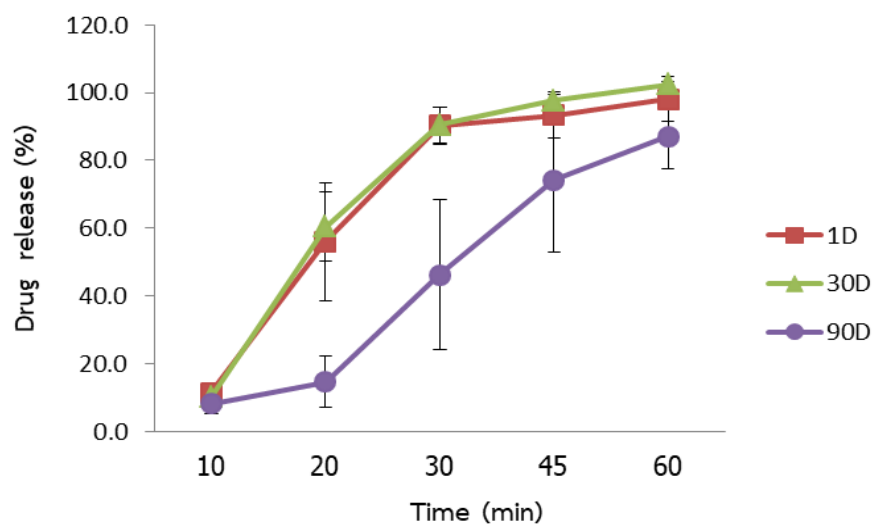
(b) CSG-9

Figure V- 12 FT-IR spectra of gelatin capsule shell of colored formulation 8 (a) and colored formulation 9 (b) containing ibuprofen at different time points

## Appendix VI Dissolution profile of ibuprofen soft gelatin capsules

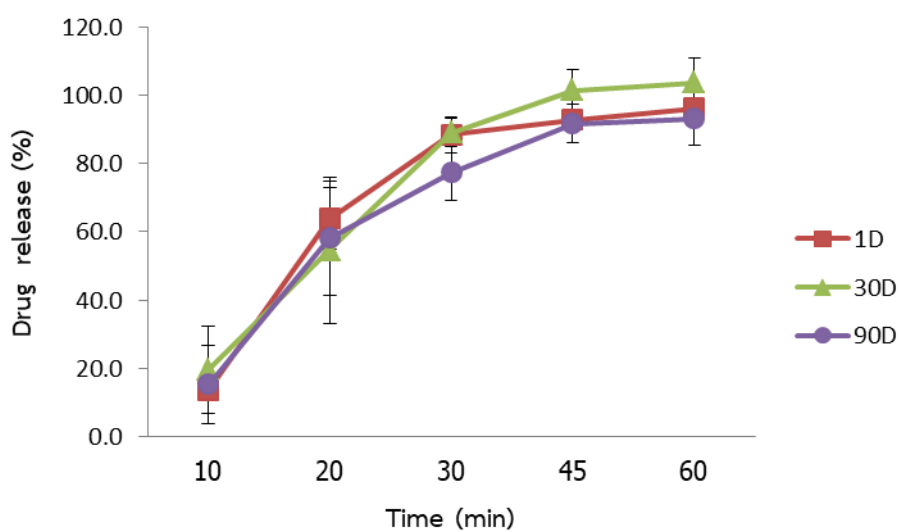
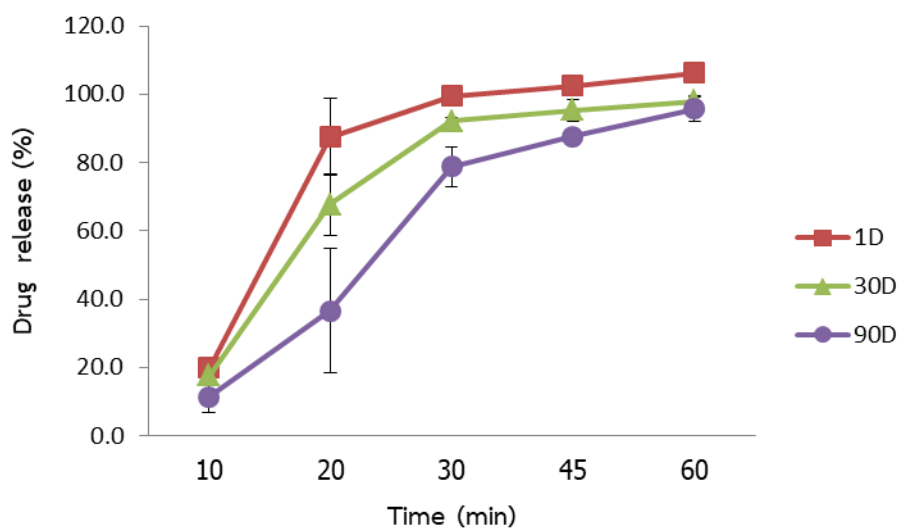


(a) CSG-1



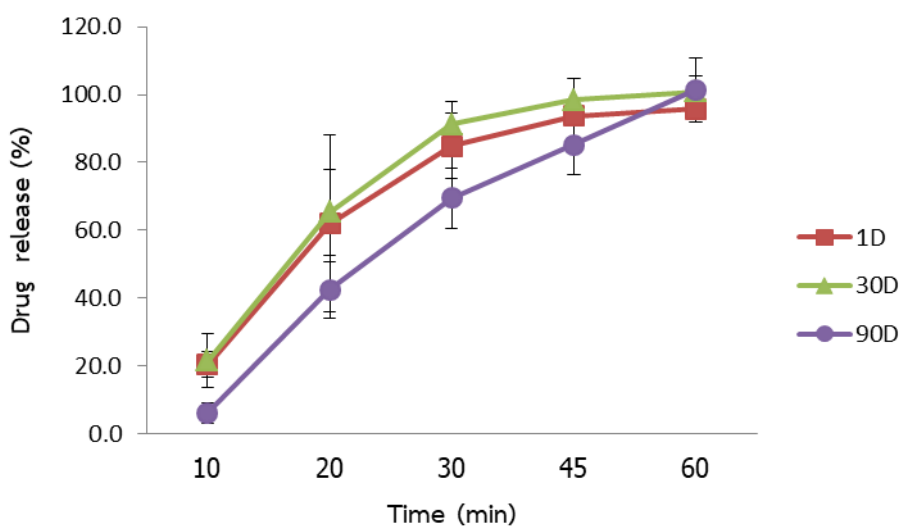
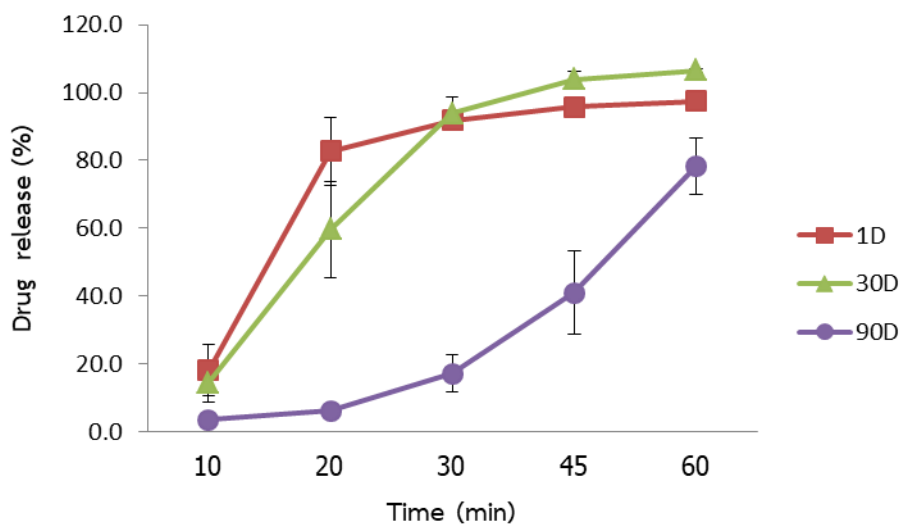
(b) CSG-3

Figure VI- 1 Dissolution profiles of ibuprofen soft gelatin capsules for colored formulation 1 (a) and formulation 3 (b) at 1 (1D), 30 (30D) and 90 (90D) days



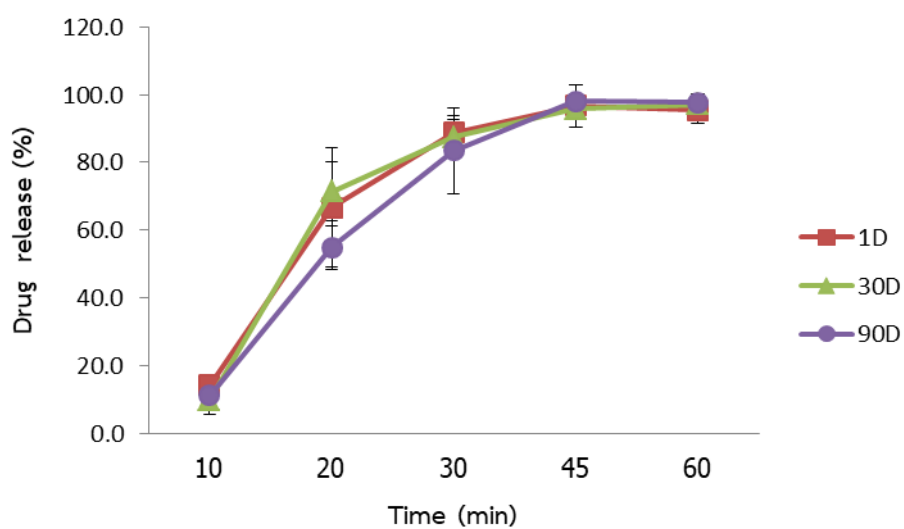
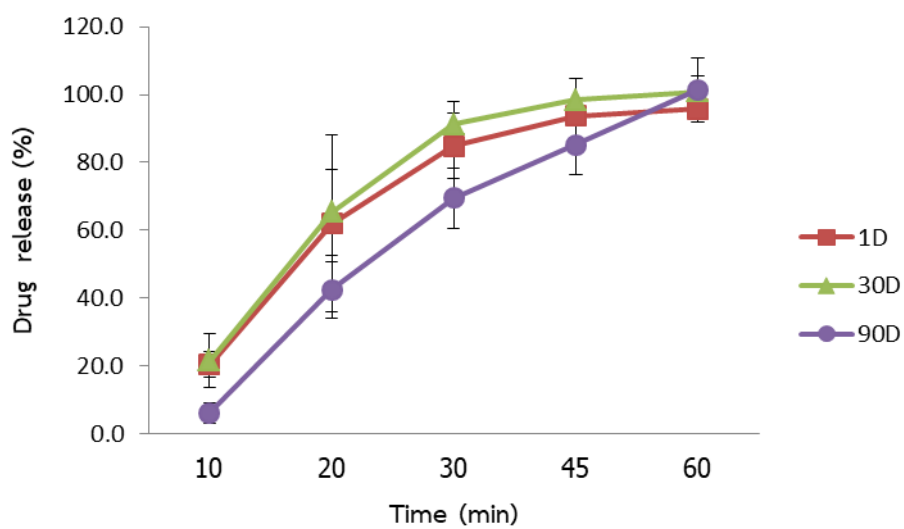
(b) CSG-5

Figure VI- 2 Dissolution profiles of ibuprofen soft gelatin capsules for colored formulation 4 (a) and formulation 5 (b) at 1 (1D), 30 (30D) and 90 (90D) days



(b) CSG-7

Figure VI- 3 Dissolution profiles of ibuprofen soft gelatin capsules for colored formulation 6 (a) and formulation 7 (b) at 1 (1D), 30 (30D) and 90 (90D) days



(b) CSG-9

Figure VI- 4 Dissolution profiles of ibuprofen soft gelatin capsules for colored formulation 8 (a) and formulation 9 (b) at 1 (1D), 30 (30D) and 90 (90D) days

## VITA

Mrs. Weena Nittayasoot was born in Bangkok, Thailand on December 12th, 1985. She received her Bachelor of Science in Pharmacy degree in 2008 from the Faculty of Pharmaceutical Sciences, Chulalongkorn University, Thailand. She presented a proceeding poster entitled "Crosslinking of soft gelatin capsules filled with polyethylene glycol 600" in the 6th Burapha University International Conference on August 3-4, 2017 at Pattaya, Chonburi, Thailand.

